The preparation of polyolefin nanofibres by solution electrospinning

By

L Keulder

Dissertation presented for the degree of Doctor of Philosophy (Polymer Science)

at

Stellenbosch University

Promoter: *Prof Albert J. van Reenen*

DECLARATION

I, the undersigned hereby declare that the work in this thesis is my own original work and that I have not previously in its entirety or in part submitted it at any university for a degree.

Date: March 2013

Abstract

Solution electrospinning is a technique used to produce polymer micro- or nanofibres. Recently a great deal of research has been done on the application of polymer nanofibres produced by this method.

The solution electrospinning of polyolefins have not been researched in-depth mainly due to the difficulty in dissolving these polymers in suitable electrospinning solvents. We managed to electrospin polypropylene copolymers at room temperature, obtaining both polymer micro- and nanofibres. A suitable solvent system was developed (cyclohexane/DMF/acetone) that allowed for the room temperature solution electrospinning of these crystalline polypropylene copolymers.

It was also shown that using propylene-1-alkene copolymers with a low comonomer content was a facile way of producing crystalline polyolefins nano – and microfibers. Similar attempts to electrospin isotactic polypropylene were unsuccessful, even though lower molecular weight materials were used than in the case of the copolymers. This lead to an investigation of solution melting temperature by SCALLS. The copolymers showed great variance in their solution melting temperatures despite the fact that they all had more or less the same crystallinity and amount of comonomer, indicating that the type of comonomer played an important role in the solubility of the copolymer.

The effect of different collectors was investigated, but in the end it was found that between spinning unto ice, foil on ice of just foil, foil still seemed to be the best collector.

Comparing crystallinity of the polymer powders with that of the polymer fibres by DSC and WAXD, it was found that there is a difference in the crystallinity of the fibres and the powders.

EVOH is a polymer with excellent properties and electropspinning of this polymer is relatively easy due to the fact that it dissolves quite easily in conductive solvents. DMF, Isopropanol/water and DMSO were all tested as suitable solvents and the morphology was compared through the use of SEM. The morphology of the fibres indicated that DMSO was the best solvent. The influence of the spinning parameters was determined for both systems of DMF and DMSO.

These nanofibres were used as reinforcement in LDPE matrix and the mechanical properties of the LDPE matrix was improved with the addition of both aligned and unaligned fibres.

The next step was the electrospinning of EVOH fibres containing MWCNT. TEM, FE-SEM and TGA were used to confirm the presence of the MWCNT as well as determine the distribution of the MWCNT inside the nanofibres. The nanotubes were distributed through the fibres; however agglomeration of the nanotubes did still take place. The nanofibres containing MWCNT were also used to make composites where the fibres were melted, leaving the MWCNT behind in the polymer matrix. This was done in both LDPE and EVOH matrices. The LDPE/MWCNT composites

did not give positive results, on the other hand the EVOH/MWCNT composite showed an improvement in the mechanical properties compared to pure EVOH.

The attachment of fluorescent dye molecules to the surface of the MWCNT was attempted and through fluorescent microscopy and the dispersion of the nanotubes inside the fibres as well as the composite could be seen.

This study proved that polyolefin nanofibres could be obtained, giving rise to more applications for these versatile polymers. It also confirmed the importance of nanofibres as reinforcement and the use of nanofibres as a way to incorporate MWCNT in a polymer matrix.

Opsomming

Elektrospin in ‘n oplosmiddel is ‘n tegniek wat gebruik word om polimeer mikro- en nanovesels te produseer. Die afgelope tyd word baie navorsing gedoen oor die aanwending van polimeer nanovesels wat geproduseer word op hierdie manier.

Daar is nog min navorsing gepubliseer wat handel oor die elektrospin van poliolefiene uit ‘n oplosmiddel, deels oor hoe moeilik dit is om ‘n geskikte elektrospin oplosmiddel te vind vir hierdie polimere. In hierdie studie het ons mikro- en nanovesels verkry deur polipropileen kopolimere te elektrospin by kamertemperatuur.

Die polimere is opgelos in ‘n oplosmiddel sisteem wat bestaan uit sikloheksaan/dimetielformamied/asetoon, by hoë temperatuur en het toegelaat dat die polimere in oplossing bly by kamertemperatuur. Hierdie diverse kopolimere het verskillende resultate gegee, sommige polimere het mikrovesels produseer, waar ander nanovesels geproduseer het. Die vessel morfologie is ondersoek deur die gebruik van Skandering Elektron Mikroskopie (SEM) en daar is gevind dat die vesels nie ‘n gladde voorkoms het nie, maar dat daar kraalvormige morfologie gesien kon word. Om dit te voorkom is sout by die oplosmiddel sisteem gevoeg. Die invloed van die verskillende parameters op die vesels se deursnit is ondersoek vir al die kopolimere. Die byvoeging van sout het gelei tot ‘n meer gladde vesel morfologie.

Die effek van die gebruik van verskillende oppervlaktes om die vesels op te vang is ondersoek en die die kristalliniteit van die polimeer poeiers is vergelyk met die kristalliniteit van die polimeer vesels met die hulp van DSC en WAXD.

‘n Poging is aangewend om isotaktiese polipropileen te elektrospin uit oplossing, maar ons kon nie daarin slag om die polimeer op te los nie, al was die molekulêre gewig minder as die van die kopolimere. Dit het gelei tot die ondersoek van die smeltpunt temperatuur in oplossing deur die gebruik van oplossing kristallisasie-analise deur laser lig verstrooing (SCALLS). Al die kopolimere het min of meer dieselfde kristalliniteit en hoeveelheid komonomer bevat, tog het hulle smeltpunt temperatuur in oplossing baie verskil. Dit het gedui op die feit dat die tipe komonomeer ‘n groot rol speel in die oplosbaarheid van die kopolimeer.

Die elektrospin van etileen-ko-vinielalkohol (EVOH) is ook ondersoek. DMF, Isopropanol/Water en Dimetielsulfoksied (DMSO) is getoets as geskikte oplosmiddels en die morfologie van die vesels is vergelyk deur die gebruk van SEM. Die tyd wat die polimeer in oplossing gebly het asook die morfologie van die vesels, het aangedui dat DMSO die mees geskikte oplosmiddel

was. Die invloed van die elektrospin parameters was vasgestel vir beide DMF en DMSO sisteme.

Hierdie nanovesels is gebruik as versterking in ‘n LDPE matriks en die meganiese eienskappe van die LDPE matriks is verbeter deur die toevoeging van beide nie-geweefde en gerigte veselsopppervlakte.

Die volgende stap was die elektrospin van EVOH vesels wat multi-ommuurde koolstof nanobuisies (MWCNT) bevat. TEM, FE-SEM en TGA was gebruik om te bevestig dat die vesels wel MWCNT bevat asook om die verspreiding van MWCNT in die vesels aan te dui. Die nanobuisies was versprei deur die vesels, maar bundels nanobuisies het tog voorkom in sommige plekke. Die nanovesels wat MWCNT bevat is ook gebruik om nanosamestellings te maak, waar die vesels gesmelt is om net MWCNT agter te laat in die polimeer matriks. Hierdie was gedoen in beide LDPE en EVOH matrikse. Geen positiewe resultate is verkry vir die LDPE/MWCNT nanosamestelling nie, maar die EVOH/MWCNT nanosamestelling het aan die anderkant ‘n groot verbetering getoon in die meganiese eienskappe in vergelyking met EVOH sonder MWCNT.

‘n Poging was aangewend om fluoreseerende molekules aan die oppervlak van MWCNT te voeg en deur fluoresensie mikroskopie kon die verspreiding van die MWCNT in die vesels asook in die nanosamestellings gesien word.

Hierdie studie het bewys dat poliolefien nanovesels gemaak kan word wat lei tot die aanwending van hierdie polimere in nog meer toepassings. Dit het ook die belangrikheid van die gebruik van nanovesels as versterking in nanosamestellings bevestig asook die gebruik van nanovesels as ‘n manier om MWCNT in ‘n matriks te plaas.

Acknowledgements

I would like to thank the following people:

Prof. Van Reenen, for your guidance, support and patience as my study leader

Madelaine Frazenberg - SEM

Mohammed Jaffer and Francois Cummings (UCT) – TEM

Miranda Waldron – FE-SEM

Dr. B. Loos and Lize Engelbrecht – Fluorescence microscopy

Roediger Agency – Tensile testing

Olefin research group, everyone of you who were there for, research support, coffee breaks and countless laughs.

Polymer students, especially Gareth Bayley for being electrospinning mentor. Nadine, Ashwell, Pritish, William, Corey, Jacques and Morne for moral support and always willing to listen

Friends and family, each of you that tried to understand what I was doing and for being supportive

And lastly but most importantly,

My parents, for allowing me to study and always being there and supporting me in every aspect

And

To God, for giving me the ability to study

Table of Contents

List of Figures

List of Tables

List of Abbreviations

AC	alternating current
AIBN	azobisisobutyronitrile
ATR	attenuated total reflectance fourier transform infra-red
CNT	carbon nanotubes
CVD	chemical vapour deposition
DC	direct current
d-DMSO	deutorated dimethylsulfoxide
DMF	N,N-dimethylformamide
DMSO	dimethylsulfoxide
DSC	differential scanning calorimetry
DWCNT	double wall carbon nanotubes
EVOH	polyethylene-co-vinyl alcohol
FE-SEM	field emission scanning electron microscopy
FITC	fluorescein isothiocyanate
FT-IR	fourier transform infrared
HDPE	high density polyethylene
HPLC	high performance liquid chromatography
KH_2PO_4	potassium dihydrogen phosphate
LDPE	low density polyethylene
LiCl	lithium chloride
LLDPE	linear low density polyethylene
MA	maleic anhydride
MAO	methyl alumoxane
MWCNT	multi-walled carbon nanotubes
NaCl	sodium chloride
NMR	nuclear magetic resonance
PEG	poly(ethylene glycol)
PMMA	polymethyl methacrylate
PP	polypropylene
PS	polystyrene
PVA	poly(vinyl acetate)
p-Xylene	para-xylene
SCALLS	solution crystallization analysis by laser light scattering
SEM	scanning electron microscopy

STDEV	standard deviation
SWCNT	single-walled carbon nanotubes
TCD	tip-to-collector distance
TGA	thermogravimetric analysis
TREF	temperature rising elution fractionation
WAXD	wide angle X-ray diffraction

Chapter 1

Introduction

1.1 Polyolefins, poly(ethylene-co-vinyl alcohol) and electrospinning

1.1.1 General introduction

In recent times, there has been a great deal of interest in the applications of polymeric nanofibres produced by solution electrospinning. The ability to produce fibres with diameters well below 1 μm in a facile manner has spawned a plethora of papers dealing with possible applications of these fibres. As will be discussed in greater detail at a later stage, the electrospinning of a polymer from solution is subject to the polymer being (a) soluble and (b) that the solvent or combination of solvents that are used is sufficiently conductive to allow for the electrospinning process to occur.

One of the most commonly used group of thermoplastic polymers, the polyolefins, have not been the subject of many electrospinning studies, because, (a) the polymers are typically only soluble in aromatic (chlorinated) hydrocarbons or longer-chain alkanes at elevated temperatures, and (b) these solvents are essentially non-conductive. Initially the research discussed in this thesis was focussed on the electrospinning of the polyolefins, but this evolved into other related areas. What follows below is a brief overview of some of the topics relevant to this thesis.

1.1.2 A general overview of polyolefins

Polyolefins are used in numerous applications. These polymers are chemically quite inert and depending on the morphology have a wide range of physical properties. Most polyolefins melt between 110 and 170 °C, which makes the processing more onerous compared to other commonly used but non-crystalline thermoplastics (like PVC and polystyrene), but at the same time the thermal stability of the polyolefins is therefore better than the aforementioned materials. Overall the polyolefins have good mechanical properties, and are resistant to chemicals (excluding the aliphatic hydrocarbons).

As a group of materials, the commercially important polyolefins are the polyethylenes (low density polyethylene, high density polyethylene and linear low density polyethylene), and polypropylene. Polypropylene is (as an isotactic homopolymer) a highly crystalline material and has numerous applications in industry. Isotactic polypropylene does have a drawback, in that it is quite brittle, particularly at low temperatures. Copolymers of polypropylene are also available. Commercially the

crystalline propylene-ethylene random copolymers (low ethylene content) and the so-called impact copolymers (higher ethylene content, produced by sequential gas-phase polymerization) are produced by heterogeneous transition metal catalysed polymerization.

The addition of the higher 1-alkenes as comonomers to polypropylene decreases the crystallinity of the polymer and thereby increases the processability of the polymer. Polypropylene is a very brittle polymer with a glass transition temperature of 0 °C. By adding the comonomer, the glass transition temperature could be lowered, producing a more flexible polymer. It was also found that the addition of 1- butene decreases the melting temperature of the polymer and the polymer was also more flexible[1]. Most of the copolymers of propylene with the higher 1-alkenes have been made (non-commercially) by homogeneous transition metal (metallocene) catalysts. These produce polymers with a much narrow molecular weight distribution than the materials produced by commercial, heterogeneously catalysed reactions[2, 3]. The copolymers of propylene and the 1-alkenes can range, as far as the morphology of the polymer is concerned, from being a completely amorphous (rubber) to highly crystalline (meltable thermoplastic). The applications of the materials are obviously affected by the physical state of the material[1].

1.1.3 Poly(ethylene-co-vinyl alcohol)

Poly(ethylene-co-vinyl alcohol) (EVOH) is a random copolymer comprising ethylene and vinyl alcohol units. This polymer is prepared by the hydrolysis of a copolymer of ethylene and vinyl acetate. Due the presence of the pendent hydroxyl groups of the vinyl alcohol monomer units, EVOH has some notable properties, one of them being exceptional oxygen barrier properties (as a film). This has led to the polymer being extensively used (in multilayer films) in the food packing industry. Apart from good barrier properties, EVOH also has outstanding thermal processability and is resistant to many solvents. The pendent hydroxyl units on the EVOH backbone make this polymer water insoluble yet hydrophilic. EVOH is also reported to be biocompatible but not biodegradable. This led to the increasing use of EVOH in biomedical applications in recent years[4, 5].

EVOH membranes can also be formed which can be used in filtration applications or in tissue engineering. Kenawy *et al*[6]. suggested that the electrospinning of EVOH is a simple way to prepare porous structures that can be used as membranes.

The surface modification of nanofibres is much easier than a polymer in any other form. Since EVOH have reactive hydroxyl groups attached to the polymer chains, the modification of the surface of EVOH nanofibres will encourage the use of this material in various applications[7, 8].

In recent years the use of nanocomposites has become quite popular. To our understanding, the term nanocomposite refers to the production of a composite containing a nanomaterial as a filler.

In most composites containing fibres, small fibres were, until recently mostly microfibers, and it is only recently that the use of nanofibres as fillers has begun. As we know, nanofibres have superior mechanical properties over microfibers. It therefor stands to reason the incorporating nanofibers in a polymer matrix will enhance the mechanical properties of the polymer, and a few papers have illustrated this[9-11]. There are a few factors that play a role when using nanofibres as reinforcement. The interaction between the nanofibres and the polymer matrix and the arrangement of the fibres inside the matrix all play a role in the manner in which the polymer will be reinforced.

It has also been shown that EVOH may be used as a compatibiliser between polyolefins and specifically wood species[12, 13]. The good interaction between EVOH and polyolefins creates the possibility to use EVOH nanofibres as reinforcement in polyolefins. It must be pointed out that the term EVOH describes the whole family of ethylene-vinyl alcohol copolymers. The grades of EVOH are mostly defined by the hydroxyl content (expressed as percentage vinyl alcohol) in the copolymer.

When talking about the use of nanofillers, the use of carbon nanotubes must be mentioned. These nanomaterials have excellent mechanical properties as well as good conductivity characteristics. The use of carbon nanotubes has spread to various applications, including in sensors, catalysts and as conductive films, to name but a few[14, 15]. One of the main complications when using nanotubes as reinforcement is the distribution of the nanotubes inside the material. In addition there is the adhesion (or lack thereof) between the polymer and the nanotubes. Nanotubes tend to agglomerate and then when placed inside a polymer matrix they will occur as bundles rather than being well dispersed throughout the material. Agglomerated nanotubes have weaker conductivity and mechanical properties, than nanotubes that are well dispersed[16, 17]. The incorporation of nanotubes inside a matrix can occur through various methods, but one of the most recent being the use of nanofibres[18, 19]. This entails that the carbon nanotubes are electrospun with a polymer, from solution. The result is polymer nanofibres containing carbon nanotubes. Research has shown that the carbon nanotubes will be well dispersed throughout the fibres and tend to agglomerate less[19]. These nanofibres containing nanotubes could then be placed inside a polymer matrix, so not only will the polymer matrix be reinforced by the fibres, but also even more by the nanotubes. Another option is the melting of the fibres inside the polymer leaving the well dispersed carbon nanotubes inside the polymer matrix.

1.1.4 Electrospinning

Electrospinning is a technique in which polymers get drawn into fibre form by the application of an electrostatic force. This technique has the ability to produce polymer material in nanometre range. Nanofibres have excellent properties including a high surface area/weight ratio, good mechanical properties and the ability to have the surface functionalised with ease[9, 20, 21]. Nanofibres are mainly

used in three areas, textiles, industrial applications and, recently, in the biomedical field. Polymers used in the electrospinning process must be chemically and thermally stable during the process and must be capable of being drawn into fibres[22].

The electrospinning technique was first observed by Rayleigh in 1897, but was patented by Formhals in 1934[9]. Formhals discovered that when a polymer solution is subjected to an electric field, the electrostatic forces will cause the solution to be drawn into fibres.

When combining the properties of the polyolefins with that of nanofibres it is obvious by producing polyolefin nanofibres will result in a strong material with numerous application possibilities.

Polyolefin nanofibres have been produced by melt electrospinning. The solution electrospinning of polyolefins has not been investigated to nearly the same degree. The main problems are the ones which were mentioned at the start of this chapter; the temperature at which polyolefins are soluble, and the conductivity of the solvents used. Larrondo *et al*[23-25]. published some of the first papers describing the electrospinning of polyethylene from a paraffin solution at 100 °C. Not only is the temperature at which electrospinning takes place the problem, but these polymers only dissolve in hydrocarbons which is not really suitable for electrospinning due to their low conductivity.

The possible advantages of being able to produce polyolefin nanofibers by electrospinning makes is worth while exploring routes to overcome the inherent problems associated with these materials.

1.1.5 Aims

The objective of this study was twofold.
In the **first instance it was an aim** to solution electrospin polyolefins. The use of high temperature was a challenge, so an electrospinning setup needed to be designed to accommodate this problem. The solubility of the polymers in suitable conductive solvents was another obstacle. Polyolefins are highly crystalline materials, but the introduction of comonomers has been shown to decrease the crystallinity of the material which in turn might make it more soluble for solution electrospinning.
The specific goals of this part of the study were as follows:

- Designing an electrospinning setup in which the solution electrospinning of polyolefins can take place.
- Optimising the electrospinning conditions to obtained beadless fibres with the smallest possible diameter.
- Investigate the influence of the different parameters namely, tip-to-collector distance, applied voltage and feed rate, on the fibre diameter.
- Explore the use of different collectors

- Consider the reasons why the usage of the polypropylene copolymers might be better in the solution electrospinning process than other polyolefins.

The **second aim of this study** was to use EVOH nanofibres as reinforcement in polyolefins, but also the electrospinning of this polymer with carbon nanotubes. These nanofibres containing nanotubes will then be used as a method to incorporate the nanotubes inside a polyolefin matrix. The more specific goals of the second aim were as follows:

- Finding a suitable solvent for the electrospinning of EVOH.
- Optimising the electrospinning conditions to obtained beadless fibres with the smallest possible diameter.
- Investigate the influence of the different parameters namely, tip-to-collector distance, applied voltage and feed rate, on the fibre diameter.
- The incorporation of the nanofibres inside a polyolefin matrix
- Mechanical testing of the formed nanocomposites as well as an investigation of the arrangement of the fibres inside the composite.
- Electrospinning of multi-walled carbon nanotubes with EVOH.
- Incorporation of the carbon nanotubes inside a polymer matrix through the use of nanofibres.
- Investigation of the influence of the nanotubes on the mechanical properties of the polymer matrix.
- Examination of the distribution of the nanotubes inside the fibres and inside the composites.
- Possible functionalization of the EVOH and the electrospinning of the functionalised EVOH.

1.2 References

1. Imanishi, Y.; Naga, N. *Progress in Polymer Science* **2001,** 26 , 1147-1198.

2. Brüll, R.; Pasch, H.; Raubenheimer, H. G.; Sanderson, R.; van Reenen, A. J.; Wahner, U. M. *Macromolecular Chemistry and Physics* **2001,** 202 (8), 1281-1288.

3. Arnold, M.; Bornemann, S.; Köller, F.; Menke, T. J.; Kressler, J. *Macromolecular Chemistry and Physics* **1998,** 199 (12), 2647-2653.

4. Ogata, N.; Lu, G.; Iwata, T.; Yamaguchi, S.; Nakane, K.; Ogihara, T. *Journal of Applied Polymer Science.* **2007,** 104 (2), 1368-1375.

5. Kroschwitz, J. I. In *Encyclopedia of Polymer Science and Technology.* John Wiley & Sons, Inc.: United States of America, 2003; Vol. 5, pp 230-233.

6. Kenawy, E.; Layman, J. M.; Watkins, J. R.; Bowlin, G. L.; Matthews, J. A.; Simpson, D. G.; Wnek, G. E. *Biomaterials* **2003,** 24 (6), 907-913.

7. Cerrada, M. L.; Sanchez-Chaves, M.; Ruiz, C.; Fernandez-Garcia, M. *Biomacromolecules* **2009,** 10 (7), 1828-1837.

8. Sánchez-Chaves, M.; Ruiz, C.; Cerrada, M. L.; Fernández-García, M. *Polymer* **2008,** 49 (12), 2801-2807.

9. Huang, Z. -.; Zhang, Y. -.; Kotaki, M.; Ramakrishma, S. *Composites Science and Technology* **2003,** 63 , 2223-2253.

10. Bergshoef, M. M.; Vancso, G. J. *Advanced Materials* **1999,** 11 (16), 1362-1365.

11. Tang, C.; Liu, H. *Composites, Part A: Applied Science and Manufacturing* **2008,** 39A (10), 1638-1643.

12. Shebani, A. N. The effect of wood composition and compatibilisers on polyethylene/wood fibre composites, Stellenbosch University, Stellenbosch, 2010.

13. Shebani, A. N.; Van Reenen, A. J.; Meincken, M. *Journal of Composite Materials* **2009,** 43 (11), 1305-1318.

14. O'Connell, M. J. In *Carbon Nanotubes,Properties and Applications.* Taylor & Francis Group: Florida, 2006; pp 329.

15. Meyyappan, M. In *Carbon nanotubes, Science and Applications.* CRC Press: Florida, 2005; pp 289.

16. Bandarian, M.; Shojaei, A.; Rashidi, A. M. *Polymer International* **2011,** 60 (3), 475-482.

17. Jose, M. V.; Dean, D.; Tyner, J.; Price, G.; Nyairo, E. *Journal of Applied Polymer Science* **2007,** 103 , 3844-3850.

18. Choi, J.; Park, E. J.; Park, D. W.; Shim, S. E. *Synthetic Metals* **2010,** 160 (23-24), 2664-2669.

19. Kim, M. J.; Lee, J.; Jung, D.; Shim, S. E. *Synthetic Methods* **2010,** 160 (13-14), 1410-1414.

20. Shin, Y. M.; Hohman, M. M.; Brenner, M. P.; Rutledge, G. C. *Applied Physics Letters* **2001,** 78 (8), 1149-1151.

21. Garg, K.; Bowlin, G. L. *Biomicrofluidics* **2011,** 5 (1), 013403/1-013403/19.

22. Mark, H. F.; Atlas, S. M.; Cernia, E. In *Man-made fibers (Science and technology).* Man-made fibers (Science and technology); John Wiley & Sons: United States of America, 1967; Vol. 1, pp 432.

23. Larrondo, L.; St. John Manley, R. *Journal of Polymer Science, Polymer Physics Edition* **1981,** 19 (6), 909-920.

24. Larrondo, L.; St. John Manley, R. *Journal of Polymer Science, Polymer Physics Edition* **1981,** 19 (6), 921-932.

25. Larrondo, L.; St. John Manley, R. *Journal of Polymer Science, Polymer Physics Edition* **1981,** 19 (6), 933-940.

Chapter 2

Background

This chapter serves to briefly introduce a number of topics that are relevant to the study that was conducted. For this purpose, the chapter is subdivided into (a) materials used, (b) nanofibres and (c) the methodology of producing them, and (d) considerations regarding polymer nanocomposites

2.1 Materials used.

2.1.1. Polypropylene copolymers

Numerous articles have been published on the synthesis of polyethylene copolymers produced by metallocene catalysts[1]. Far fewer papers have been published regarding the polymerization of polypropylene with α-olefins, but a there are several good examples [1-7].

The copolymers used in this study were polymerized with metallocene catalyst, and were primarily propylene-higher α-olefin copolymers with a low comonomer content [8, 9].

As these polymers were made by metallocene catalysts, a brief introduction to these types of catalysts follow in Section 2.1.1.1.

2.1.1.1. A brief discussion of metallocene catalysts

Metallocene catalysts consist of two (substituted) cyclopentadienyl ligands, bound to a central group 4B transition metal, which in turn is σ-bonded to two additional ligands. The catalytic behaviour is determined by the substituents on the cyclopentadienyl ligands, the stereochemistry of the bound ligands, the type of transition metal as well as the cocatalyst. By varying these factors one can change the activity of the catalyst, the stereospecificity of the monomer insertion and the reactivity of the catalyst towards certain monomers. These catalysts are typically “single-centre” catalysts which allows for the production of polymers with narrow molecular weight distribution. These catalysts allow the control of molecular weight, molecular weight distribution and tacticity to a greater degree than other transition metal catalyst systems. One of the biggest advantages of these catalysts is that by changing the chemical structure of the catalyst you can control the performance [10-13]. The history and development of these catalysts is well-documented [11,12].

It is also necessary to point out that the cocatalyst that is most commonly used is methyl alumoxane or MAO. This is a complex molecule, the structure of which is still not fully resolved. Examples of reported structures are given in Figures 2.1 and 2.2 [14,15].

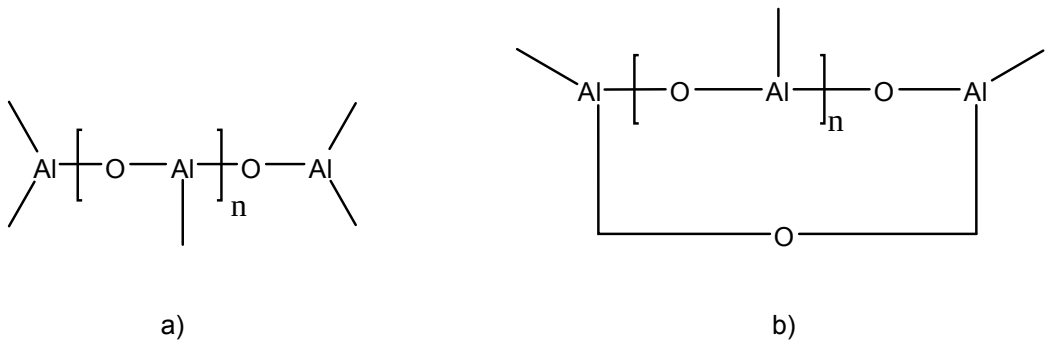

Figure 2.1 Proposed structures of MAO: a) linear and b) cyclic where n = 4-20 [14].

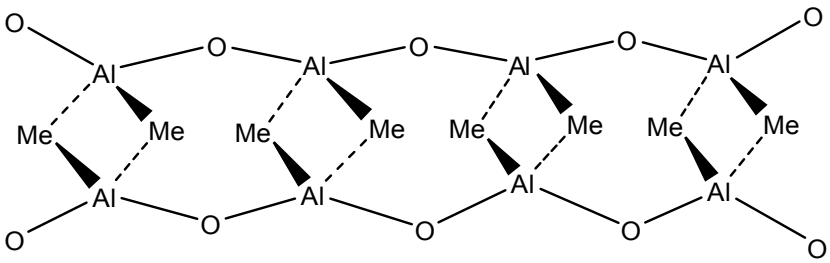

Figure 2.2 The structure of MAO proposed by Sungano *et al* [14, 15]. with a coordination number of 4.

MAO undergoes fast ligand exchange with a metallocene dichloride (the precatalyst), so fast methylation takes place. The next step is a partial demethylation, in which CH_3^- is taken from the metallocene by the Al centre of the MAO. The weakly coordinating MAO anion that is formed will stabilize the catalyst active centre (the cationic metallocene). The MAO also acts as scavenger for impurities and potential catalyst poisons [14, 16, 17]. Other alkyl aluminium compounds can also perform these roles, but MAO also enhances the catalytic activity more than any other alkyl aluminium compound. One of the reasons is that when MAO stabilizes the cationic active centre, it does so by forming a “crown-alumoxane complex”. Conventional cationic polymerization mostly gets terminated by an anionic species attacking the cationic active centre; therefore the stabilization of the cationic centre is very important. Another function of the MAO is to reactivate dormant catalyst species[14].

Figure 2.3 outlines the proposed mechanism of polymerization of a metallocene catalyst [11, 17, 18].

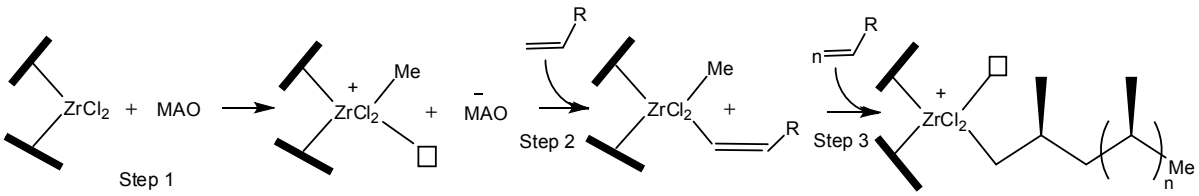

Figure 2.3 Proposed mechanism of polymerization of a metallocene catalyst [17]

The activity of the catalyst as well as the properties of the resultant polymer is dependent on the nature of the metallocene. This includes the type of transition metal centre, structures of the Cp ligands and the way the catalysts and the monomer interacts [14,18].

The copolymerization of polypropylene with α-olefins have been reported for both isospecific Ziegler-Natta catalysts and more importantly for isospecific metallocene catalysts [3, 4, 6, 19-23]. The advantage of using an isospecific metallocene catalyst is that these catalysts have high reactivity towards α-olefins and the copolymers produced from them are usually very homogeneous. This meant that polymers with a narrow molecular weight distribution (typically less than 2) and a random distribution of comonomer can be produced [3, 24]. Like in the case of linear low density polyethylene, which is produced when copolymerizing small amounts of α-olefins with ethylene, the addition of the comonomer during the polymerization of propylene decreases the crystallinity of the resultant polymer. This has, inter alia, the effect of increasing the processability of the polymer. It has been reported in literature that the melting temperature of propylene/1-butene copolymers decreases with an increase in comonomer content. With higher α-olefins was shown that the melting temperature of the copolymers did decrease with increasing comonomer content, but that this decrease was independent of the chain length of the comonomer [6, 23, 24]. The appeal of producing propylene copolymers is that not so much that the melting point is decreased, but that the glass transition temperature is lowered from the 0 °C for isotactic polypropylene homopolymer. This glass transition temperature has the effect the iPP cannot be used for low temperature applications. By adding the comonomer, the lower Tg has the result of a tougher, less stiff material at low temperatures. The propylene copolymers can range from being a thermoplastic elastomer to a semicrystalline thermoplastic. The resultant polymers can now be used in a wider range of applications than iPP alone [3].

2.1.2. Poly(ethylene-co-vinyl alcohol)

Poly(ethylene-co-vinyl alcohol) (EVOH) is a random copolymer consisting of ethylene and vinyl alcohol units. The molecular formula of this copolymer is $–(CH_2\text{-}CH_2)_m\text{-}(CH_2\text{-}CH(OH))_n$ [25, 26]. These polymers are produced in two variations. First, these materials are produced (via the ethylene-vinyl acetate copolymer route) as materials with high ethylene content (82 – 90 mole%) as either an

ethylene-vinyl alcohol copolymer or as an ethylene-vinyl acetate-vinyl alcohol terpolymer. These materials are usually used as adhesives. The second variation is made by fully hydrolysing poly(ethylene-co-vinyl acetate) with an ethylene content of 25 to 45% to produce EVOH with 60-75 mole% vinyl alcohol. This type of EVOH has exceptional properties, which include excellent barrier properties, which means that this polymer has a high resistance to gas diffusion [26]. These polymers also have good solvent resistance and processability [27].

The excellent barrier properties can be attributed to the molecular structure of EVOH. The molecular structure is very symmetrical and there strong hydrogen bonding is present due to the pendent hydroxyl groups. This makes the diffusion of oxygen through the polymer very difficult, since the movement of the segments that are necessary for oxygen diffusion is limited by the high inter- and intramolecular cohesive energy. When the ethylene content increases, the inter- and intramolecular hydrogen bond strength decreases. The segments will be able to move and oxygen will be able to diffuse through the material more easily. Because of the excellent barrier properties, EVOH is usually used as packaging material. EVOH is usually coextruded or blended with other polymers [28], like HDPE, for the formation of films. EVOH is very sensitive to humidity and the humidity can change the resistance of the polymer to oxygen diffusion [29]. The greater the amount of hydroxyl pendant groups, the more the polymer will be influenced by moisture and humidity [26]. The moisture acts as plasticiser and increases the oxygen permeability [30]. EVOH is thus normally sandwiched between two moisture barrier resins, so the oxygen barrier properties will be retained even the packaging film is exposed to moisture [27]. The properties of EVOH will vary according to the vinyl alcohol content. It was found that with an increase in the vinyl alcohol content there is also an increase in the hardness of the material [31].

Another feature of EVOH (due to the presence of the hydroxyl groups) is that the polymer is hydrophilic whilst still being water-insoluble. EVOH is reported to be biocompatible but non-biodegradable. Due to these properties EVOH can be used as a biomaterial [25, 32]. Recent studies have highlighted the use of EVOH in biomaterial applications. EVOH can be electrospun and used as nanofibrous mats for cell growth, as membranes [33-37] and in tissue engineering [25].

EVOH generally has a low reactivity towards active compounds at low temperature. To improve this property, functional groups can be added to the structure by reacting with the hydroxyl groups on the polymer [25, 32, 38, 39-40]. As an example of this, EVOH can be reacted with amminosaccharides to produce glycopolymers that can be used as membranes [41].

2.2 Nanofibres in general

Nanofibres have received quite a bit of attention in the past few years. These fibres can be used in a variety of applications. The definition of a nanomaterial is varied, but nanofibres can be described as threadlike materials with a diameter of less than 400 to 500 nm.

Polymeric fibres can be produced by spinning, either from solution or from the melt. For a polymer to be spinnable it needs to be thermally and chemically stable during the spinning process. It must also be possible for the polymer to be pulled into threads and converted into a solid fibre [42].

The ability to produce polymeric nanofibres (for example by electrospinning) has created some interesting possible applications. Tissue engineering is one of the applications for nanofibres and is probably one the most extensively studied areas. Biodegradable material can be spun unto a wound directly. This covering will boost the skin growth and the wound will heal faster [43-45]. Biocompatible nanofibrous mats of polymer and protein can be added to prosthetic implants, and will act as an interface between the tissue and the implant [44, 46]. Bognitzki *et al* [47]. took a polymer that can be electrospun easily, but will degrade at high temperatures and coated it with a desired thermally stable material that will form a wall on the outside of the fibre. Once this is done, the polymer inside is degraded and you are left will a tubular form of the coated material which can be used in a variety of applications. These are is just a few examples of the ways in which nanofibres can be applied.

Ramakrishna *et al* [48]. have discussed various ways of producing nanofibres, drawing, phase separation, self-assembly, template synthesis and electrospinning. For the purpose of this study we will only discuss electrospinning.

2.3 Methodology

2.3.1. Electrospinning

Electrospinning is a fibre-forming process in which a polymer melt or solution gets drawn into fibres. This technique has become popular in the industry the past few years, especially in the biomedical field [49]. This is due to the fact that is a relatively easy process to produce nanofibres that can be used in a wide variety of applications [50-52]. One of the main areas that are being researched is the use of nanofibres in tissue engineering, since the electrospinning of the material creates a mat that has a high surface area as well as high porosity [53, 54].

Rayleigh first detected this phenomenon in 1897 and eventually it was patented by Formhals in 1934 [55]. Formhals discovered that if a solid material is dissolved in a liquid and passed through an electrical field, the formation of fibres will take place [56]. The process works is that when, for example, a polymer solution is subjected to an electrical field; the electrostatic forces will cause the polymer to be drawn into fibres. One advantage of electrospinning is that it produces fibres with a diameter in the nanometer range that have a very high ratio of surface area to mass. Polymers in this form also have better mechanical properties and functionalization of the surface is also much easier than for similar polymeric fibres in the micrometer range [45, 51, 57].

There are two types of electrospinning, melt electrospinning and solution electrospinning. Melt electrospinning implies that the electrospinning takes place out of a polymer melt. With solution electrospinning the polymer is dissolved and then electrospun out of the solution.

The solution electrospinning setup usually requires a capillary which will supply the polymer solution, a high voltage supply and a grounded collector plate. The solution may be gravity fed through a capillary tube. Another option is to place the solution in a syringe and to use a syringe pump to deliver the polymer solution in a controlled fashion. An electrode is attached to the syringe or capillary and one with an opposite charge is attached to the grounded collector plate. A droplet of the polymer solution is suspended at the tip of the needle. The droplet will be subjected to two forces, the first being the surface tension of the droplet and the second the electrostatic forces of the electrical field. The surface tension of the droplet will be in equilibrium with the electrical field and the electrical charges in the solution will interact with the electrical field and the drop will elongate in conical shape, namely a Taylor cone. The angle of a Taylor cone is about 30°. At a given point the surface tension will be overcome by the electrostatic forces and the polymer solution will then erupt in a jet at the tip of the Taylor cone and in a whipping motion get drawn towards the grounded collector plate [44, 48, 52, 58-63].

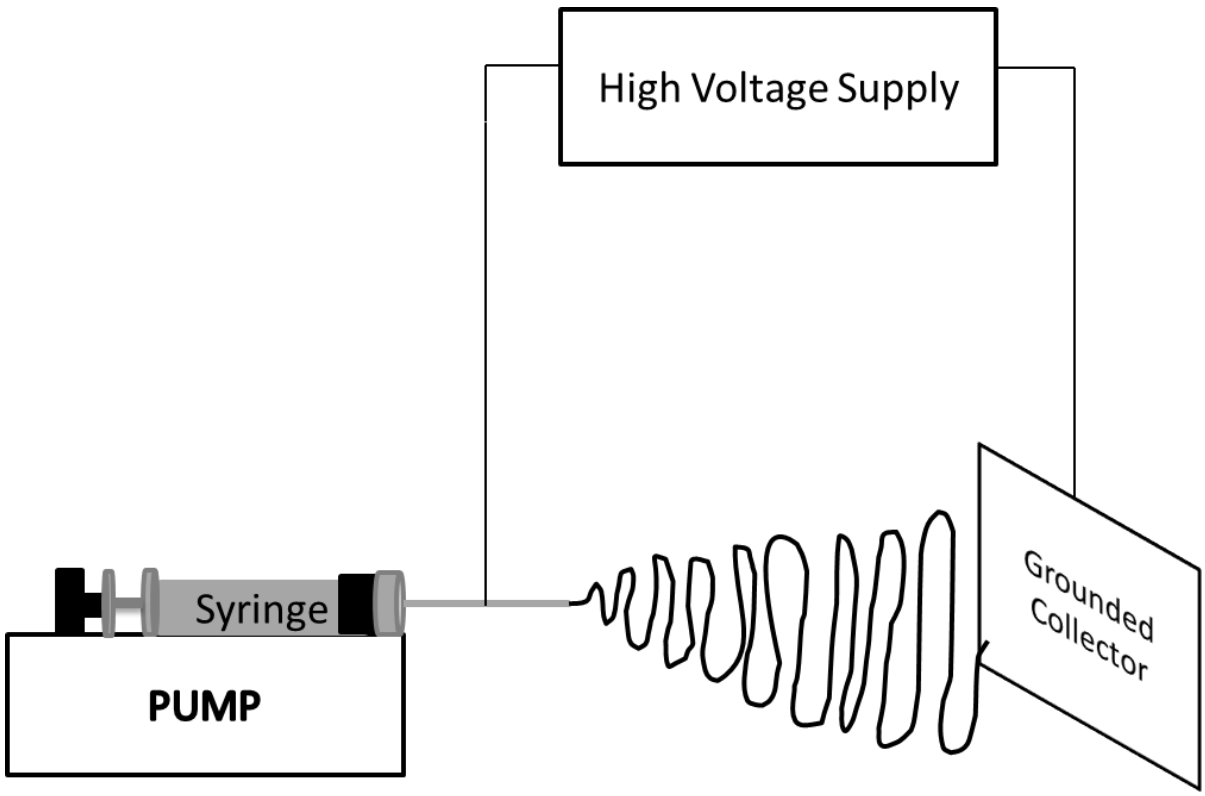

Figure 2.4 Electrospinning setup

The electrospinning process seems quite simple, but on closer examination it is actually quite complex. There are some factors that are quite important and by varying them the whole process can change. For example, while the jet appears to follows direct path toward the collector plate, this is not the case. The jet will start to move from side to side (called the whipping of the jet) in the form of a cone with its opening going towards the collector plate. This whipping motion leaves room for instabilities to occur.

Hohman *et al* [64, 65]. looked in detail at the instabilities of the jet. According to these papers, there are two types of instabilities. In the first case the centre of the jet remains stable, but the radius gets modulated and in the second case this is reversed. Hohman *et al* [64, 65]. also postulated three modes that are unstable. First there is the Rayleigh mode, where the electrical effects plays the biggest role, second there is the axisymmetric mode and third the whipping conducting mode. The latter two modes only exist when the solution conductivity is limited. When the Rayleigh instability is decreased by increasing the electrical field, the conducting mode is favoured. These authors concluded that the core of electrospinning is the whipping of the jet and that charge density on the jet interacts with the external field and an instability is created. It is not only the jet that will influence the electrospinning process, although it plays an important role. The shape of the fibres can vary, from being flat ribbons to very broad fibre diameters [52]. Other factors include the type of solvent, the viscosity of the solution, the voltage applied and the distance between the needle and the grounded collector plate [48, 52, 55].

The factors influencing the process can be divided into two categories, parameters relating to the polymer solution and those relating to the conditions of the electrospinning process [48].

2.3.1.1. Polymer solution parameters

Solution viscosity, molecular weight and solution concentration

For electrospinning to take place, the solution needs to have a certain viscosity. The viscosity of the solution will be influenced by the molecular weight and concentration of the polymer in solution. The molecular weight (and therefore viscosity) plays a role, because when the jet leaves the needle tip, the molecular entanglement of the polymer chains cause the jet to be continuous and stable [48, 58].

There are two ways to increase the viscosity of the solution. The molecular weight of the polymer could be increased or the concentration could be increased. The entanglement density will increase with an increase in molecular weight [48, 66]. With polymer solutions, the molecular weight plays an important role and can have an effect on electrical and rheological properties, for example surface tension, viscosity, dielectric strength and conductivity [67]. Overall it was observed that fibre diameter becomes smaller and more uniform with an increase in the solution concentration [52, 68].

The morphology of the fibre or artefact will change as follows with an increase in concentration: at low concentration only beads will form, then beads and emerging fibres will form, then beaded fibres, then only fibres and finally spherical fibres or macrobeads [66, 67]. When the viscosity is too low, surface tension will be the overriding influence. There will be more solvent molecules and fewer polymer chain entanglements, leading to bead formation or the formation of drops instead of fibres [68-70]. When the viscosity increases there are more chain entanglements and the charges will stretch the solution. The solvent molecules will be distributed among the chains [48]. Rayleigh instability occurs when the jet becomes unstable and breaks up into droplets. When the viscosity is too low, there will be no resistance against Rayleigh instability. Spherical droplets can be formed due to the lack of chain molecules, but a complete break-up is prevented. These droplets will repel each other and will not combine. If there is an increase in the charge density on the surface of the droplets, they will burst into even smaller droplets. This process is known as electrospraying. Bead formation usually takes place when Rayleigh instability occurs for long-chain molecules. These molecules cannot be break up into droplets that easily and rather cause beaded fibres [55].

On the other hand, if the viscosity is too high, the solution may dry at the tip of the needle, before it can be electrospun and a high viscosity could also make it difficult to pump the solution through the syringe. When this happens the fibres that are formed are not uniform, or no fibres at all may be produced [68, 71]. The fibre diameter will also increase, due to the fact that solution will resist stretching [48, 58, 72-69].

Some interesting fibre morphologies have also been found when varying the solution concentration. A solution of polyvinyl alcohol was electrospun by Holzmeister *et al* [73]. at different solution concentrations. When using an 8 wt% solution they found smooth fibres, whereas using 4 to 6 wt% solutions they observed the formation of barbed fibres. They explained this phenomenon, saying that is due to the slow charge relaxation compared to the formation of the secondary instabilities which will deform the jet.

Surface Tension

The polymer in solution needs to overcome the surface tension to be able to be electrospun. Surface tension effectively decreases the surface area per unit mass of a fluid. This could cause the jet to break up into droplets because of Rayleigh instability [48, 55]. The surface tension will cause the molecules to aggregate together when there is a high concentration of free solvent molecules and will cause bead formation. When the viscosity is high, the interaction between the polymer and the solvent molecules is better. So when the solution is subjected to charge, the solvent molecules spread out over the entanglements of the polymer molecules. This will reduce the chances of the solvent molecules aggregating. Certain solvents have low surface tension and will be ideal to use.

Another method of reducing the surface tension of a solution is by adding a surfactant or a salt to the solution [48].

Dielectric effect of a solvent

The dielectric constant of a solvent gives an indication of the polarity of the solvent. The dielectric constant is very important in the electrospinning process. It was found that a solvent with a high dielectric constant decreases bead formation and fibre diameter [48, 74-76]. Hsu and Shivkumar [74] also found that when adding N,N-diemthylformamide (DMF) to chloroform when electrospinning poly(caprolactone) the deposition rate also increases. Jarusuwannapoom *et al* [77]. tested the influence of different solvents on the fibre morphology of polystyrene fibres. They found that solvents with a high dipole moment and conductivity produce fibres more easily. If the polymer dissolves well in the given solvent, a higher dielectric constant solvent will generally lead to thinner fibres and less beading during the electrospinning process.

This decrease in beading and fibre diameter is not always the case, however. When a solvent with a high dielectric constant is used, but the polymer does not interact well with the solvent, the formation of beads may occur, in addition to an increase in fibre diameter [48].

Conductivity of the solution

During electrospinning the solution gets stretched due to the charges that are repulsed on the surface of the solution. When the conductivity of the solution is increased more charges can be carried by the jet. An increase in the conductivity means that electrostatic forces can now overcome the surface tension much easier [48, 78]. The more charges the jet carries, the more the solution will be stretched and the more the solution is stretched, the lesser is the chance of bead formation and thinner fibres will also be produced [48, 67]. The increase in charges also causes the jet to have greater bending instability which in turn will lead to a greater deposition area. The solution however can only be stretched up until a certain point, viscoelastic charges will be working against the coulombic forces of the charges and this limits the amount of stretching the solution can undergo. Results have also shown that if the conductivity is too high, only droplets are formed [79]. In some cases it is very difficult to find solvents that will dissolve the polymer as well as being conductive enough. In these cases, an ionic salt could be added to the mixture, thereby increasing the conductivity of the solution. When ionic salts are used (like NaCl, LiCl, and KH_2PO_4) beadless fibres are usually obtained [48, 67, 80, 81-40]. The salts do have an effect on the morphology of the fibre though. Due to higher conductivity the solution will get stretched more and thinner fibres can be formed [75]. Qin *et al* [78, 80]., Demir *et al* [69]. and Fong *et al* [82]. all found that fibre diameter decreases with the addition of an ionic salt. In another experiment it was found that if the conductivity of the solution is already high, adding salt can cause aggregation and fusion of the fibres [81]. Qin *et al* [80]. found that when comparing different salts, LiCl produces the fibres with the largest diameter. They

said the salt increased the conductivity of the solution and this leads to an increase in the surface charge of the jet, which in turn will lead to more fluent spinning, now the amount of solution in the jet increases and then eventually the fibre diameter increase.

Processing parameters

These are the external factors that influence the electrospinning process.

Size and diameter of the needle

A smaller internal diameter of a needle was found to produce thinner fibres. With a smaller internal diameter the size of the droplet at the tip of the needle is reduce and the surface tension of the droplet will increase. If the same voltage is used over different diameter sizes, you will find for the smaller diameter size a bigger coulombic force is needed to initiate the jet. This will decrease the acceleration of the jet and the solution will undergo more stretching before it reaches the collector plate. The smaller diameter also prevents the solution from blocking the opening and this might be due to the fact that the solution is less exposed to the atmosphere.

The diameter cannot be too small; otherwise the solution cannot be drawn from the tip of the needle [48].

Feed rate

For a stable Taylor cone to be formed the process requires a certain voltage and for a certain voltage there is a certain feed rate to produce a stable Taylor cone. The amount of solution that is available to be electrospun is determined by the feed rate. The fibre diameter usually increases with an increase in the feed rate; this can be explained by the fact that there is now more solution that needs to be drawn away from the needle tip. The increase of fibre diameter occurs only up to a certain point. If the feed rate equals the rate at which the solution is taken by die electrospinning jet, an increase in feed rate will cause an increase in the charges. This implies that the solution will get stretched more and thus a smaller diameter fibre will be obtained.

A high feed rate may also lead to a situation where fibres fuse together. When there is a high feed rate, more solution needs to get drawn from the tip of the needle and the jet will take a longer time to dry. This means that all the solvent might not be evaporated by the time the fibre reaches the collector plate and this may cause the fibres to fuse together. At a lower feed rate the solvent will have more time to evaporate [48].

Voltage

The applied voltage will initiate the electrospinning process. This is done by the fact that it induces the electrostatic force on the solution by the charges that it gives to the solution. As soon as the electrostatic forces overcome the surface tension of the solution, the polymer will be electrospun.

For electrospinning DC voltage supply is mostly used, but AC can be used as well. The jet will be initiated by the charging of the solution. This usually takes place quite quickly and when using an AC supply, this will occur before the voltage alternates. In this case the jet contains positive and negative charges. This will reduce the bending instability of the jet, because bending instability is due to the columbic repulsive forces in the jet and the positive or negative charges will reduce these forces. Fibres produced with AC generally have a larger diameter compared to those spun with a DC supply (of the same voltage). However a thicker layer of fibres can be obtained by an AC supply. Since there will be fewer like charges that accumulate on the fibres, the fibres will pack close together.

The high voltage causes the formation of the Taylor cone at the tip of the needle. The stability of the jet is dependent on the amount of voltage that is applied. The higher the voltage the more solution gets drawn from the tip of the needle; in this case the Taylor cone might be smaller and less stable. If the feed rate is too slow while the voltage is too high, it may cause the Taylor cone to recede into the needle [48].

The high voltage also has an influence on the morphology of the fibres. It was found that with higher voltage there is more bead formation. During higher voltage the solution gets stretched more and with more stretching you would assume there would be less beading. One reason for the bead formation could be that the Taylor cone is not that stable or even has receded into the needle [48, 67].

The diameter of the fibre is also influenced by the voltage. Usually thinner fibres would be expected with a higher charge, because the solution gets stretched more. Also if the viscosity of the solution is low, the higher voltage may cause secondary jets and this reduces the fibre diameter [48]. However, it was also found that with high voltage the fibre diameter actually increases. This is said to be due to more polymer being ejected at a higher voltage, encouraging the formation of thicker fibres [48, 67]. With an increase in the voltage, the electrical field is increased and this should encourage the formation of thinner fibres, however Baumgarten [79] found that with an increase in the field strength, the fibre diameter goes through a minimum and at certain field strength, the fibre diameter becomes larger with an increase in field strength. This can be related to the feed rate of the polymer [46].

There have been some cases where a lower voltage leads to fibres with a smaller diameter. At a lower voltage the time of flight of the jet is longer and the jet gets more time to stretch and elongate.

The crystallinity of the fibres is also influenced by the amount of voltage that is applied. Polymer molecules can become more ordered due to the electrostatic field and therefore have greater crystallinity. Too high voltage can decrease the crystallinity. When the voltage increase the time of flight of the jet increases, this implies that the molecules will have less time to orientate themselves before they reach the collector plate, leading to less crystalline fibres[48].

The effect of the collector

For the electrospinning process to begin there must be an electrical field present between the source and the collector. The collector plate can be conductive or non-conductive, though conductive is usually preferred. Aluminium foil is a good example of a conductive collector, but because of the difficulty transferring the fibres from the foil, other collectors like conductive cloth or paper, rotating rod or wheel or liquid non-solvent can be used [48, 67]. The use of different collectors can have a great influence on the morphology and physical properties of the fibres and the type of collector will also influence the packing density of the fibres as well as the arrangement of the fibres [83, 84]. When a non-conductive collector is used, the charges of the jet will accumulate on the collector, this leads to fewer fibres on the collector. The more charges that are accumulated on the collector will cause repulsive forces and the fibres will not pack as closely together as on a conductive collector.

A honey-comb structure can form when using a non-conductive collector. As the density of the charge on the initial fibre mesh builds up, this will cause repulsion of the fibres forming after that and this will lead to the honey-comb structure. Since nanofibres are non-conductive, this may also occur when using a conductive collector. When a lot of fibres are collected and the mesh becomes quite thick, the accumulation of charges can also take place, causing a dimple-like structure on the fibre mesh [48].

Static or moving collectors also have an influence on the fibre morphology. A rotating collector will produce aligned fibres but also drier fibres since the rotating collector gives the solvent more time to evaporate. This is especially useful when using a conductive solvent with a high boiling point like DMF [48, 67]. The rotation speeds also has an influence on the collection. At lower speeds, the fibres tend to be collected randomly although still aligned. When the speed increases a centrifugal force develops near the boundary of the drum, this elongates the fibres that are collected. When the rotational speed is too high, fibres will tend to break up and non-continuous fibres are formed [45, 83]. Edwards *et al* [85]. found that with a collector speed slower than the spinning rate, the fibres will only be partially aligned. At even higher speeds, more crystalline fibres will be obtained, but at certain threshold the fibres will start to deform and a drop in crystallinity will be seen. Konghlang *et al* [86]. found that by varying the rotating collector's speed they could influence crystal morphology and molecular orientation.

When using a porous collector it was found that the fibres also seem to have a lower packing density. With a smooth surface you may get the accumulation of solvents around the fibres. When using a porous collector the solvent will evaporate more quickly because of the higher surface area. When the fibres dry faster, charge will build up on the fibres and that then will repulse the next fibres to pack closely. On a smooth surface the solvent will cause the charges to be lead away to the conductor [48]. Acharya *et al* [87]. did some work by using a dual electric field. They could control the orientation of the fibres by applying a secondary electric field perpendicular to the primary field.

Distance between the tip and the collector

The electrospinning process depends strongly on the time of flight of the fibres as well as the strength of the electric field. Both these factors are influenced by the distance between the tip of the needle and the collector plate. When the distance is decreased, the jet will have a shorter distance to travel and because the electric field now also increase, the jet will accelerate faster. This might not give the solvent enough time to evaporate and this may lead to the fibres merging and forming a connected mesh [48, 67].

The morphology of the fibres can also be affected by the distance between tip and collector. Beads may be observed when using a shorter distance. When the distance decreases the electric field strength increases. When the field strength is too high it may lead to greater instability of the jet and this may cause the formation of beads. The distance can be set to achieve optimal field strength and then bead formation may not occur [48, 67-71].

The fibre diameter has also found to decrease with an increase in the distance. When the distance is longer, the jet can be stretched and elongate more, leading to a smaller fibre diameter. However the distance become too large, the fibre diameter might increase due to the fact the electrical field strength is weaker and no sufficient stretching and elongations can take place [48].

The shape of the fibre can also be influenced by the distance. It has been found that with shorter distances, flatter. More ribbon-like fibres are produced and as the distance increases, the more rounded the fibres become [48, 67].

Temperature of the solution

The higher the temperature of the solution the less viscous the solution will be and the better the solvent will evaporate. Literature also indicates that certain polymers produce a more uniform fibre diameter when spun at a higher temperature. The lower viscosity of the solution allows more equal stretching of the solution. Higher temperature may also lead to thinner fibre diameter. When the solution is less viscous and the polymer molecules more mobile, the Coulombic forces can stretch the solution more, resulting in thinner fibres [48, 67]. It has to be noted though, that functionality on

some molecules could be affected by the higher temperature, like when working with biological molecules [48].

Ambient parameters

This is the effect of the surroundings on the electrospinning process. This area has not yet been thoroughly investigated.

Humidity and temperature

Humidity and the temperature of the atmosphere surrounding the electrospinning setup can have an influence on the fibre morphology. With an increase in temperature the solvent evaporation increases and the viscosity of the solution decreases. Both these factors will greatly influence the fibre morphology [88]. At higher temperature smaller fibres may be obtained, this was in fact described by Supaphol *et al* [89]. with polyamide-6 fibres. They explained it by concluding that the increase in temperature expanded the polymer molecules so the degree of chain entanglements reduced, leading to lower viscosity. The lower viscosity will lead to lower viscoelastic forces to counter the Coulombic stretching force, therefore the material will be stretched more and thinner fibres are obtained. Wang *et al* [90]. found that with an increase in temperature of a polyacrylonitrile/DMF solution, the solution viscosity and surface tension decreases, but there is an increase in the solution conductivity and thinner fibres were formed. When the humidity is high water may condense on the surface of the fibre and this may cause pores on the surface of the fibre [48]. These were seen when using polystyrene, polycarbonate and poly(methyl methacrylate) [59, 91]. As the humidity increases the size of the pores increase as well, and as they get larger they may combine, forming larger structures on the fibre [48]. Casper *et al* [59]. found that when using polystyrene, higher humidity leads to increases in the pore diameter and pore size distribution. With atomic force microscopy it was proven that the depth of the pores also increase with an increase in humidity but only up to a certain point. The water vapour usually condenses on the surface when the surface of the jet is cooled by the rapid evaporation of the solvent. When both the solvent and the water evaporate eventually pores are formed [48, 59].

When looking at the influence on electrostatic charges, it was found that at a higher humidity there were no charges in the particles, but as the humidity decreased, the amount of charges on the particles increased.

The rate of the evaporation of the solvent is also influenced by the humidity. In very low humidity the solvent will evaporate very quickly and the solvent may evaporate quicker than the rate at which the solvent is removed from the tip of the needle, causing that after a few minutes the needle might be blocked and the electrospinning process will stop. At higher humidity the solvent evaporate rate will decrease and the fibre will have longer time elongate, leading to thinner fibres

[92]. The humidity effect has also been shown to have an influence on the melting and crystallinity of certain polymer fibres [93].

Pressure

Low pressure usually does not have a positive influence on the electrospinning process. At pressure below atmospheric pressure, the solution just flows out the needle and the initiation of the jet will not be stable. The further the pressure the decreases, the solution will start to bubble at the tip of the needle. Then at very low pressure, the electrical charges will be directly discharged, making electrospinning impossible [48].

The electrospinning process can also take place in a vacuum. A few scientists have reported that fibres with better properties and morphology are obtained in a vacuum. For example, Rangkupan and Reneker obtained much thinner fibres when melt-spinning polypropylene in a vacuum [52].

Type of atmosphere

By changing the atmosphere in which the electrospinning takes place, the electrospinning process may be influenced. Under high electrostatic field, gases will behave differently depending on the breakdown voltage of the gas. A gas with a high break-down voltage, like Freon®-12, will produce thicker fibres compared to the same solution spun in an air atmosphere. If helium is used as atmosphere, no electrospinning is possible, due to the breakdown of the gas under the electrostatic field [48].

The above-mentioned factors and how they influence the electrospinning process can usually be applied to melt electrospinning as well. There are some differences though.

The biggest difference is that the reservoir, in which the polymer solution is kept, should be heated constantly to keep the solution in the molten state.

The polymer solution may be more viscous depending on the temperature of the solution; therefore a higher voltage is required for the initiation of the jet. Increasing the field strength produces smaller fibres.

With melt electrospinning the distance between the tip of the needle and the collector is also much smaller, more in the range of 2 cm.

2.3.1.2. Solution electrospinning of polyolefins

Not a lot of work has been published on the solution electrospinning of polyolefins. One of the main reasons for this may be the difficulty of dissolving polyolefins in a solvent that will be suitable for electrospinning. Polyolefins usually dissolve in nonpolar solvents, which have a low dielectric constant and that leads to poor conductivity [94]. Polyolefins also need to be dissolved at high

temperatures and will only stay in solution if kept at a high temperature. This causes a lot of problems when using a conventional setup and therefore acquires that the setup should be altered. Larrondo and Manley [95-97] have spun polyethylene out of melt and in a paraffin solution at 100 °C. One of the main problems of this was that the paraffin had to be removed after spinning. This could only be done by washing the fibres with xylene.

Givens *et al* [94]. used *p*-xylene to electrospin linear low density polyethylene. *P*-xylene will evaporate during the electrospinning process, so no post treatment will be needed. The dielectric constant of *p*-xylene however is still low and the solution needed to be at a high temperature. Givens overcame this problem by adding a salt, *tert*-butylammonium, and altering the electrospinning setup. They used an infrared emitter to keep the spinning setup at 110 °C [94]. The fibre diameter was in the micrometre range.

Rabolt *et al* [98, 99]. used a solvent system comprising of three different solvents, cyclohexane, DMF and acetone. They reported that they were able to electrospin polyolefins at room temperature.

2.4 Polymer composites

The word composite refers to two or more materials that has been put together to form one material. In the case of polymer composites it is usually a polymer that contains another material. This material usually enhances the properties of the polymer. Making nanocomposites is one of the subjects that have been studied extensively the past few years. The reason for this is that you can form a new material with two different materials and the composites will have the properties of the two different materials. So by forming composites we can formulate materials with distinct properties.

2.4.1. Particular reinforcement

To use particles as a reinforcing material is probably the technique that is used the most. Particles mostly enhance the yield strength and the elastic modulus. When these particles are too big, they will scatter light and if a transparent material is required, that will influence the appearance of the material. This is one of the reasons why nanoparticles are preferred in a variety of applications. One of the problems with nanoparticles, though, is the fact they tend to agglomerate when higher volumes of nanoparticles are used. When the particles agglomerate or do not disperse uniformly, it can cause the material to have weaker mechanical properties than the neat material [100]. Several studies have focussed on producing a better method to disperse these nanoparticles in a material, with as little agglomeration as possible.

2.4.2. Platelets

Platelet fillers usual exist as a layered material in their natural state. To use these fillers in a material, the layers should be separated and well disperse throughout the material. The separation of these fillers can be described in three ways. In the first instance, we have the miscible state; here the spacing between the layers of the particle is very small. In the (second) intercalated state there is a space between the different layers. There are two ways of preparing intercalated polymer/clay composites; melt – intercalation and solution polymerization intercalation. Melt – intercalation is the preferred method, since it does not require solvents in which both polymer and clay can be dissolved in [101]. The third state is the exfoliated state where the layers of the platelets are totally separated [100].

The most popular platelet fillers are graphite and clay. A lot of research has been done on polymer-clay composites. These nanocomposites have great advantages like improved thermal stability, stiffness, strength and toughness over the unfilled matrix polymer.. The clay is usually quite hydrophilic and the polymer usually hydrophobic. Because of these differences, the clay tends to agglomerate inside the matrix. To overcome this, the surface of the clay can be modified [100]. Lui *et al* [102]. added clay particles to electrospun fibres, thereby increasing the thermal and mechanical properties of these fibres.

When looking at graphite fillers, one of the main advantages is the increase in the conductivity of the material when adding these platelets to the polymer material [100].

2.4.3. Fibrous materials

Fibres are frequently used in polymers as reinforcement. In early applications, microfibres have been used. Recently research has been focussed on using nanofibres as reinforcement. Nanofibres are mainly preferred due to the fact that they possess even better mechanical properties than microfibres. Incorporating them in polymer materials will enhance the properties of these composites [45]. Neppalli *et al* [103]. prepared composites of polycaprolactone reinforced with electrospun nylon fibres. The stiffness of the material as well as the ductility was increased. This was different to what was found when using other fillers. Kim *et al* [104]. used poly(benzimidazole) as reinforcement in epoxy and rubber matrices. The Young's modulus and fracture toughness of the epoxy were increased by the addition of nanofibres. In the rubber matrix, the fibres increased the Young's modulus of the rubber. In other research, by Bergshoef *et al* [105]., Nylon 4, 6 fibres were incorporated in an epoxy matrix. By this means they were able to produce a transparent material and the fibres had a reinforcing effect on the epoxy. Recently Tang *et al* [106]. used cellulose fibres to reinforce poly(vinyl alcohol). The fibres enhanced the Young's modulus by 600 % compared to the pure polymer and the visible light transmittance for the composites was 75 %.

Swart *et al* [107]. prepared silicone laminated composites by distributing non-woven fibres of poly(methyl methacrylate-*graft*-poly(dimethyl siloxane) inside a silicone matrix. They found that the strength, stiffness and surprisingly the toughness of the material increased when adding the fibres. Bayley *et al* [108]. used polyacrylonitrile-*graft*-poly(dimethyl siloxane) fibres as reinforcement inside a silicone matrix. Both non-woven and aligned fibres were used as reinforcement and the aligned fibres showed the greatest increase in the stiffness of the material. What was interesting was that the unaligned fibres showed an immense increase in the extendibility of the material compared to the composite filled with aligned fibres and the unfilled composite. They ascribed this to a complex failure mechanism

There are still many areas of research regarding the use of nanofibres as reinforcement that are essentially wide open. For example, the bonding of the nanofibres to the surface of the polymer and also the effect the nanofibres have on the mechanical properties. In addition, there is also the effect of the arrangement of the fibres in the composites, the use of aligned or unaligned fibres etc. have on the properties of the composites [45].

2.4.4. Carbon nanotubes

Carbon nanotubes are often favoured as nanofillers in materials and more specifically polymers. They have excellent conductivity as well as reinforcement characteristics. Carbon nanotubes can be used in many applications, varying from conductive films, catalysts and catalyst supports to sensors. Carbon exists in three solid phase allotropic forms: diamond, graphite and fullerenes. In the diamond form, each carbon atom is sp^3 hybridized and bonded to four other carbon atoms and arranged in a tetrahedral form. These sp^3 hybridized bonds are responsible for diamond's electrically insulating properties. In graphite the carbon atoms are sp^2 hybridized and they are bound together in a hexagonal network. Layered planar sheets of these carbon atoms forms graphite. The carbon atoms are only bonded to 3 other atoms. Because of this graphite is conductive, since the free electrons in the unhybridized *p* orbital can move around from one *p* orbital to another and they form a delocalised π network. The last form is fullerenes; they involve cylindrical molecules made up out of carbon sp^2 hybridized atoms [109, 110]. In 1991 Iijima discussed the preparation of a new type of carbon structure in the form of needle-like tubes. He grew graphite carbon needles on a carbon electrode. They observed on electron microscopy that each needle was made up of coaxial tubes of graphite sheets which varied from 2 to 50 sheets. The carbon-atom hexagons are arranged in a helical form around the axis of the needle [111]. To describe it in a less complex way, carbon nanotubes (CNT) comprises of graphite sheets that are rolled up in a cylinder shape. This cylindrical structure is seamless and hollow. They consist of hexagonal carbon networks and are usually capped on one or both ends by a hemispherical fullerene

molecule [112-114]. The bonding in carbon nanotubes is sp^2. Due to the fact that it is in cylindrical form, the three σ bonds are marginally out of the plane and the π orbital will be delocalized outside the tube [110]. The length of the CNT is usually in the micrometer range and the diameter up to 100 nm. They are very complex because of the formation of bundles and these bundles become entangled forming a network [112].

CNT can be used in polymers as nanofillers because of their excellent properties. These properties include a large aspect ratio, high flexibility, low mass density and most important excellent electrical and conductive properties [115-118]. These graphite structures have carbon atoms with sp^2 hybridisation and therefore are covalently bonded [111, 113]. Due to this covalent bonding the surface area to volume ratio is very high and they have good tensile strength and a high elastic modulus. Their flexibility can be attributed to the fact that they can deform under large stress without breaking [113]. They can have a large number of different chiralities and helicities [109].

Ajayan *et al*[119]. was the first person to use CNT in a polymer as a nanofiller.

Before looking at CNT as carbon fillers, it is best to look at the different type of CNT available as well as their properties.

2.4.4.1. Single-walled carbon nanotubes (SWCNT)

A single sheet of graphite is wrapped into a tubular form to create SWCNT. The edges of the sheet are fused and form a seamless tube [114]. As described earlier each carbon atom is covalently bonded to three other carbon atoms next to it [116]. The structural parameters of SWCNT will determine whether it is semi-conducting or metallic.

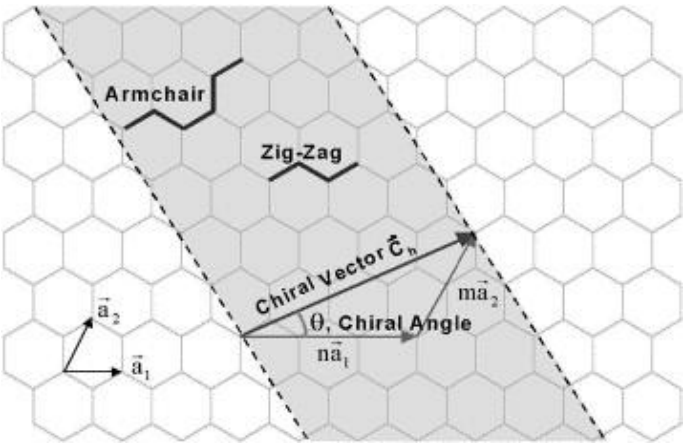

Figure 2.5 Schematic drawing to show the way in which a hexagonal graphite sheet will be rolled, creating a carbon nanotube [120]

The tube chirality is use to described the way in which the sheets are rolled. The chirality is changed by the way in which the sheets are rolled up. The tube chirality is defined by the equation

$\vec{C}_h = n\vec{a_1} + m\vec{a_2}$, where *n* and *m* are the number of steps along the unit vectors of the hexagonal lattice and $\vec{a_1}$ and $\vec{a_2}$ are the unit vectors [114, 116, 118]. The chiral angle is determined by the following equation

$$\text{chiral angle } \theta = \tan^{-1}\left[\sqrt{3}\left(\frac{n}{2m+n}\right)\right]$$

The chiral angle is used to divide the nanotubes into three types: zigzag, where *m* = 0 and $\theta = 0°$ and arm chair where *n* = *m* and $\theta = 30°$, and all the other types, which are specified as chiral [109]. The relationship between *n* and *m* determines their conductive properties. Arm chair SWCNT are always metallic and they have a band gap of 0 eV. Zigzag tubes can either be metallic or semiconducting. If the SWCNT have *n* – *m* = 3 or a multiple of 3, they are semi-metallic and have band gap of a few meV. When SWCNT have *n* – *m* not equal to 3 or a multiple of 3, they are semi-conducting with a band gap of 0.5 – 1 eV [109, 116, 118]. When looking at the probable nanotube conformations from a statistical point of view, it can be seen that one-third of the possible conformations are metallic and two-thirds, conducting. Up and till now, only nanotubes with mixed chirality have been produced [114].

The diameter of the nanotubes can be calculated by the following equation

$$d_t = \sqrt{3}\left[a_{c\text{-}c}(m^2 + mn + n^2)^{1/2}/\pi\right] = C_h/\pi$$

Where C_h is the length of the chiral vector and $a_{c\text{-}c}$ is the bond length of C-C [109, 121].

2.4.4.2. Multi-walled carbon nanotubes (MWCNT)

These nanotubes were the first nanotubes to be discovered by Iijima. They observed nanotubes that had between 2 - 20 layers. MWCNT were also more used than SWCNT and the first applications involved MWCNT being used. The reason for this was that they were far easier to manufacture in industrial scale [109] than SWCNT. MWCNT are layers of graphite sheets that have been rolled-up. They have a spacing of about 0.34 nm between them, which correlates to the inter-layer spacing of graphite, which is 0.335 nm. When looking at tube chirality for MWCNT, they have a multiple tube chiralities because the different layers will all have different chiralities and that makes their properties very hard to predict [116, 118]. The typical MWCNT has an outer diameter smaller than 100 nm and the inner diameter is usually greater than 2 nm [110]. Double-wall carbon nanotubes (DWCNT) do also exits. In this case the nanotubes are made up out of two graphite sheets, rolled into a cylinder. They usually have higher toughness than MWCNT because they are smaller and also have a higher flexural modulus than SWCNT because they have two walls instead of one [118]. When looking at the electronic structure it was found that the current flows only

through tube on the outside of MWCNT. There is not much interlayer electronic coupling and they can alternate between metallic or semi-conducting. Though there is not much coupling between the different layers, it cannot be totally ignored. The coupling between the different tubes can affect the band structure considerably[116].

2.4.4.3. Production of carbon nanotubes

Carbon nanotubes are mostly produced by three methods.

Arc discharge

The synthesis of carbon nanotubes, more specifically MWCNT, was first observed by Iijima [111] using this method. Now SWCNT are also produced by this method [109, 122]. The setup for this method consists out of two highly pure graphite rods, which are the anode and cathode. They are usually between 5 to 20 mm in diameter [109]. The anode will act as the carbon source and will get smaller as it gets consumed. An arc will be produced in the gap between the two electrodes. Under a helium atmosphere, the two rods are brought together and a high voltage is applied till a stable arc is reached. A gap between the anode and cathode is kept by moving the anode. The material deposit on the bigger cathode and consists out of an outer shell that is made up out of fused material and an inner core, which is softer and contains the nanotubes. Soot and fullerenes are also found on the cathode [109, 120-122]. When making SWCNT the electrodes are usually fixed with some metallic catalyst particles [120]. The most widely used catalyst is a Y:Ni mixture and this produces a 90% yield of SWCNT with a diameter of between 1.2 – 1.4 nm [109]. This process usually takes place at temperatures between 2 000 – 3 000 °C. The metals then evaporate with the carbon and agglomerate into bunches. This acts as the base from which the nanotubes are grown [114]. The nanotubes are usually found in the soot that is generated. This technique do require that the nanotubes must be purified before use, this is done by heating the tubes in air till 420 °C and then washing it in a low concentration of HCl [109, 114, 120, 122].

These days the most common environment to grow the nanotubes in is a mixture of Ar and He. The ratio of these two gases determines the diameter of the SWCNT. When using more Ar, SWCNT with smaller diameter are obtained. The pressure of the gas also determines the percentage yield [109].

This method is not ideal for the formation of aligned CNT, but the growth temperature is much higher, resulting in more perfect and crystalline CNT and a much higher yield [122].

Laser ablation

This technique was used for the production of fullerenes and was adapted for the production of SWCNT [123, 124]. A graphite target, that consists out of graphite and 1.2% cobalt/nickel, is put in an oven at about 1 200 °C, in an inert atmosphere of Ar or He and then the target is vaporized by a

laser [109, 120]. With the vaporized graphite, nano-sized metal particles are also formed. They act as the catalyst which induces the growth of the SWCNT [109, 114, 122]. Unfortunately many by-products are formed as well, which includes amorphous and graphitic carbon, fulleroid spheres and small fullerenes. This means that the nanotubes must undergo extensive purification afterwards [109, 114, 120]. The nanotubes and the by-products condenses on a cold surface which is located downstream from the graphite target. The yields are usually between 20 – 80 % for SWCNT and the diameter between 1.0 – 1.6 nm [109]. The advantages of this method are that the quality of SWCNT that are produced is quite high and there is good control over the diameter of the SWCNT [122, 123].

Chemical vapour deposition (CVD)

The previous two techniques produced very crystalline nanotubes, because of the high temperatures at which they are produced [114], but in both the previous two methods, the amount of sample that can be prepared was very limited. This was due to the fact that it depends on the graphite source, which was the anode or target for the two different techniques. Also with these two techniques it was necessary to purify the sample to get rid of all the unwanted by-products [114, 120]. Another disadvantage was that when the nanotubes were purified they were dispersed in a solvent and then put on the material by dipping, spraying etc. This method is not appropriate when producing nanotubes for use in microelectronic systems [114].

Because of these disadvantages, CVD was developed. The first (defective) MWCNT was produced by this method in 1993 by Endo *et al* [125]. In CVD a carbon-containing gas (usually methane or acetylene) is decomposed to form the nanotubes. The gas is flowed over nanoparticles that are made of transition metal. The carbon then reacts with these particles and then the nanotube grows from this [109, 114, 120, 122]. This reaction can take place between 500 – 1 200 °C [109]. More nanotubes can be produced by this method, since the carbon source is flowing gas that can be replaced the whole time. Since it is only gas that decomposes the purity of the nanotubes is much higher and usually limited purification is necessary. This technique also allows the control to produce carbon nanotubes with a certain diameter and length, since the catalyst particle can be changed [114, 120], for example individual aligned SWCNT can be produced. The SWCNT produced by this method usually have a better atomic quality and the yield is quite high, it can exceed 99%[109]. One of the disadvantages of this technique compared with the previous two is that the arc discharge and laser ablation techniques produce CNT with fewer defects than those produced by CVD. This can be explained due to the fact that the growth of the nanotubes takes place at much higher temperatures with the previous mentioned techniques and therefore better annealing takes place in the tubular sheets [110]. Straight MWCNT are produced by the higher temperature methods, whereas with CVD the MWCNT are usually bent [110]. Another disadvantage is that the CNT produced with this method is not as crystalline [122]. Despite the drawbacks, the advantages

outweigh the disadvantages, and CVD is usually the preferred method for the production of CNT [109].

2.4.4.4. The use of carbon nanotubes in composites

Carbon nanotubes have a diameter of only a few nanometers and lengths of a few hundred nanometres. These characteristics lead to CNT having a very high aspect ratio. They are conducting and have a high elastic modulus. Al these factors contribute to improving the mechanical and thermal stability properties of the polymer when these CNT are added in a composite [126, 127].

One of the key aspects when using them in a polymer matrix, is the uniform dispersion of the CNT in the polymer matrix and the adhesion between the CNT and the polymer [126, 127].

Functionalization of carbon nanotubes

Carbon nanotubes are insoluble. For CNT to be used in polymer materials, better solubility and dispersion is needed. There are great cohesive forces present in CNT and therefore we will find that CNT usually occur in the form of bundles. Because of the formation of these bundles they have limited solubility and cannot be very well dispersed throughout a polymer matrix. It is also found that when dispersing pristine CNT in a matrix, they tend to agglomerate, which will lead to decreasing the mechanical strength of the composites. The CNT also do not bind to the matrix, so when put under stress, the CNT usually gets pulled out of the matrix. These bundles need to be separated and then dispersed uniformly throughout the matrix. One way of doing this is by functionalizing the CNT. The modification of the surface of the nanotubes increases their interactions with the polymer matrix [100, 109]. By functionalizing the CNT, they can also be separated by type. For example, the semiconducting SWCNT will not react as fast as the metallic SWCNT [109].

The nanotubes are usually either functionalized by irradiation with ions or electrons or by chemical methods [100].

We find both non-covalent and covalent functionalization. In non-covalent functionalization the CNT is usually wrapped in a surfactant [109].

When using chemical methods, chemical bonds are attached to the side walls or to the ends of the nanotubes. The nanotubes caps are highly reactive because of their curvature and they can react with strong acids[100].

The incorporation of carbon nanotubes in polymers

CNT has been incorporated in a few polymers, enhancing the conductive and the mechanical properties of these materials. The main factors that influences the performance of the CNT in the composite is the dispersion and the alignment of the CNT.

The nanotubes tend to agglomerate due to van der Waals bonding. When looking at the different types of nanotubes, SWCNT tends to cluster and MWCNT are tangled.

For CNT to be aligned is very difficult because of their size. The better we can control their orientation in a material, the better they will perform inside the matrix[100].

The formation of polymer/CNT composites can be achieved by various methods, which include extrusion, injection moulding, solvent casting and melt mixing. All of these techniques should disperse the CNT and avoid agglomeration, enhance filler alignment and improve the bonding of the CNT and the polymer so that better load transfer can take place between the two surfaces. It should be avoided to decrease the aspect ratio or terminate their integrity[113, 128]. The structure of the CNT in the polymer will also determine its properties, for example for high strength well aligned CNT is necessary[128].

There are a few methods available incorporating CNT into polymers.

Through solution blending

This is the most common method for preparing polymer/nanotube composites. The polymer and the nanotubes are mixed together in a solvent. The solvent is evaporated to leave a composite film. When dissolving the nanotubes in the solvent, they will disperse and will not aggregate, so that when the solvent is evaporated the nanotubes will be well dispersed within the film. The best method of solution blending is by sonicating the solution. The most effective way of doing this is by adding the nanotubes to solvent, sonicating it and then adding the polymer and sonicating the solution again or by using variations of this method [129-131]. The mechanical properties of these materials were mostly improved, a greater improvement was found above the Tg of the materials, indicating that reinforcement for softer material was greater [130].

Through melting mixing

This method is ideal for polymers that are insoluble and especially for thermoplastic polymers. The polymer will be heated to above its T_g or melting temperature and then the CNT will be mixed by either shear mixing, injection moulding or compression moulding. There are some drawbacks to this technique. The carbon nanotubes will increase the viscosity of the material and, for example, when extruding this material, the polymer might degrade due to higher shear rates required with the increase of viscosity [129]. Potschke *et al* [132]. found that the CNT were well distributed with this method and the composites were reinforced and conductive. Polypropylene (PP)/CNT composites have also been prepared by Banbury-type processing. It was found that there was no agglomeration of the nanotubes inside the PP. The CNT enhanced thermal stability of the PP, but the tensile strength was unaffected. This is attributed to the matrix inability to crystallize further under stress, due to the constraint caused by the fibre dispersion [133]. Another method used is to first disperse the nanotubes through solution and then melt press the composite. The composite is

then broken up into pieces and melted again and after repeating it a few times the composite was extruded in fibre form. It was found that the dispersion improved after each melting cycle [129, 134].

Using thermosets and films

Mostly for this method the CNT gets dispersed in an epoxy prepolymer by sonication. Afterwards a hardener is added and the nanotubes are cured within the epoxy. Variations on this method include dispersing the CNT in solvents or in solvent with a block-copolymer [135], sonicating it and then adding the epoxy before sonicating it again. Afterwards the solvent is evaporated and the hardener is added. Lastly the epoxy goes into an oven to get cured. The dispersion of the CNT is quite good, but there might be some traces of the solvent left in the composite, and different solvents will influence the properties of the composite to differing degrees [129, 136].

By in-situ polymerization

The main advantages of this method are that it can be used for the production of composites from thermally unstable or insoluble polymers that cannot undergo melting or solution. The in-situ polymerization of a monomer takes place in the presence of CNT. The polymer gets grafted onto the nanotubes and then polymer composites are made from the resulting material. Not only do you get a high CNT loading, but this material will also interact very well with other polymers. One example of this was reported by Jia *et al* [137]. They in-situ polymerized methyl methacrylate (MMA) with 2,2'-azobisisobutyronitrile (AIBN) in the presence of CNT. The AIBN opens the π bonds of the CNT allowing it to take part in the polymerization. This method was also used by Kumar *et al*[138]. Other examples are reported as well [132, 139, 140]. Saeed *et al* [141]. prepared MWCNT/polycaprolactone nanocomposites through in-situ polymerization. They then electrospun these polymers and compared functionalized and unfunctionalized nanotubes with each other. It was found that as the carbon nanotube content increases, bead formation in the fibres increased as well.

Polymers have been used in many ways to disperse the nanotubes in a matrix. The nanotubes can either be covalently bound to the polymer, or they can be grafted onto the polymer either by grafting to or grafting from methods [142].

By incorporation into nanofibres

Electrospinning has become quite a popular technique to fabricate fibres that can be used in nanocomposites. Carbon nanotubes can be electrospun into nanofibres using a suitable polymer carrier, thereby providing a method to disperse the carbon nanotubes inside a polymer matrix [143]. This technique allows the CNT be aligned along a single axis without damaging the structure of the CNT [113]. The stretching of the jet in the electrostatic field will allow the alignment of the CNT inside the fibre. Huang *et al* [45]. explained it by saying that the conductivity mismatch between the CNT and the polymer causes dielectrophoretic forces which in combination with the high shear force of

the electrospinning will align the CNT along with fibre axis. Comparing this to when just simply embedding the CNT in the fibres, we find that the CNT do not agglomerate. This allows better bonding with the polymer, which in turn will cause a better aspect ratio and leads to better reinforcement [144]. Kim *et al* [144]. prepared carbon nanotubes/polycarbonate nanofibres to be used in polymer composites. They found that MWCNT were well aligned along the fibre axis. The load of stress will now be better transferred from the matrix to the MWCNT. The strain of break of the fibres is also enhanced because of the slippage of the individual nanotubes in the fibres. Bayley et al[108]. electrospun polyacrylonitrile-*graft*-poly(dimethyl siloxane) containing carbon nanotubes. The nanotubes were well aligned and distributed inside the fibre. These nanotubes containing fibres were then used as reinforcement inside a silicone matrix. The composites containing aligned fibres with carbon nanotubes showed an significant increase in the stiffness of the material.

Another example is the case of MWCNT electrospun with polyvinyl alcohol (PVA). The fibres were prepared by first functionalizing the MWCNT to create carboxyl groups on the nanotubes. The functionalized MWCNT were then reacted with poly(ethylene glycol) (PEG) in ethanol. The MWCNT with the PEG attached on the surface were then added to a solution of PVA and electrospun. The adding of the MWCNT to the fibre, greatly enhanced the conductivity of the fibres [145].

Sometimes adding the MWCNT can change the structure of the fibres. It was found that by adding MWCNT to a polyurethane (PU) solution and then electrospinning it, a web-like structure was found in between the fibres which were not seen in the pure PU fibres. The authors attributed this to strong secondary electrofields that is present during electrospinning between the MWCNT [146]. Mathew *et al* [147]. added 5 wt% MWCNT to poly(butylene terephthalate) in hexafluoroisopropanol. The morphology of the fibres changed by being broader and having a rougher surface due to some of the CNT on the surface of the fibres. The thermal stability of the fibres however was improved by 8-9 °C and the mechanical modulus enhanced. A broader fibre morphology was also found by Mazinani *et al* [148]., but fewer beads were observed when using CNT. The CNT also increased the crystallinity of the fibres and again the CNT enhanced the mechanical properties of the material.

The main problem with the incorporation of the CNT in the polymer fibres is that a well dispersed solution of CNT in the polymer solution is needed before electrospinning. Therefore surfactants or amphiphilic polymers (poly(vinyl pyrrolidone) or sodium dodecyl sulphate) will be added to the CNT dispersion [149]. This dispersion will be sonicated, to make sure the CNT are dispersed throughout the dispersion. The dispersion will then be mixed with the polymer solution. Mazinani *et al* [150]. added a copolymer (Styrene-butadiene-styrene) to their CNT/PS solution to enhance the dispersion of the CNT in the solution.

Some examples of gel spinning can also be found. Ruan *et al*[151]. demonstrated the increase in tensile properties of ultra-high molecular weight polyethylene fibres with CNT prepared by gel-spinning.

One of the aspects that should be taken note of is the sonication time. Sonication may cause the CNT to break up or to be damaged. Therefore there is an optimum sonication time, too short and the CNT will not be dispersed and too long, they will be damaged or break [152]. Better dispersion of the CNT could also be obtained by the ball milling technique, polymer wrapping or AC electrophoresis. These techniques will overcome the van der Waals forces between the nanotubes and prevent them from agglomerating. Another way of gaining better dispersion is by functionalizing the surface of the CNT [113].

Another method is to electrospin the polymer and then to simply immerse the fibres in a solvent containing the CNT. The nanotubes will then adsorb unto the surface of the fibres. Choi *et al*[143]. used nylon fibres that have been immersed in a solution of functionalized CNT to detect low molecular weight alcohol vapours.

2.5 References

1. Benavente, R.; Perena, J. M.; Bello, A.; Perez, E.; Locatelli, P.; Fan, Z.; Zucchi, D. *Polymer Bulletin (Berlin)* **1996,** 36 (2), 249-256.

2. Fan, Z.; Yasin, T.; Feng, L. *Journal of Polymer Science Part A: Polymer Chemistry* **2000,** 38 (23), 4299-4307.

3. Arnold, M.; Bornemann, S.; Köller, F.; Menke, T. J.; Kressler, J. *Macromolecular Chemistry and Physics* **1998,** 199 (12), 2647-2653.

4. Forlini, F.; Fan, Z.; Tritto, I.; Locatelli, P.; Sacchi, M. C. *Macromolecular Chemistry and Physics* **1997,** 198 (8), 2397-2408.

5. Shiono, T.; Azad, S. M.; Ikeda, T. *Macromolecules* **1999,** 32 (18), 5723-5727.

6. Arnold, M.; Henschke, O.; Knorr, J. *Macromolecular Chemistry and Physics* **1996,** 197 (2), 563-573.

7. De Rosa, C.; Talarico, G.; Caporaso, L.; Auriemma, F.; Galimberti, M.; Fusco, O. *Macromolecules* **1998,** 31 (26), 9109-9115.

8. Graef, S. M.; Wahner, U. M.; Van Reenen, A. J.; Brüll, R.; Sanderson, R. D.; Pasch, H. *Journal of Polymer Science Part A: Polymer Chemistry* **2002,** 40 (1), 128-140.

9. Van Reenen, A. J.; Brull, R.; Wahner, U. M.; Raubenheimer, H. G.; Sanderson, R. D.; Pasch, H. *Journal of Polymer Science Part A: Polymer Chemistry* **2000,** 38 (22), 4110-4118.

10. Hamielec, A. E.; Soares, J. B. P. *Progress in Polymer Science* **1996,** 21 (4), 651-706.

11. Kashiwa, N.; Imuta, J. *Catalalysis Survey in Japan* **1997,** 1 (1), 125-142.

12. Reddy, S. S.; Sivaram, S. *Progress in Polymer Science* **1995,** 20 (2), 309-367.

13. Kaminsky, W. *CatalalysisToday* **2000,** 62 (1), 23-34.

14. Huang, J.; Rempel, G. L. *Progress in Polymer Science* **1995,** 20 (3), 459-526.

15. Sugano, T.; Matsubara, K.; Fujita, T.; Takahashi, T. *Journal of Molecular Catalysis* **1993,** 82 (1), 93-101.

16. Soga, K.; Shiono, T. *Progress in Polymer Science* **1997,** 22 (7), 1503-1546.

17. Kaminsky, W.; Laban, A. *Applid Catalysis A* **2001,** 222 (1-2), 47-61.

18. Kroschwitz, J. I. In *Encyclopedia of Polymer Science and Technology.* 2003; Vol. 7, pp 35-103.

19. Forlini, F.; Tritto, I.; Locatelli, P.; Sacchi, M. C.; Piemontesi, F. *Macromolecular Chemistry and Physics* **2000,** 201 (4), 401-408.

20. Kim, I. *Macromolecular Rapid Communications* **1998,** 19 (6), 299-303.

21. Schneider, M. J.; Muelhaupt, R. *Journal of Molecular catalysis A: Chemistry* **1995,** 101 (1), 11-16.

22. Jüngling, S.; Mülhaupt, R.; Fischer, D.; Langhauser, F. *Die Angewandte Makromolekulare Chemie* **1995,** 229 (1), 93-112.

23. Imanishi, Y.; Naga, N. *Progress in Polymer Science* **2001,** 26 , 1147-1198.

24. Brüll, R.; Pasch, H.; Raubenheimer, H. G.; Sanderson, R.; van Reenen, A. J.; Wahner, U. M. *Macromolecular Chemistry and Physics* **2001,** 202 (8), 1281-1288.

25. Ogata, N.; Lu, G.; Iwata, T.; Yamaguchi, S.; Nakane, K.; Ogihara, T. *Journal of Applied Polymer Science* **2007,** 104 (2), 1368-1375.

26. Kroschwitz, J. I. In *Encyclopedia of Polymer Science and Technology.* John Wiley & Sons, Inc.: United States of America, 2003; Vol. 5, pp 230-233.

27. Park, S. H.; Lee, G. J.; Im, S. S.; Suh, K. D. *Polymer Engineering and Science* **1998,** 38 (9), 1420-1425.

28. Faisant, J. B.; Aït-Kadi, A.; Bousmina, M.; Descheˆnes, L. *Polymer* **1998,** 39 (3), 533-545.

29. Ait-Kadi, A.; Bousmina, M.; Yousefi, A. A.; Mighri, F. *Polymer Engineering and Science* **2007,** 47 (7), 1114-1121.

30. Cava, D.; Cabedo, L.; Gimenez, E.; Gavara, R.; Lagaron, J. M. *Polymer Testing* **2006,** 25 (2), 254-261.

31. Fonseca, C.; Perena, J. M.; Benavente, R.; Cerrada, M. L.; Bello, A.; Perez, E. *Polymer* **1995,** 36 (9), 1887-1892.

32. Ruiz, C.; Sanchez-Chaves, M.; Cerrada, M. L.; Fernandez-Garcia, M. *Journal of Polymer Science, Part A: Polymer Chemistry* **2008,** 46 (21), 7238-7248.

33. Matsumoto, T.; Nakamae, K.; Ochiumi, T.; Horie, S. *Journal of Membrane Science* **1981,** 9 (1-2), 109-119.

34. Sakurada, Y.; Sueoka, A.; Kawahashi, M. *Polymer Journal* **1987,** 19 (5), 501-513.

35. Young, T.; Hu, W. *Biomaterials* **2003,** 24 (8), 1477-1486.

36. Young, T.; Lai, J.; You, W.; Cheng, L. *Journal of Membrane Science* **1997,** 128 (1), 55-65.

37. Young, T.; Wang, D.; Hsieh, C.; Chen, L. *Journal of Membrane Science* **1998,** 146 (2), 169-178.

38. Fernandez, M. J.; Fernandez, M. D. *Polymer* **2005,** 46 (5), 1473-1483.

39. Sánchez-Chaves, M.; Ruiz, C.; Cerrada, M. L.; Fernández-García, M. *Polymer* **2008,** 49 (12), 2801-2807.

40. Fallahi, D.; Rafizadeh, M.; Mohammadi, N.; Vahidi, B. *e-Polymers.* **2008,** No pp. given.

41. Cerrada, M. L.; Sanchez-Chaves, M.; Ruiz, C.; Fernandez-Garcia, M. *Biomacromolecules* **2009,** 10 (7), 1828-1837.

42. Mark, H. F.; Atlas, S. M.; Cernia, E. In *Man-made fibers (Science and technology).* Man-made fibers (Science and technology); John Wiley & Sons: United States of America, 1967; Vol. 1, pp 432.

43. Fertala, A.; Han, W. B.; Ko, F. K. *Journal of Biomedical Materials Research* **2001,** 57 (1), 48-58.

44. Sawicka, K. M.; Gouma, P. *Journal of Nanoparticle Research* **2006,** 8 , 769-781.

45. Huang, Z. -.; Zhang, Y. -.; Kotaki, M.; Ramakrishma, S. *Composites Science and Technology* **2003,** 63 , 2223-2253.

46. Buchko, C. J.; Chen, L. C.; Shen, Y.; Martin, D. C. *Polymer* **1999,** 40 (26), 7397-7407.

47. Bognitzki, M.; Hou, H.; Ishaque, M.; Frese, T.; Hellwig, M.; Schwarte, C.; Schaper, A.; Wendorff, J. H.; Greiner, A. *Advanced Materials* **2000,** 12 (9), 637-640.

48. Ramakriskna, S.; Fujihara, K.; Teo, W. E.; Lim, T. C.; Ma, Z. *An Introduction to Electrospinning and Nanofibers;* World Scientific Publishing Co. Pte. Ltd: Singapore, 2005; .

49. Zeng, J.; Xu, X.; Chen, X.; Liang, Q.; Bian, X.; Yang, L.; Jing, X. *Journal of Controlled Release* **2003,** 92 (3), 227-231.

50. Kenawy, E.; Layman, J. M.; Watkins, J. R.; Bowlin, G. L.; Matthews, J. A.; Simpson, D. G.; Wnek, G. E. *Biomaterials* **2003,** 24 (6), 907-913.

51. Garg, K.; Bowlin, G. L. *Biomicrofluidics* **2011,** 5 (1), 013403/1-013403/19.

52. Greiner, A.; Wendorff, J. H. *Aangewandte Chemie International Edition* **2007,** 46 , 5670-5703.

53. Agarwal, S.; Wendorff, J. H.; Greiner, A. *Advanced Materials* **2009,** 21 (32-33), 3343-3351.

54. Agarwal, S.; Wendorff, J. H.; Greiner, A. *Polymer* **2008,** 49 (26), 5603-5621.

55. Burger, C.; Hsiao, B. S.; Chu, B. *Annual Review of Materials Research* **2006,** 36 , 333-368.

56. Formhals, A. United States of America Patent 1975504, 1934.

57. Shin, Y. M.; Hohman, M. M.; Brenner, M. P.; Rutledge, G. C. *Applied Physics Letters* **2001,** 78 (8), 1149-1151.

58. Frenot, A.; Chronakis, I. S. *Current Opinion in Colloid and Interface Science* **2003,** 8 , 64-75.

59. Casper, C. L.; Stephens, J. S.; Tassi, N. G.; Chase, D. B.; Rabolt, J. F. *Macromolecules* **2004,** 37 , 573-578.

60. Agarwal, S.; Greiner, A.; Wendorff, J. H. *Advanced Functional Materials* **2009,** 19 (18), 2863-2879.

61. Doshi, J.; Reneker, D. H. *Journal of Electrostatics.* **1995,** 35 (2&3), 151-160.

62. Reneker, D. H.; Chun, I. *Nanotechnology* **1996,** 7 (3), 216-223.

63. Subbiah, T.; Bhat, G. S.; Tock, R. W.; Parameswaran, S.; Ramkumar, S. S. *Journal of Applied Polymer Science* **2005,** 96 (2), 557-569.

64. Hohman, M. M.; Shin, M.; Rutledge, G.; Brenner, M. P. *Physics of Fluids* **2001,** 13 (8), 2201-2220.

65. Hohman, M. M.; Shin, M.; Rutledge, G.; Brenner, M. P. *Physics of Fluids* **2001,** 13 (8), 2221-2236.

66. Shenoy, S. L.; Bates, W. D.; Frisch, H. L.; Wnek, G. E. *Polymer* **2005,** 46 , 3372-3384.

67. Bhardwaj, N.; Kundu, S. C. *Biotechnology Advances* **2010,** 28 (3), 325-347.

68. Deitzel, J. M.; Kleinmeyer, J.; Harris, D.; Beck Tan, N. C. *Polymer* **2001,** 42 (1), 261-272.

69. Demir, M. M.; Yilgor, I.; Yilgor, E.; Erman, B. *Polymer* **2002,** 43 (11), 3303-3309.

70. Eda, G.; Shivkumar, S. *Journal of Material Science* **2006,** 41 (17), 5704-5708.

71. Ding, W.; Wei, S.; Zhu, J.; Chen, X.; Rutman, D.; Guo, Z. *Macromolecular Materials and Engineering* **2010,** 295 (10), 958-965.

72. Rutledge, G. C.; Fridrikh, S. V. *Advanced Drug Delivery Reviews* **2007,** 59 , 1384-1391.

73. Holzmeister, A.; Yarin, A. L.; Wendorff, J. H. *Polymer* **2010,** 51 (12), 2769-2778.

74. Hsu, C.; Shivkumar, S. *Macromolecular Materials and Engineering* **2004,** 289 (4), 334-340.

75. Son, W. K.; Youk, J. H.; Lee, T. S.; Park, W. H. *Polymer* **2004,** 45 (9), 2959-2966.

76. Wannatong, L.; Sirivat, A.; Supaphol, P. *Polymer International* **2004,** 53 (11), 1851-1859.

77. Jarusuwannapoom, T.; Hongrojjanawiwat, W.; Jitjaicham, S.; Wannatong, L.; Nithitanakul, M.; Pattamaprom, C.; Koombhongse, P.; Rangkupan, R.; Supaphol, P. *European Polymer Journal* **2005,** 41 (3), 409-421.

78. Qin, X.; Wang, S. *Materials Letters* **2008,** 62 (8-9), 1325-1327.

79. Baumgarten, P. K. *Journal of Colloid and Interface Science* **1971,** 36 (1), 71-79.

80. Qin, X.; Yang, E.; Li, N.; Wang, S. *Journal of Applied Polymer Science* **2007,** 103 (6), 3865-3870.

81. Arumugam, G. K.; Khan, S.; Heiden, P. A. *Macromolecular Materials and Engineering* **2009,** 294 (1), 45-53.

82. Fong, H.; Chun, I.; Reneker, D. H. *Polymer* **1999,** 40 , 4585-4592.

83. Baji, A.; Mai, Y.; Wong, S.; Abtahi, M.; Chen, P. *Composites Science and Technology* **2010,** 70 (5), 703-718.

84. Liu, H.; Hsieh, Y. *Journal of Polymer Science Part B: Polymer Physics* **2002,** 40 (18), 2119-2129.

85. Edwards, M. D.; Mitchell, G. R.; Mohan, S. D.; Olley, R. H. *European Polymer Journal* **2010,** 46 (6), 1175-1183.

86. Kongkhlang, T.; Tashiro, K.; Kotaki, M.; Chirachanchai, S. *Journal of the American Chemical Society* **2008,** 130 (46), 15460-15466.

87. Acharya, M.; Arumugam, G. K.; Heiden, P. A. *Macromolecular Materials and Engineering* **2008,** 293 (8), 666-674.

88. De Vrieze, S.; Van Camp, T.; Nelvig, A.; Hagstrom, B.; Westbroek, P.; De Clerck, K. *Journal of Materials Science* **2009,** 44 (5), 1357-1362.

89. Supaphol, P.; Mit-Uppatham, C.; Nithitanakul, M. *Journal of Polymer Science Part B: Polymer Physics* **2005,** 43 (24), 3699-3712.

90. Wang, C.; Chien, H.; Hsu, C.; Wang, Y.; Wang, C.; Lu, H. *Macromolecules* **2007,** 40 (22), 7973-7983.

91. Megelski, S.; Stephens, J. S.; Chase, D. B.; Rabolt, J. F. *Macromolecules* **2002,** 35 , 8456-8466.

92. Tripatanasuwan, S.; Zhong, Z.; Reneker, D. H. *Polymer* **2007,** 48 (19), 5742-5746.

93. De Vrieze, S.; De Schoenmaker, B.; Ceylan, O.; Depuydt, J.; Van Landuyt, L.; Rahier, H.; Van Assche, G.; De Clerck, K. *Journal of Applied Polymer Science* **2011,** 119 (5), 2984-2990.

94. Givens, S. R.; Gardner, K. H.; Rabolt, J. F.; Chase, D. B. *Macromolecules* **2007,** 40 , 608-610.

95. Larrondo, L.; St. John Manley, R. *Journal of Polymer Science, Polymer Physics Edition* **1981,** 19 (6), 909-920.

96. Larrondo, L.; St. John Manley, R. *Journal of Polymer Science, Polymer Physics Edition* **1981,** 19 (6), 921-932.

97. Larrondo, L.; St. John Manley, R. *Journal of Polymer Science, Polymer Physics Edition* **1981,** 19 (6), 933-940.

98. Rabolt, J. F.; Lee, K. H.; Givens, S. R. United States of America Patent , 2007.

99. Lee, K.; Ohsawa, O.; Watanabe, K.; Kim, I.; Givens, S. R.; Chase, B.; Rabolt, J. F. *Macromolecules* **2009,** 42 (14), 5215-5218.

100. Thostenson, E. T.; Li, C.; Chou, T. *Composites Science and Technology* **2005,** 65 (3-4), 491-516.

101. Zhang, X.; Yang, M.; Zhao, Y.; Zhang, S.; Dong, X.; Liu, X. *Journal of Applied Polymer Science* **2004,** 92 , 552-558.

102. Liu, Y.; Li, C.; Chen, S.; Wachtel, E.; Koga, T.; Sokolov, J. C.; Rafailovich, M. H. *Journal of Polymer Science, Polymer Physics Edition* **2009,** 47 (24), 2501-2508.

103. Neppalli, R.; Marega, C.; Marigo, A.; Bajgai, M. P.; Kim, H. Y.; Causin, V. *European Polymer Journal* **2010,** 46 (5), 968-976.

104. Kim, J.; Reneker, D. H. *Polymer Composites* **1999,** 20 (1), 124-131.

105. Bergshoef, M. M.; Vancso, G. J. *Advanced Materials* **1999,** 11 (16), 1362-1365.

106. Tang, C.; Liu, H. *Composites, Part A: Applied Science and Manufacturing* **2008,** 39A (10), 1638-1643.

107. Swart, M.; Olsson, R. T.; Hedenqvist, M. S.; Mallon, P. E. *Polymer Engineering & Science* **2010,** 50 (11), 2143-2152.

108. Bayley, G. M.; Hedenqvist, M.; Mallon, P. E. *Polymer* **2011,** 52 (18), 4061-4072.

109. O'Connell, M. J. In *Carbon Nanotubes,Properties and Applications.* Taylor & Francis Group: Florida, 2006; pp 329.

110. Meyyappan, M. In *Carbon nanotubes, Science and Applications.* CRC Press: Florida, 2005; pp 289.

111. Iijima, S. **1991,** 354 , 56-58.

112. Tasis, D.; Tagmatarchis, N.; Bianco, A.; Prato, M. *Chemical Reviews* **2006,** 106 (3), 1105-1136.

113. Yeo, L. Y.; Friend, J. R. *Journal of Experimental Nanoscience* **2006,** 1 (1-4), 177-209.

114. Hierold, C. In *Carbon Nanotubes Devices.* Brand, O., Fedder, G.K., Hierold, C., Korvink, J.G., Tabata, O., Ed.; Wiley-VCH: Weinheim, 2008; Vol. 8, pp 363.

115. Spitalsky, Z.; Tasis, D.; Papagelis, K.; Galiotis, C. *Progress in Polymer Science* **2010,** 35 (3), 357-401.

116. Bandaru, P. R. *Journal of Nanoscience and Nanotechnology* **2007,** 7 (4/5), 1239-1267.

117. Meng, Z. X.; Zheng, W.; Li, L.; Zheng, Y. F. *Materials Science and Engineering: C* **2010,** 30 (7), 1014-1021.

118. Moniruzzaman, M.; Winey, K. I. *Macromolecules* **2006,** 39 (16), 5194-5205.

119. Ajayan, P. M.; Dhinojwala, A. Patent Application Country: Application: US; Patent Country: US; Priority Application Country: US Patent 20080280137, 2008.

120. Thostenson, E. T.; Ren, Z.; Chou, T. -. *Composite Science and Technology* **2001,** 61 (13), 1899-1912.

121. Dresselhaus, M. S.; Dresselhaus, G.; Eklund, P. C. *Science of Fullerenes and Carbon Nanotubes;* ACADEMIC PRESS: United States of America, 1995; , pp 965.

122. Ando, Y.; Zhao, X.; Sugai, T.; Kumar, M. *Materials Today* **2004,** 7 (10), 22-29.

123. Guo, T.; Diener, M. D.; Chai, Y.; Alford, M. J.; Haufler, R. E.; McClure, S. M.; Ohno, T.; Weaver, J. H.; Scuseria, G. E.; Smalley, R. E. *Science* **1992,** 257 (5077), 1661-1664.

124. Thess, A.; Lee, R.; Nikolaev, P.; Dai, H.; Petit, P.; Robert, J.; Xu, C.; Lee, Y. H.; Kim, S. G.; et al *Science* **1996,** 273 (5274), 483-487.

125. Endo, M.; Takeuchi, K.; Igarashi, S.; Kobori, K.; Shiraishi, M.; Kroto, H. W. *Journal of Physics and Chemistry of Solids* **1993,** 54 (12), 1841-1848.

126. Bandarian, M.; Shojaei, A.; Rashidi, A. M. *Polymer International* **2011,** 60 (3), 475-482.

127. Jose, M. V.; Dean, D.; Tyner, J.; Price, G.; Nyairo, E. *Journal of Applied Polymer Science* **2007,** 103 , 3844-3850.

128. Breuer, O.; Sundararaj, U. *Polymer Composites* **2004,** 25 (6), 630-645.

129. Coleman, J. N.; Khan, U.; Blau, W. J.; Gun'ko, Y. K. *Carbon* **2006,** 44 (9), 1624-1652.

130. Shaffer, M. S. P.; Windle, A. H. *Advanced Materials* **1999,** 11 (11), 937-941.

131. Qian, D.; Dickey, E. C.; Andrews, R.; Rantell, T. *Applied Physics Letters* **2000,** 76 (20).

132. Pötschke, P.; Bhattacharyya, A. R.; Janke, A.; Goering, H. *Composite Interfaces* **2003,** 10 (4), 389-404.

133. Lozano, K.; Barrera, E. V. *Journal of Applied Polymer Science* **2001,** 79 (1), 125-133.

134. Haggenmueller, R.; Gommans, H. H.; Rinzler, A. G.; Fischer, J. E.; Winey, K. I. *Chemical Physics Letters* **2000,** 330 (3,4), 219-225.

135. Li, Q.; Zaiser, M.; Koutsos, V. *Physica Status Solidi (a)* **2004,** 201 (13), R89-R91.

136. Lau, K.; Lu, M.; Lam, C.; Cheung, H.; Sheng, F.; Li, H. *Composites Science and Technology* **2005,** 65 (5), 719-725.

137. Jia, Z.; Wang, Z.; Xu, C.; Liang, J.; Wei, B.; Wu, D.; Zhu, S. *Materials Science & Engineering, A: Structural Materials: Properties, Microstructure and Processing* **1999,** A271 (1-2), 395-400.

138. Velasco-Santos, C.; Martinez-Hernandez, A. L.; Fisher, F. T.; Ruoff, R.; Castano, V. M. *Chemistry of Materials* **2003,** 15 (23), 4470-4475.

139. Kumar, S.; Dang, T. D.; Arnold, F. E.; Bhattacharyya, A. R.; Min, B. G.; Zhang, X.; Vaia, R. A.; Park, C.; Adams, W. W.; Hauge, R. H.; Smalley, R. E.; Ramesh, S.; Willis, P. A. *Macromolecules* **2002,** 35 (24), 9039-9043.

140. Zhao, C.; Hu, G.; Justice, R.; Schaefer, D. W.; Zhang, S.; Yang, M.; Han, C. C. *Polymer* **2005,** 46 (14), 5125-5132.

141. Saeed, K.; Park, S.; Lee, H.; Baek, J.; Huh, W. *Polymer* **2006,** 47 (23), 8019-8025.

142. Ford, W. T. *Macromolecular Symposia* **2010,** 297 (1), 18-24.

143. Choi, J.; Park, E. J.; Park, D. W.; Shim, S. E. *Synthetic Metals* **2010,** 160 (23-24), 2664-2669.

144. Kim, G. -.; Michler, G. H.; Pötschke, P. *Polymer* **2005,** 46 (18), 7346-7351.

145. Kim, M. J.; Lee, J.; Jung, D.; Shim, S. E. *Synthetic Methods* **2010,** 160 (13-14), 1410-1414.

146. Kimmer, D.; Slobodian, P.; Petrá?, D.; Zatloukal, M.; Olejník, R.; Sáha, P. *Journal of Applied Polymer Science* **2009,** 111 (6), 2711-2714.

147. Mathew, G.; Hong, J. P.; Rhee, J. M.; Lee, H. S.; Nah, C. *Polymer Testing* **2005,** 24 (6), 712-717.

148. Mazinani, S.; Ajji, A.; Dubois, C. *Journal of Polymer Science, Polymer Physics Edition* **2010,** 48 (19), 2052-2064.

149. Dror, Y.; Salalha, W.; Khalfin, R. L.; Cohen, Y.; Yarin, A. L.; Zussman, E. *Langmuir* **2003,** 19 (17), 7012-7020.

150. Mazinani, S.; Ajji, A.; Dubois, C. *Polymer* **2009,** 50 (14), 3329-3342.

151. Ruan, S.; Gao, P.; Yu, T. X. *Polymer* **2006,** 47 (5), 1604-1611.

152. Kearns, J. C.; Shambaugh, R. L. *Journal of Applied Polymer Science* **2002,** 86 (8), 2079-2084.

Chapter 3

Experimental

3.1 Materials

3.1.1 Polymers

The polypropylene copolymers used was previously produced by Brüll et al. [1], using a metallocene catalyst, $(CH_3)_2Si$(2-methylbenz[e]indenyl) $ZrCl_2$, donated by H.-H. Britzinger [2].
Poly(ethylene-co-vinyl alcohol) (EVOH) was purchased from Sigma Aldrich (44 mole% ethylene).

3.1.2 Solvents

For the solution electrospinning of the polypropylene copolymers, cyclohexane (CHROMASOLV® HPLC grade with 99.9% purity (Sigma Aldrich)), reaction grade acetone (99% pure (Sigma Aldrich)) and *N,N,*-dimethylformamide (GC 99% (Sigma Aldrich)) was used.
EVOH was electrospun from *N,N*,-dimethylformamide (used as received), dimethyl sulfoxide (dried over molecular sieves) and anhydrous 2-propanol (99.5% (Sigma Aldrich)).

3.2 Electrospinning

Electrospinning was performed on an setup built in-house, based on a setup described in literature [3-5]. The solution reservoir was a Hamilton® SGE gas-tight syringe, which was placed in a Kent Scientific (Genie Plus) pump. This was used to deliver the polymer solution at a predetermined rate. The spinneret was a stainless steel blunt tip 50 mm needle (16 gauge) and in some cases 60 cm teflon tubing (Separations), fitted with luer-locks, was used to connect the syringe and needle. The electrical field was supplied by a high voltage supply (manufactured at Stellenbosch University) that is connected to the needle and grounded collector plate. The unit was capable of supplying up to 50 kV. Non-aligned fibres were collected on aluminium foil and aligned fibres on a rotating drum that was earthed and controlled by Reliance electric motor (E243) that was connected to an Eagle HP005B HEP-613) power supply.

3.3 Composite formation

Composites were produced in Grasby Specac 15.011 ton press. Two films of LDPE were pressed to a 15 µm thickness. Typically, a small amount of material (LDPE) was pressed between two

MYLAR® films at 140 °C in multiple steps. The material was placed inside the press and kept at a 140 °C for 5 min. Then 5 T pressure was applied for 30 seconds and this step was repeated. The film was then allowed to cool to room temperature.

To form the composite the electrospun nanofibre mat was placed between the two LDPE films and placed inside the press. The materials were heated to and kept at 140 °C for a minute and 2.5 T pressure was then applied for 5 seconds. The thickness of the composite was 50 μm. Dumbbell shaped composites for tensile testing were prepared in the same fashion, except the thickness of the dumbbell was 300 μm.

EVOH films were prepared in the same way, except that these films were pressed at a temperature of 180 °C.

Composites containing MWCNT were prepared by pressing two films of the LDPE polymer as described previously. The nanofibre mat containing the MWCNT was placed in between the two films and pressed in multiple steps at 180 °C. The two films with the fibre matt was placed inside the press and kept at 180 °C for 5 min. Then 5 T pressure was applied for 20 seconds. Dumbbell shape composites for tensile testing were prepared in the same except the thickness of the dumbbell was 300 μm.

3.4 Functionalising MWCNT

Two methods were employed to functionalise the MWCNT. The first method was done as described in the PhD thesis of G.M. Bayley. Typically 2 g MWCNT and $NaNO_3$ powder (2:1) were added to 250 ml round-bottom flask. The mixture was placed in an ice-bath and 46 ml of a 93 wt% H_2SO_4 solution was carefully added while magnetically stirring the solution. After 10 minutes 300 g $KMNO_4$ was slowly and carefully added, while keeping the temperature below 20 °C. The stirring speed was increased and after the addition the mixture was vigorously stirred for another 10 minutes. The round-bottom flask was removed from the ice-bath and heated to 98 °C. As soon as the mixture turned a brown-grey colour, 92 ml distilled water was slowly added. The solution was kept, after the addition of water, at 98 °C for 15 minutes. The volume of the solution was increased to 200 ml by adding a 3 wt% solution of H_2O_2 in water. This mixture was then stirred for a further 20 minutes. The solution was transferred to a centrifuge tube and centrifuged and washed with deionised water repeatedly until a pH of 7 was obtained. In the second method, 2 g MWCNT was added to 50 g 6M Nitric acid. The solution was heated to 145 °C and refluxed for 48 hours. After 48 hours the solution was transferred to a centrifuge tube and centrifuged and washed with deionised water repeatedly till a pH of 7 was obtained. The solution was freeze-dried to obtain functionalised MWCNT.

3.5 Attaching fluorescent dye molecules to MWCNT

3.5.1 Rhodamine B

10 wt% Rhodamine B for fluorescence (Sigma) was added to the MWCNT. This reaction took place in acetone,(reaction Grade, 99% purity) containing 1 drop of concentrated H_2SO_4. The reaction mixture was refluxed at 50 °C for 2 hours. After the 2 hours, the mixture was centrifuged and then repeatedly washed with deionised water until a neutral pH was obtained. The solution was subsequently freeze-dried to obtain dried MWCNT with Rhodamine B attached to it.

3.5.2 Fluorescein

The reaction of the fluorescein was based on the article by Nielsen et al.[6] Fluorescein 5(6)-isothiocyanate (0.001 g, BioReagent, Sigma Aldrich) was added to 0.1 g functionalised MWCNT in 10 mL aqueous NaOH. The reaction was stirred at room temperature for 72 hours in the dark. After 72 hours the solution was centrifuged in aqueous NaOH until all the unreacted dye was washed out and then in deionised water until a pH of 7 was obtained. Subsequently the mixture was freeze-dried to obtain dried and dyed MWCNT.

3.6 Analytical Techniques

3.6.1 Scanning electron microscopy

The samples were placed on SEM stubs and gold coated. SEM analysis were performed with a Leo 1430VP scanning electron microscope fitted with backscatter, cathodoluminescence, variable pressure and energy dispersive detectors, including a Link EDS system and software for microanalysis.

The samples for FE-SEM were fixed on SEM stubs and carbon coated. The analysis was done on a FEI Nova Nanosem 230 fitted with a field emission gun.

3.6.2 Transmission electron microscopy

Fibre samples were placed directly on a copper grid and then placed in the transmission electron microscope. Images were taken on a JEOL 1200 EXII instrument.

The composite samples were placed in agar resin and microtomed to obtain thin cross-sections which were then analysed using the TEM.

3.6.3 High temperature size exclusion chromatography

Molecular weight and polydispersity of the polypropylene copolymers were determined with high temperature SEC. A small amount of the polymer (1.5-2 mg) was dissolved in 2 ml of 1, 2, 4-trichlorobenzene containing 0.0125% 2, 6-di-tert-butyl-4-methylphenol (BHT). The samples were

dissolved at 160 °C before injection. Molecular weights were determined on a PL-GPC 220 high temperature chromatograph from Polymer Laboratories, operating at 145 °C. The 4 columns were packed with polystyrene/divinylbenzene copolymer (PL gel MIIXED-B [9003-53-6]) from Polymer Laboratories. Each column had a length of 300 mm and a diameter of 7.5 mm. The particle size was 10 μm. A differential refraction index detector was used. The calibration of the instrument was done with monodisperse polystyrene standards (Easical from Polymer Laboratories).

3.6.4 ATR

A Thermo-Nicolet iS10 FT-IR with ATR attachment was used for the ATR analysis. The FT-IR is equipped with a ZnSe crystal. Fibres and powders was analysed as received.

3.6.5 Fluorescence microscopy

Fluorescence microscopy images were taken with a Olympus Cell® system which was attached to an IX 81 inverted fluorescence microscope fitted with a F-view-II CCD camera. The light source was a Xenon-Arc burner (Olympus Biosystems GMBH) and the images were attained using either the 492 nm or 572 nm excitation filter. The emissions were collected by using a UBG triple bandpass emission filter cube by Chroma. The z-stack image frame were acquired by using a step width of 0.5 μM, an Olympus Plan Apo N 60x/1.4 Oil objective and Cell® imaging software. The fluorescence image was overlaid with a transmission image; the processing and background-subtraction were done by using Cell® software.

3.6.6 DSC

The melting point and percentage crystallinity was determined with a TA Instruments Q100 DSC. The instrument was calibrated using Indium metal according to a standard procedure. About 2-5 mg of each sample was weighed off and sealed in a standard DSC pan for analysis. All measurements were conducted in a nitrogen atmosphere.

The sample was subsequently heated to 220 °C at a rate of 10 °C/min and then equilibrated at 220 °C for 5 minutes. The sample was then cooled down to -40 °C at a rate of 10 °C/min and then left to equilibrate at that temperature for 5 minutes. The sample was then heated again to 220 °C at a rate of 10 °C. Both the first and second heating was considered for the analysis of the melting behaviour of the polymer.

3.6.7 TGA

The mass loss profile of the EVOH samples was determined on Perkin Elmer TGA 7. The samples were run from 25 °C to 750 °C at a heating rate of 20 °C/min under a nitrogen atmosphere.

3.6.8 Tensile testing

Tensile bar shaped samples were pressed on a Grasby Specac 15.011 ton press. Tensile tests were performed on a LLOYD LRX Tensile Tester. The samples had a gauge length of 25.3 cm and a deformation area of 0.36 mm x 6.65 mm. Tensile tests were conducted at 50 mm/min.

3.6.9 WAXD

WAXD was performed on a PANalytical X'Pert PRO Multi-Purpose Diffractometer with X'Celerator detector. The diffractometer is coupled to a source of CuKα radiation. The powder and fibre samples were directly placed underneath the beam and were scanned at a diffraction angle of 2θ ranging from 5 ° to 35 °.

3.6.10 SCALLS

The measurements were done on a SCALLS instrument. A laser beam (635 nm diode laser) is directed through a heated solution of a polyolefin and the intensity measured by three photodiode detectors upon controlled cooling. The reverse could also be done (heating experiment).
Cooling experiments were conducted a rate of 1.5 °C/minute (heating) and 1 °C/minute (cooling) respectively. Polymer solutions (0.5 mg/ml) in 1, 2, 4 – trichlorobenzene were prepared at 140 °C, equilibrated in the instrument at 100 °C and then cooled to 30 °C. Controlled heating followed directly afterwards (to 120 °C).

3.7 References

1. Brüll, R.; Pasch, H.; Raubenheimer, H. G.; Sanderson, R.; van Reenen, A. J.; Wahner, U. M. *Macromolecular Chemistry and Physics* **2001,** 202 (8), 1281-1288.

2. Stehling, U.; Diebold, J.; Kirsten, R.; Roell, W.; Brintzinger, H. H.; Juengling, S.; Muelhaupt, R.; Langhauser, F. *Organometallics* **1994,** 13 (3), 964-970.

3. Frenot, A.; Chronakis, I. S. *Current Opinion in Colloid and Interface Science* **2003,** 8 , 64-75.

4. Ramakriskna, S.; Fujihara, K.; Teo, W. E.; Lim, T. C.; Ma, Z. *An Introduction to Electrospinning and Nanofibers;* World Scientific Publishing Co. Pte. Ltd: Singapore, 2005; .

5. Reneker, D. H.; Chun, I. *Nanotechnology* **1996,** 7 (3), 216-223.

6. Nielsen, L. J.; Eyley, S.; Thielemans, W.; Aylott, J. W. *Chemical Communications* **2010,** 46 (47), 8929-8931.

Chapter 4

Electrospinning of polyolefins

4.1. Introduction

Electrospinning has become a popular technique for the production of polymer fibres, primarily because this is a facile method of producing nano-scale polymeric artefacts. Solution electrospinning is the method preferred for the production of nanofibres where limited amounts of polymer are available. Melt electrospinning requires substantial amounts of polymer to be effective [1].

4.2. Electrospinning of linear-low density polyethylene (LLDPE)

Polyolefins are already used in a wide variety of applications. As we have been actively involved in the synthesis and characterization of polyolefins, the pursuit of solution electrospun polyolefins nanofibres seemed a natural path to follow. These fibres could be effective in a number of possible applications, including membranes for filtration and protective clothing. Relatively few papers have been published detailing the solution electrospinning of polyolefins. One of the first published was a paper by Larrondo, who described the electrospinning of polyethylene in a paraffin solution at 100 °C [1-3]. Subsequently, very few papers have appeared [4-6]. There are a few problems encountered when wanting to electrospin these polymers. In the first place, the crystalline polyolefins are only soluble at high temperatures and will only stay in solution at high temperatures. In the second place the polyolefins are only soluble in the higher alkanes, aromatic hydrocarbons and chlorinated aromatic hydrocarbons. None of these solvents are very conductive. The simple answer would seem to be to design an electrospinning setup where electrospinning can be done at high temperatures. Unfortunately this type of design is not trivial and you are still faced with the problem of making the solution more conductive.

The solution for both these problems might be to find a suitable solvent or solvent system that will keep the polymer in solution even at room temperature and that is also conductive enough to allow the electrospinning of the polymer. To increase the conductivity seems to be the easiest problem to solve. By adding a conductive solvent to the solvent responsible for the dissolving of the polymer, the conductivity of the solution may be increase. If the conductive solvent is a non-solvent for the polymer, finding the correct ratio of the solvent/conductive non-solvent will be very important, since too little of the conductive solvent may not increase the conductivity enough and too much may cause the polymer to become insoluble. In order to tackle this problem, we first attempted to electrospin a fairly soluble polyolefin (one that still has some crystallinity, however)

namely linear low density polyethylene (LLDPE). The LLDPE (Sasol Grade LM3040P) used in this study is a copolymer of ethylene and 1-butene with a 1-butene content of 3.2 wt%.
The LLDPE was treated with several combinations of a known solvent for polyolefins and a conductive non-solvent. The solvent/non-solvent combinations are detailed in Table 4.1. The temperature at which the solutions were kept was varied between 100 – 140 °C.

In the case where the polymer dissolved, we attempted to electrospin the resultant solution.

Table 4.1. Solvent/non-solvent combinations for the electrospinning of LLDPE

Weight % polymer	Solvents	Ratio of solvents	Solution	Electrospinning
0.2	Cyclohexanone/p-Xylene	50/50	✓	No spinning
2	Cyclohexanone/p-Xylene	50/50	✓	No spinning
2	Cyclohexanone/p-Xylene	40/60	✓	No spinning
2	Cyclohexanone/p-Xylene	80/20	✓	No spinning
2	Cyclohexanone/p-Xylene	70/30	✓	No spinning

The solvent/non-solvent combinations used were selected according to literature reports. Ultra-high molecular weight polyethylene was reported to be dissolved in a solvent system consisting of *p*-xylene and cyclohexanone, and was subsequently solution electrospun [5]. *p*-Xylene is a known solvent for polyethylene, but is not very conductive. By adding the cyclohexanone, which has a higher dielectric constant, the solution would be more conductive and electrospinning might be possible. Solubility tests were first performed with LLDPE, to establish which solvent combinations would indeed dissolve the polymer. Thereafter we attempted to electrospin the polymer form the solution. The main concern was that as soon as the temperature decreases, the polymer would not stay in solution and the electrospinning cannot take place. This was a very important aspect, since the electrospinning setup in our laboratory would not allow electrospinning at high temperatures.
Preparing 2% solutions of LLDPE in cyclohexanone/xylene mixtures resulted in polymer dissolution at high temperatures across a whole range of solvent/non-solvent mixtures. However, we could not successfully electrospin these solutions, as the polymer crystallized from solution as soon as the mixture was cooled even slightly.
We therefore investigated other solvents/solvent combinations. The addition of a cycloaliphatic hydrocarbon was thought to be a possible way of improving the low-temperature solubility, but the addition of even a small amount of cyclohexane resulted in polymer precipitating from the *p*-xylene solution.
From literature it is clear that we needed to add a solvent with a higher dielectric constant[7]. N,N-dimethylformamide is one of the solvents known to improve the fibre morphology [8] and is usually

added to the solution to increase the dielectric property of the solution[9]. Rabolt *et al* [10]. described in a patent the electrospinning of polyolefins at room temperature. They claimed this could be achieved by using a solvent combination that consisted of cyclohexane/acetone/DMF in an 80/10/10 ratio. Polyolefins were reportedly dissolved at 100 °C and when the solution was allowed to cool down, the polymer stayed in solution at room temperature for a sufficient period of time for solution electrospinning to be done. We attempted this approach. As can be seen in Table 4.2 various solvent combinations were tested, but only a few were able to dissolve LLDPE, but as soon as the temperature was decreased, the polymer crystallized from solutions.

Table 4.2. Solubility tests of LLDPE

Weight % polymer	Solvent	Ratio of solvent	Solubility of LLDPE
2	Cyclohexane/Acetone/DMF	80/10/10	×
0.5	Cyclohexane/Acetone/DMF	80/10/10	×
2	Xylene/Acetone/DMF	80/10/10	Dissolves, but crystallizes out very quickly
2	Cyclohexane/Acetone/DMF	80/10/10	×
2	Xylene/DMF	80/20	Dissolves, but crystallizes out very quickly
5	Xylene/DMF	80/20	×
4	Xylene/Cyclohexanone	30/70	Dissolves, but crystallizes out very quickly
2	Xylene/DMF	50/50	×
2	Xylene/DMF	70/30	×
2	Cyclohexane/Xylene/Acetone	60/30/10	×
2	Cyclohexane/Xylene/Acetone	40/20/20	Dissolves, but crystallizes out very quickly
2	Xylene/Acetone	70/30	×
2	Cyclohexane/Xylene/Propanol	40/40/20	Dissolves, but crystallizes out very quickly

Even though the polymer crystallized out of solution rapidly, electrospinning was tried on those samples that did dissolve. The solvent combinations and solution concentration of each sample can be seen in Table 4.3 and the images of the results in Figure 4.1.

Table 4.3. Solvents and solution concentration for the electrospinning of LLDPE

Sample	Weight % polymer	Solvent	Ratio of solvent
A	2	Xylene/DMF/Acetone	80/10/10
B	1	Cyclohexane/Xylene/Acetone	60/30/10
C	2	Cyclohexane/Xylene/Propanol	60/20/20

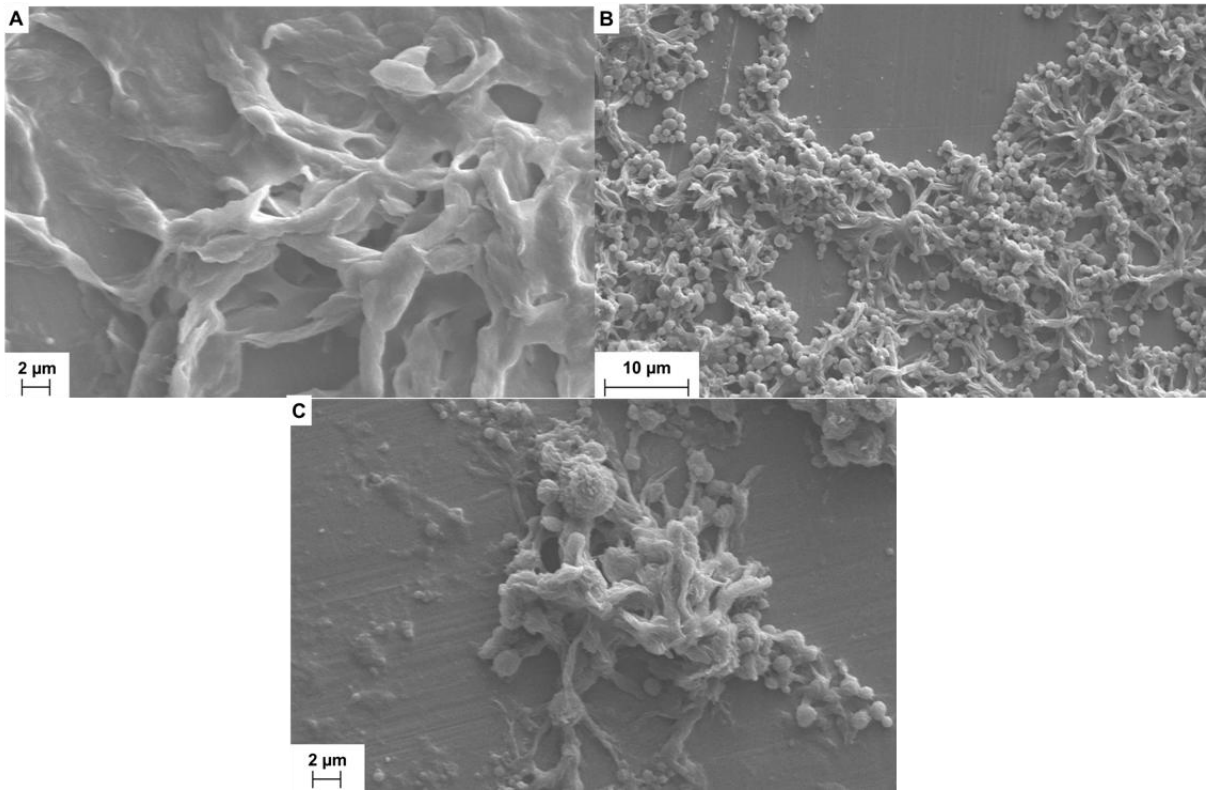

Figure 4.1. SEM images of products of attempted electrospinning of LLDPE

As can be seen in Figure 4.1,A, some stretching of the polymer did take place, but clearly not enough to encourage fibre formation. In B and C polymer beads can be observed, indicating that minimum or no stretching took place. The fused form of the polymer droplets points to the fact that solvent evaporation was not satisfactory. There are various reasons why the electrospinning was not successful; the solvent systems may not be conductive enough and there might not be enough charges carried by the jet, the evaporation of the solvent might be too slow, leading to the formation of wet fibres and lastly the polymer might be crystallizing out too quickly. The solubility of the polymer might also be inadequate, leading to unstable jet formation, which will cause electrospraying and not spinning. Nonetheless, the fact that we were able to produce a few artifacts by solution electrospinning was quite encouraging.

4.3. Solution electrospinning of polypropylene copolymers

4.3.1 Initial solution electrospinning

In a patent, Rabolt *et al* [10]. described the solution electrospinning of polyolefins at room temperature by using a solvent combination that consisted out of cyclohexane, acetone and dimethylformamide (DMF) in a ratio of 80/10/10. When dissolving the polymer at 100 °C in this solvent system and then cooling it down, the polymer stays in solution long enough to be electrospun. As can be seen in previous section, this still didn't work for the LLDPE samples and the problems with the LLDPE led us to try different polyolefins. First we tried a commercial isotactic polypropylene (Table 4.4, iPP 1 and iPP 2). These polymers did not, however, dissolve in the solvent system described by Rabolt *et al* [10].

We therefore thought that using polypropylene copolymers might be the way forward. We had previously synthesized a whole series of propylene-1-alkene copolymers. These polymers appeared to be reasonably crystalline yet much more soluble than the pure isotactic homopolymers. Therefore these materials appeared to be good candidates for solution electrospinning.

In Table 4.4 the data of the molecular weight, comonomer content and crystallinity of each polypropylene copolymer sample is given. The numeric code refers to the type of linear 1-alkene used as comonomer: 8 refer to 1-octene, 10 to 1-decene and 14 to 1-tetradecene.

Table 4.4. Molecular weight, crystallinity and comonomer data for polypropylene copolymers

Polymer	Mw (g/mol)	PD	Comonomer (mole %)	Crystallinity (%)
8A	506700	2.4	0.86	25.4
8B	662400	2.9	0.98	25.1
8C	643500	2.3	0.57	32.4
8D	722100	2.5	0.47	32.1
10A	98900	2.1	2.31	55.1
10B	467300	2.3	1.07	28.4
10C	517000	2.4	0.42	32.7
10D	196400	3.1	0.47	46.0
14A	309000	3.07	0.5	29.9
14B	190000	3.07	0.26	30.0
iPP 1	420500			51.1
iPP 2	468000			41.1

For the sample in Figure 4.2 (Polymer 8A) the tip-to collector distance and the flow rate were kept constant at 20 cm and 0.1 ml/min respectively. The solution concentration was only 2 wt%, but even though the weight percentage of the solution was quite low, the viscosity was quite high and when using a lower flow rate, the needle tended to get blocked. The voltage was varied, until it seemed a stable jet was obtained.

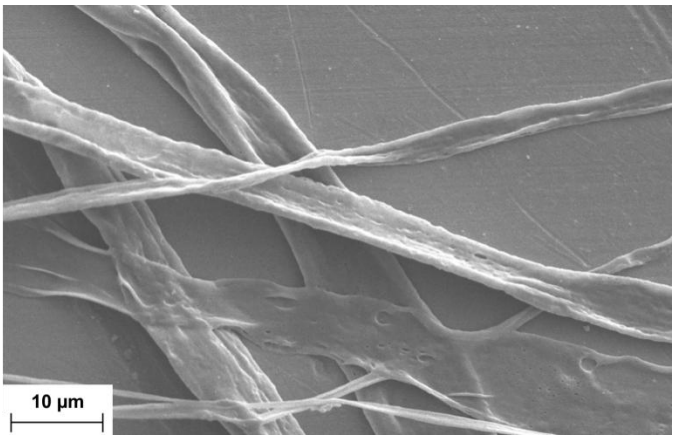

Figure 4.2. SEM image of electrospun polymer 8A

The solvent combination (cyclohexane, acetone and DMF, 80/10/10) and polymer concentration seemed to be appropriate and the formation of fibres took place. These initial fibres were mostly broad and flat, and some distance from being in the nanometer range. The isotactic polypropylenes were also treated with the same solvent system, but these polymers did not dissolve. What was interesting to see is that the copolymers mostly have a higher molecular weight

than that of the isotactic polypropylene, but dissolving them seemed to be easier. More on this aspect will be discussed later in this chapter.

The fibres found, however, were still relatively wet, indicating bad solvent evaporation. The next step was to vary the numerous spinning parameters to see if better fibre morphology could be found. The aim was the formation of nanofibres and these fibres were still in the micrometre range, so by changing the various parameters, optimum conditions could be obtained for the thinnest fibres.

Each copolymer will be discussed separately.

4.3.2 Poly(propylene–co–1–decene)

The first polymer to be electrospun was the poly(propylene–co–1–decene) copolymer. There were different samples of this copolymer, differing in the molecular weight, crystallinity and comonomer content. The first one to be tried was 10A (2.31 mole% 1-decene) and for this sample the flow rate was kept constant at 0.05 ml/min, the tip to collector distance (TCD) varied between 15 cm and 20 cm, the voltage varied between 10 – 15 kV. As the viscosity of the polymer solutions was quite high, we used a 1 wt% solution for the initial experiments

Results are shown in Figure 4.3.

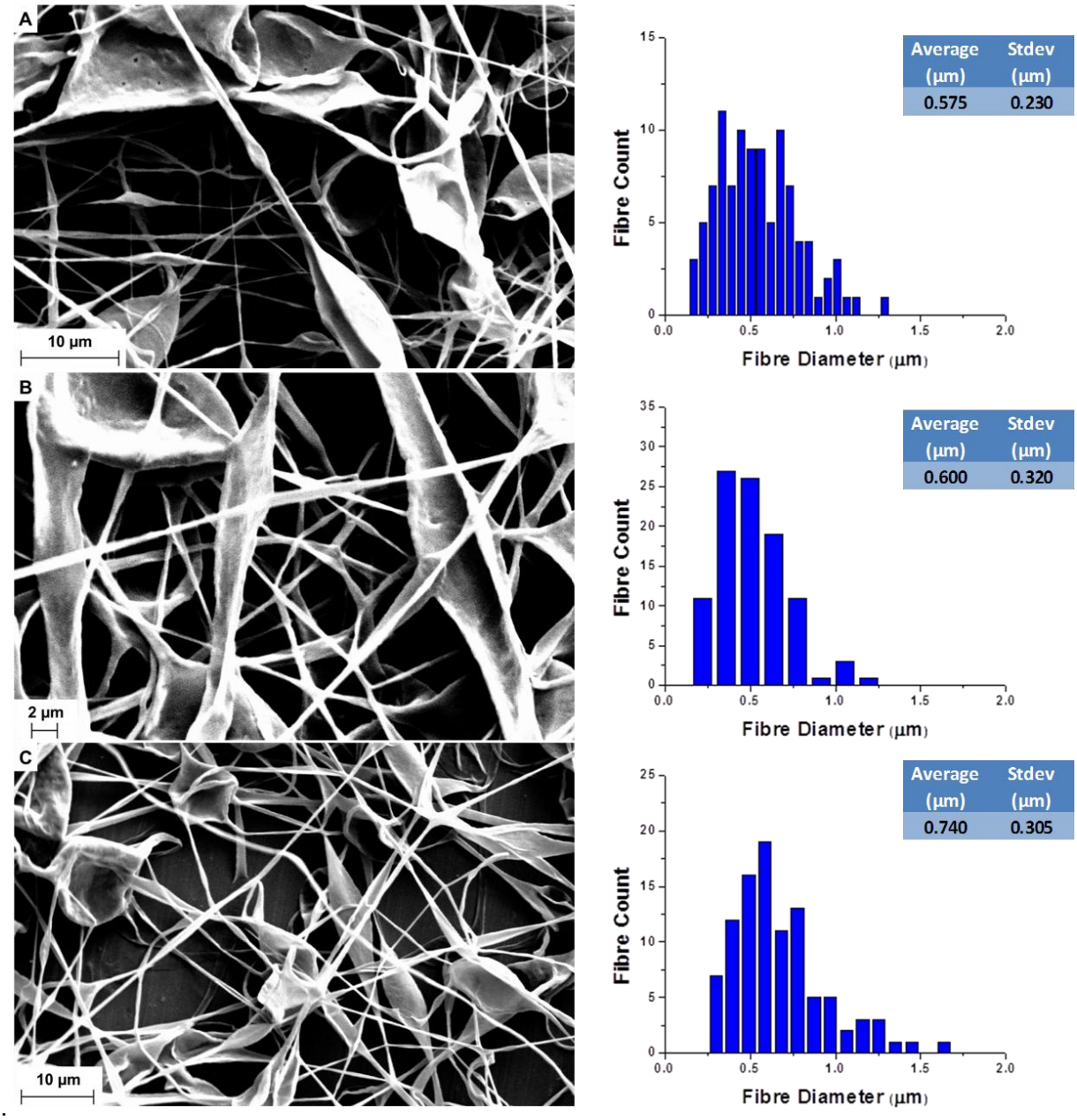

Figure 4.3. SEM images of electrospun PP-1-decene copolymer (10A): A, 10 kV, TCD: 15 cm, B, 15 kV, TCD: 15 cm and C, 15 kV, TCD: 20 cm

Varying the voltage did not have a big effect on the fibre morphology (Figure 4.3, A and B), and the average fibre diameter more or less stayed the same. Baumgarten[11] found that with an increase in the voltage, the fibre diameter goes through a minimum and then start to increase. With an increase in distance (Figure 4.3, B and C), a broader fibre diameter was observed. This was possibly due to the electrical field being too weak at greater distances, leading to less stretching of the polymer solution. For all three examples the fibres were highly beaded, indicating that sufficient stretching of the polymer fibres from solution did not take place and this is due to the solvent combination still not being conductive enough. In addition to that, the 10A polymer had a

significantly higher comonomer content than most of the other polymers (2.3 mole%). This might also influence the solubility of the polymer and thereby hinder the solvent evaporation.

This experiment was repeated using a different polypropylene-co-1-decene, this time with a lower comonomer content (10B, 1.07 mole% 1-decene). The flow rate again was kept constant at 0.05 ml/min and the voltage and TCD was changed. Results are shown in Figure 4.4.

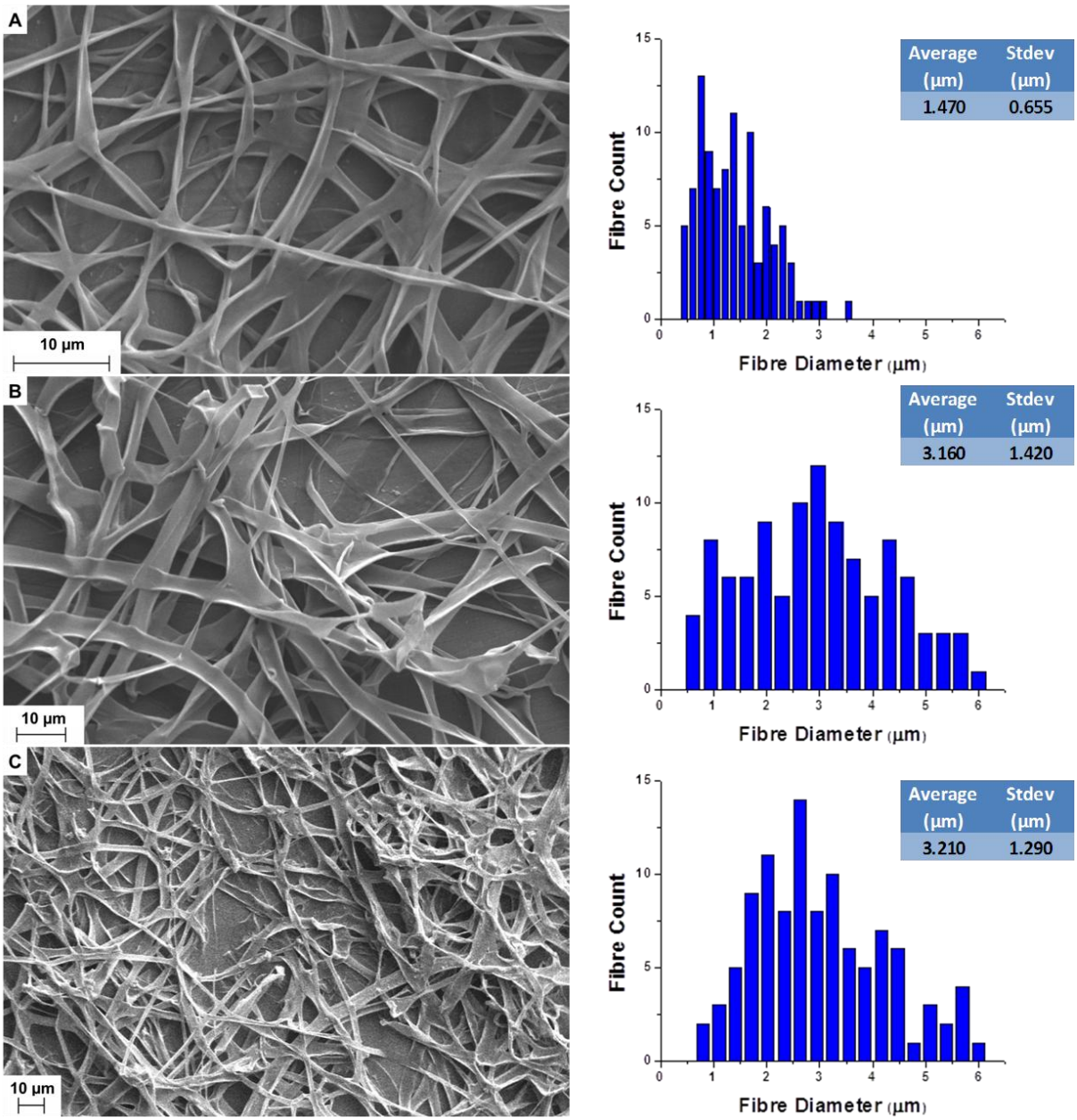

Figure 4.4. SEM images of electrospun PP-1-decene copolymer (10B): A, 10 kV, TCD: 20 cm, B, 15 kV, TCD: 20 cm and C, 15 kV, TCD: 15 cm

The fibre morphology of polymer 10 B is quite a different than that of polymer 10A (Figure 4.4). It was seen that the thinnest fibres were obtained by using the lowest voltage (Figure 4.4, A and B) and the greatest distance (Figure 4.4, B and C). The fibre diameter also tends to increase when

decreasing the distance and this polymer produced beadless fibres. This polymer's molecular weight was much higher and the comonomer content much lower than that of the 10A copolymer. It is obvious that the difference in fibre morphology between the two samples must be due these two factors. However, as there are two parameters that might play a role here, the reason is not completely clear, We do know that molecular weight and solubility plays an important role in the morphology of the fibre. In this case, using the same spinning conditions for both samples, (Figure 4.3, B and Figure 4.4, C), a difference in the fibre morphology could still be observed. Therefore, spinning conditions, in this sample, did not, in our opinion, have an influence on the changes in morphology. What was evident in these fibres was the noticeable branching of the fibres. In solutions with high viscosity, like with these samples, and in high electrical fields, splitting of the electrospinning jet could occur. The evaporation of the solvent and the elongation of the jet my cause changes in the shape of the jet and the jet will become unstable. For stabilization of the jet, a smaller jet will form from the surface of the primary jet[12].

The fibres appeared to be wet and flat. This morphology was also observed by Hsu *et al*[13]. who postulated that this is caused by incomplete solvent evaporation by the time the fibres reach the collector plate. These wet fibres can coalesce or re-dissolve, leading to flat, big fibres. Another reason could be that some solvent is trapped inside the collected fibre and as the solvent evaporates the fibres will collapse, leading to flat fibres[14].

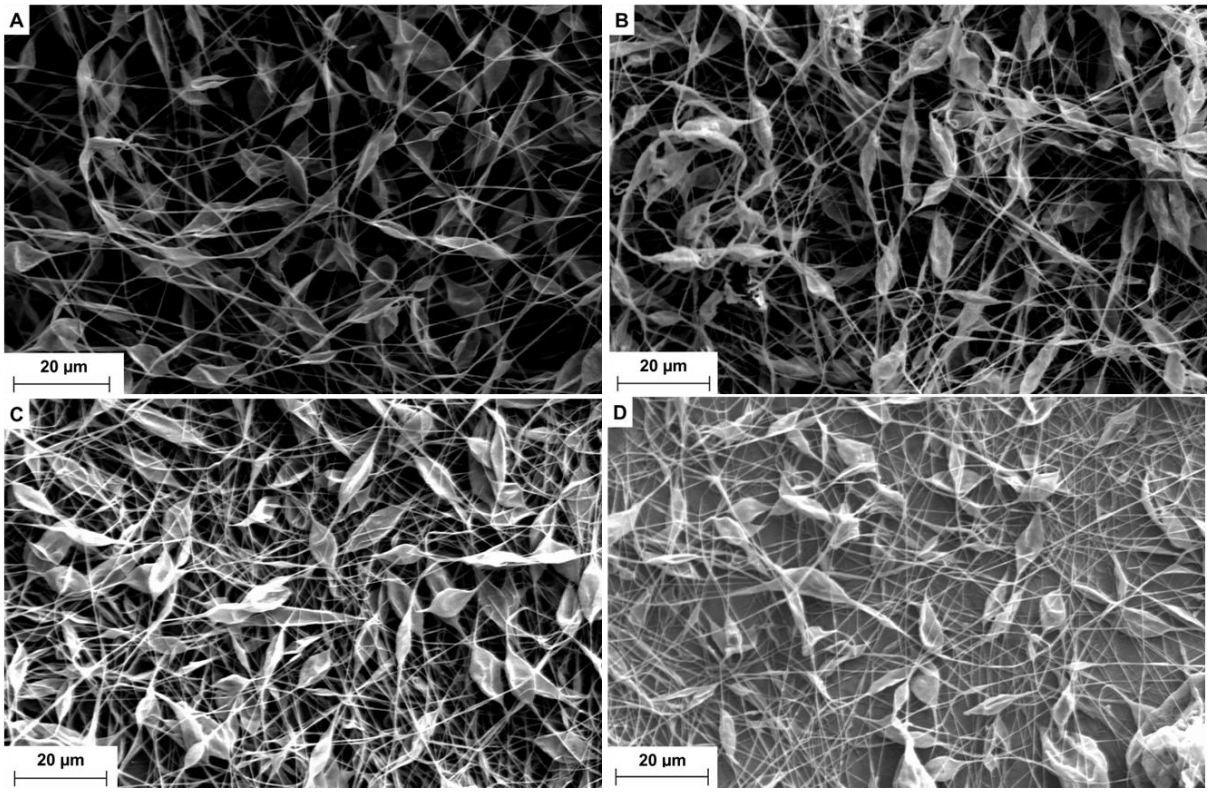

Figure 4.5. SEM images of polymer 10D with a solution concentration of 1 wt% and all spun at a flow rate of 0.05 ml/min A)15 kV and TCD: 15 cm, B) 10 kV and TCD: 15 cm, C) 15 kV and TCD: 20 cm and D) 10 kV and TCD: 20 cm

The next polymer to be electrospun was polymer 10D (Figure 4.5). These fibres were particularly beaded. The occurrence of beads can be attributed to instability of the polymer jet. Later in the chapter the occurrence of beads will be discuss as well as how the changing of the parameters could influence it. The variation of the distance (Figure 4.5, A and C) or the voltage (Figure 4.5, A and B) had no impact on the morphology of the fibres and all the fibres produced were quite beaded. The molecular weight of this polymer is quite low compared to 10B (190 000 g/mol), this will imply there will be fewer chain entanglements in the solution, which may cause the bead formation. This will be discussed in depth later in the chapter. It must be noted that the comonomer content and crystallinity of this polymer also differed from that of 10A and 10B. The crystallinity was quite high (46 % as determined by DSC) and the comonomer content was quite low (0.47 mole%).

What emerged from these experiments is that even small changes in the properties of a chemically identical copolymer have significant effects on the fibres obtained by solution electrospinning. We therefore decided to investigate some of the other copolymers as well.

4.3.3 Poly(propylene–co-1–tetradecene)

The poly(propylene-co-1-tetradecene) copolymer was the next to be electrospun. The first polymer to be electrospun in this series, was 14A (0.5 mole % 1-tetradecene). For this polymer the flow rate was kept constant at 0.05 ml/min and the distance and voltage varied. Results are shown in Figure 4.6.

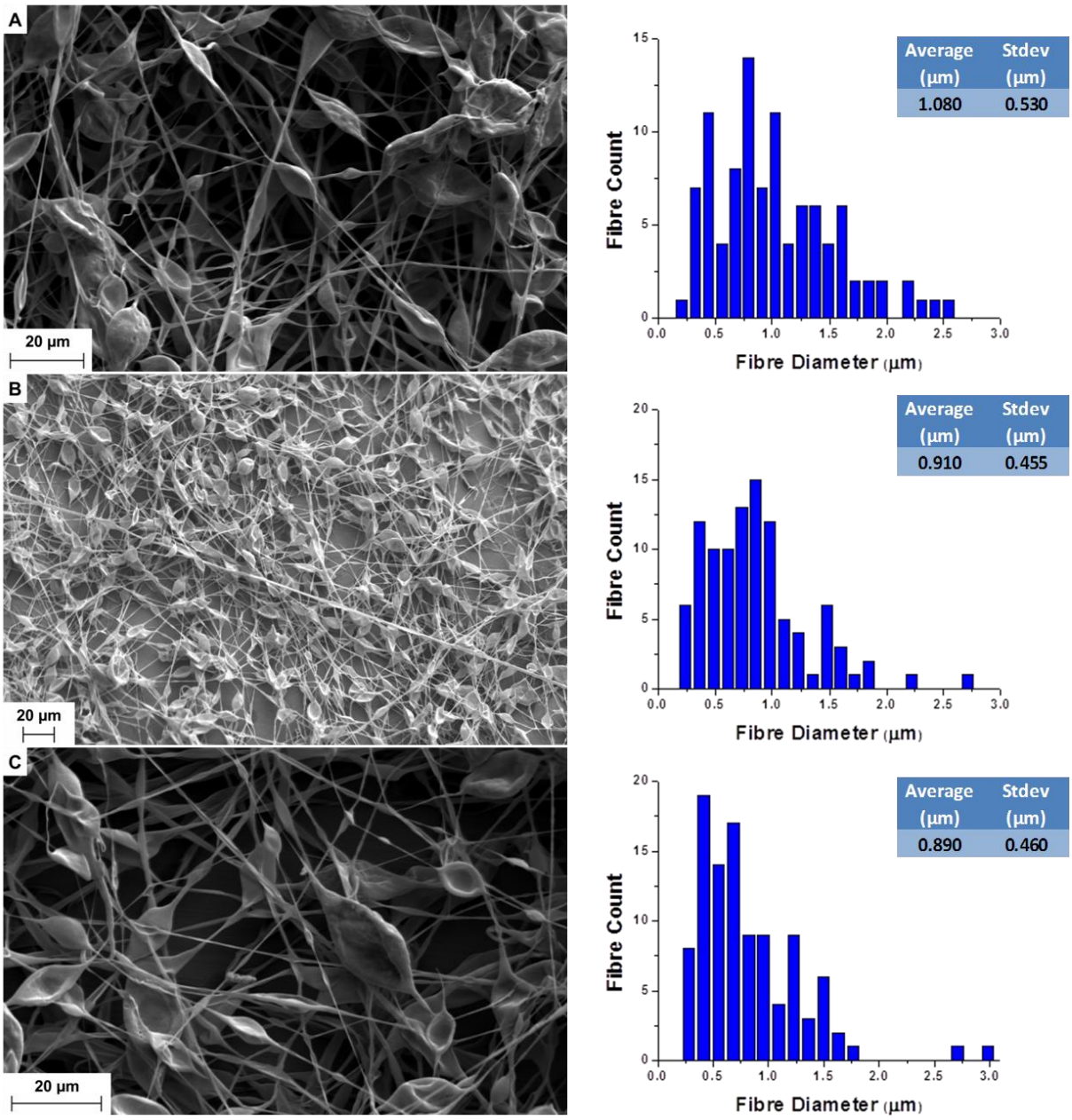

Figure 4.6. SEM images of electrospun polymer 14 A. A) 10 kV, TCD: 15 cm, B) 15 kV, TCD: 15 cm and C) 15 kV, TCD: 20 cm

Neither the distance nor the voltage seemed to make a big difference in the fibre diameter. At higher voltage (Figure 4.6, A and B), there did seem to be a slight decrease in the diameter and at

lower voltage and smaller distance the fibre diameter distribution seemed to be quite broad. In most cases higher voltage will lead to a reduction in fibre diameter, due to better stretching of the solution[15]. It is noticeable that the fibres were very beaded. At this stage it did appear as if copolymer with lower comonomer content resulted in fibres that were more beaded, leading us to postulate that the overriding issue here was solubility. It is clear that a higher comonomer content leads to more soluble copolymers.

The next polymer in this series (14B) could not be electrospun. The molecular weight of this sample is quite low (only 19 000 g/mol. The reason for this is that a low molecular weight sample will be less viscous in a solution and also contain less chain entanglements. Sufficient molecular entanglements are necessary for the material to be stretched as it is moving towards the collector plate[15].

4.3.4 Poly(propylene–co- 1– octene)

Polymer 8D was the first polymer to be electrospun in this copolymer series. The flow rate was kept constant at 0.05 ml/min, and the TCD and the voltage varied. Results are shown in Figure 4.7.

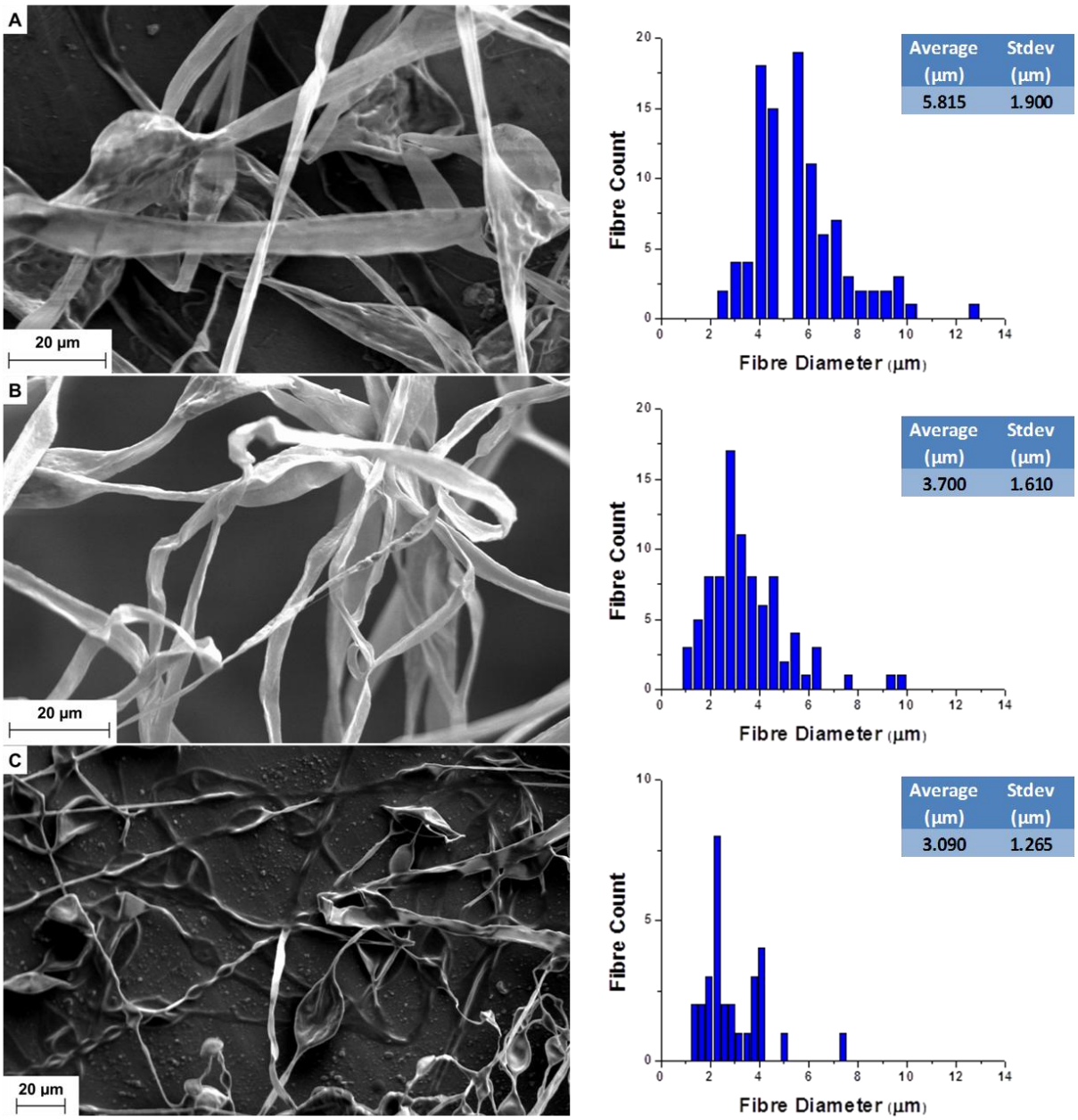

Figure 4.7. SEM images of 8D. A) 10 kV, TCD: 20 cm, B) 15 kV, TCD: 20 cm and C) 10 kV, TCD: 15 cm

For this sample (Figure 4.7) at shorter distances (Figure 4.7, A and C), fibre formation was inadequate in addition to the fibres being wet. Increasing the distance to 20 cm improved the fibre formation. At higher voltages (Figure 4.7, A and B) less beaded fibres were produced. Yet beading still occurred, as in the case of the other copolymers with low comonomer content. The reason for this is twofold; 1) At higher voltage more charges are carried by the jet. This will lead to the jet being stretched more and the formation of thinner fibres, 2) At high voltage the occurrence of a secondary jet can take place, leading to thinner fibres [15]. The next copolymer used was 8A (Figure 4.8).

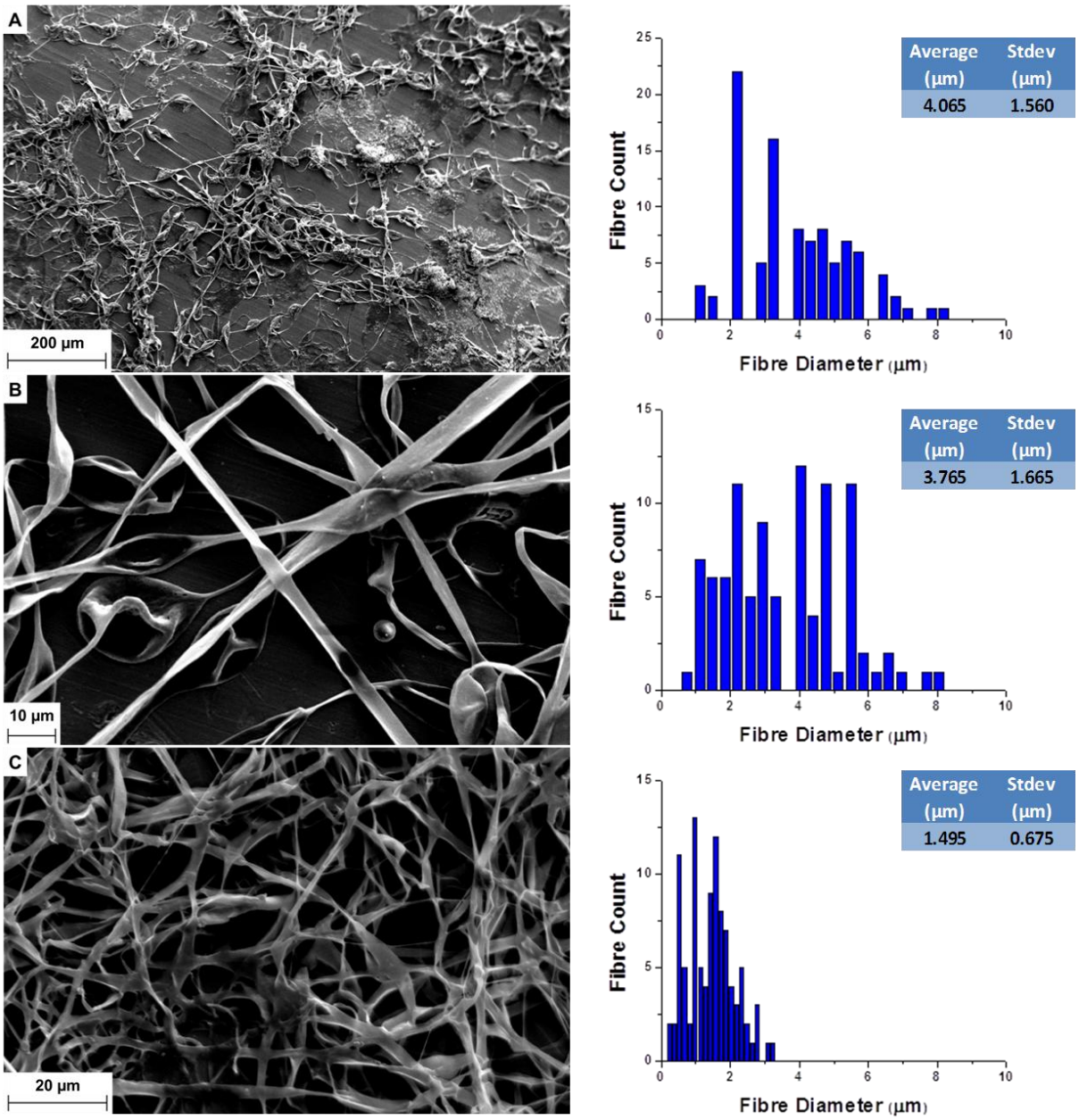

Figure 4.8. SEM images of electrospun polymer 8A. A) 10 kV, TCD: 15 cm, B) 15 kV, TCD: 15 cm and C) 20 kV, 15 cm

Up and till this point electrospinning could only be performed till 15kV, however, for this sample a new voltage supply was used, allowing the use of higher voltages. For polymer 8A (Figure 4.8) the same phenomenon was found regarding the increase in the voltage. The fibre morphology improved with an increase in voltage and the fibre diameter decreased. This sample, however, produces much thicker fibres than sample 8D. When comparing the molecular weight and commoner content of 8A and 8D, 8D has a much higher molecular weight. The higher the molecular weight, the more molecular entanglements will be present in the solution. These molecular entanglements will cause the jet to be stable [15, 16]. It was not possible to determine the viscosity of these samples, since the nature of the solutions changed over time. It could be

observed though that polymer 8D was more viscous than 8A. The viscosity of the solution is related to the molecular entanglements in that solution. A more viscous solution will have more entanglements, which in-turn will lead to stable jet formation. Therefore, a solution with a higher viscosity will produce fibres with a smaller diameter [17, 18].

4.3.5 Influence of the different parameters on the fibre diameter

A lot of research has been done on the influence of the different parameters on the fibre morphology and many of the reported results seem conflicting. It does however appear that for different polymers, different results have been obtained.

Since the copolymers of each range behaved so differently compared to each other, the influence of the parameters on each copolymer range were investigated. From the initial results it seems clear that the amount of comonomer, the comonomer type and the molecular weight (and maybe even the molecular weight distribution) all affected the fibres that were obtained.

The copolymers with different types of comonomer were compared; with one sample taken from each range. The first parameter to be investigated was the influence in the change of the voltage; the other two parameters were kept constant. We compared 8A (0.86 mole % comonomer, molecular weight 500 000 g/mole), 10B (1 mole % comonomer, molecular weight 470 000 g/mole) and 14 A (0.5 mole %, molecular weight 310 000 g/mole). Results are shown in Figure 4.9.

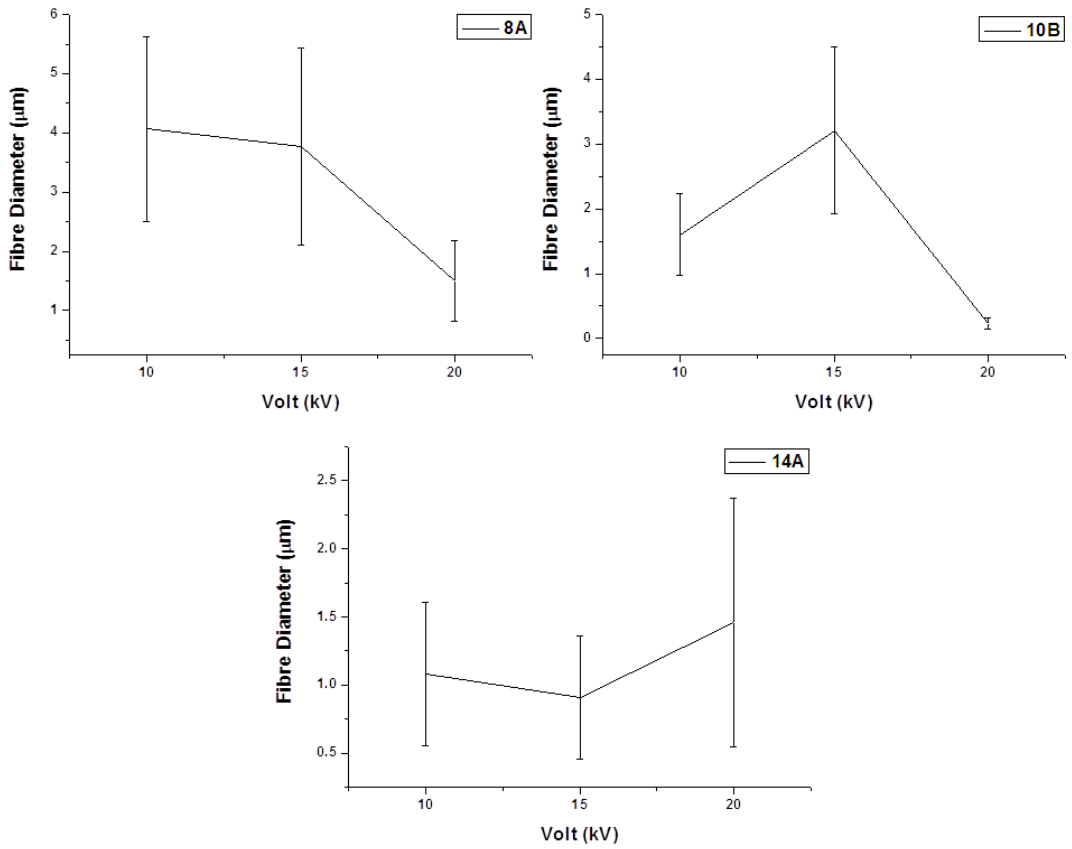

Figure 4.9. Influence of voltage on the fibre diameter for the different copolymers

Looking at Figure 4.9, for the 8A sample there is a decrease in the fibre diameter as the voltage increases. The greater voltage causes more charges to be carried by the jet and, therefore, the solution will undergo more stretching, producing thinner fibres. The solution we used may also be of lower viscosity and this may cause a secondary jet to be formed and this will encourage the formation of thinner fibres[19].For sample 14A an increase in voltage from 10kv to 15kV, showed a slight decrease in the fibre diameter. The increase in charges due to the higher voltage will encourage the stretching of the jet. However, when increasing the voltage to 20kV, there is a significant increase in the fibre diameter. At high voltage the electrical field could be unstable, which in-turn will influence the stability of the jet. An unstable jet causes an increase in the fibre diameter. Sample 10B was the one polymer that behaved quite different. To interpret the fibre diameter for this polymer was quite difficult, as these fibres were particularly beaded.

When regarding the influence of the flow rate (Figure 4.10), the copolymers again behaved differently. It has been reported that the flow rate has little or no effect on the fibre diameter[19]. However, since these polymers behaved so differently with respect to each other, it was thought worthwhile to investigate this parameter. Polymer 10B yet again did not follow any trend as regards to the flow rate. Even at these flow rates, the fibres stayed beaded and the thin fibres were in-

between enormous beads. For 8A the fibre diameter decreased slightly as the flow rate increased. For flow rates higher than 0.05 ml/min there was a slight increase in the fibre diameter, but this increase is relatively insignificant, especially when looking at the standard deviation of each sample.

Polymer 14B exhibited an increase in the fibre diameter as the flow rate increases. With an increase in flow rate, more polymer will be present at the tip of the needle. More material will led to thicker fibres being produced. Also, at a higher feed rate and more polymer, the solvent evaporation might be inadequate and wet fibres will be collected. The fusing of these wet fibres, will lead to a broader fibre diameter.

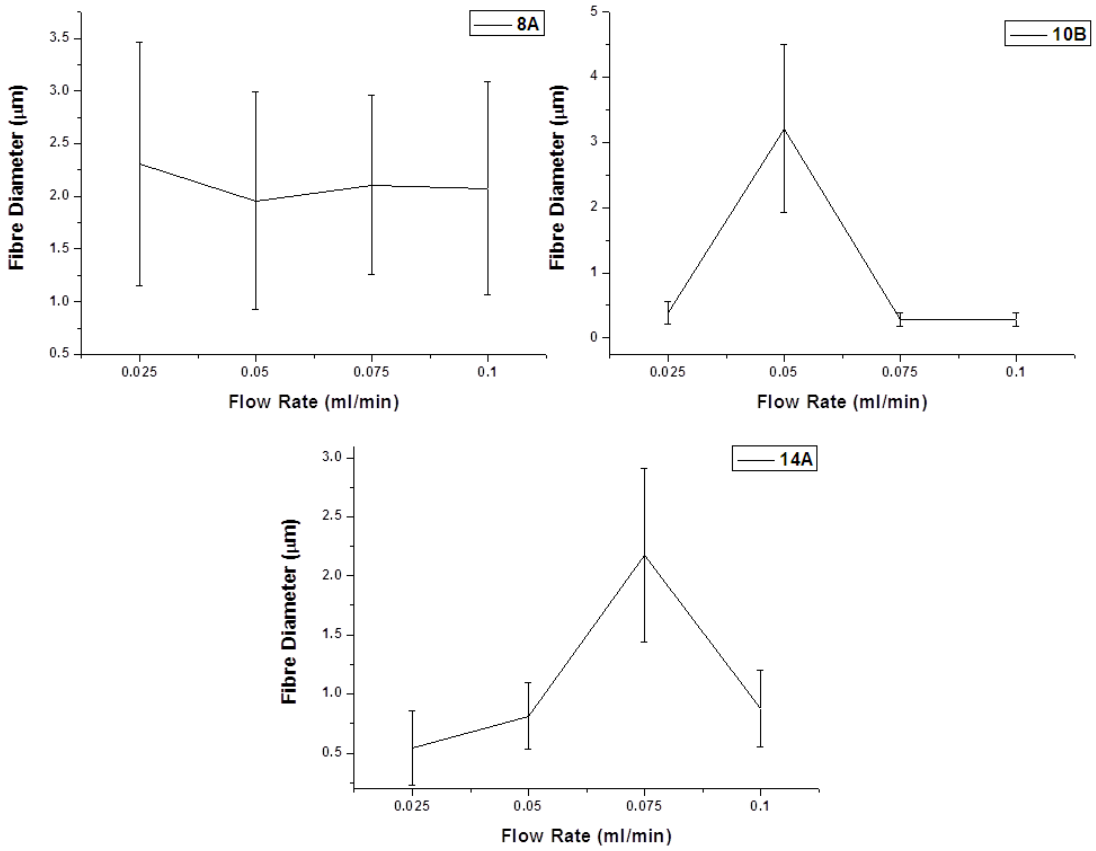

Figure 4.10. Influence of different flow rates on the fibre diameter for the different copolymers

Last, the influence of the distance between the needle tip and the collector was investigated (Figure 4.11). Again it should be noted for 10B, although there is a big difference in the fibre diameter, the fibre was really beaded. The optimum spinning parameters for this polymer was determined to be at 15 cm, 15 kV and a flow rate of 0.05 ml/min.

For sample 14B a slight increase in fibre diameter with an increase in distance can be seen. Again the standard deviation for each distance is relatively big, making this increase minor. For polymer 8A, this increase in diameter with distance is more prominent. In most cases, the fibre diameter

decrease with an increase in distance. This is due to the polymer having more time to be stretched before reaching the collector. In our case, the increase might be explained if it is assumed that the distance becomes too large, and coupled with the low conductivity of the solvent system, the electrostatic field strength weakens to the point where elongation of the jet no longer occurs[19]. This is clear in the jump in fibre diameter between 15 cm and 20 cm for 8A.

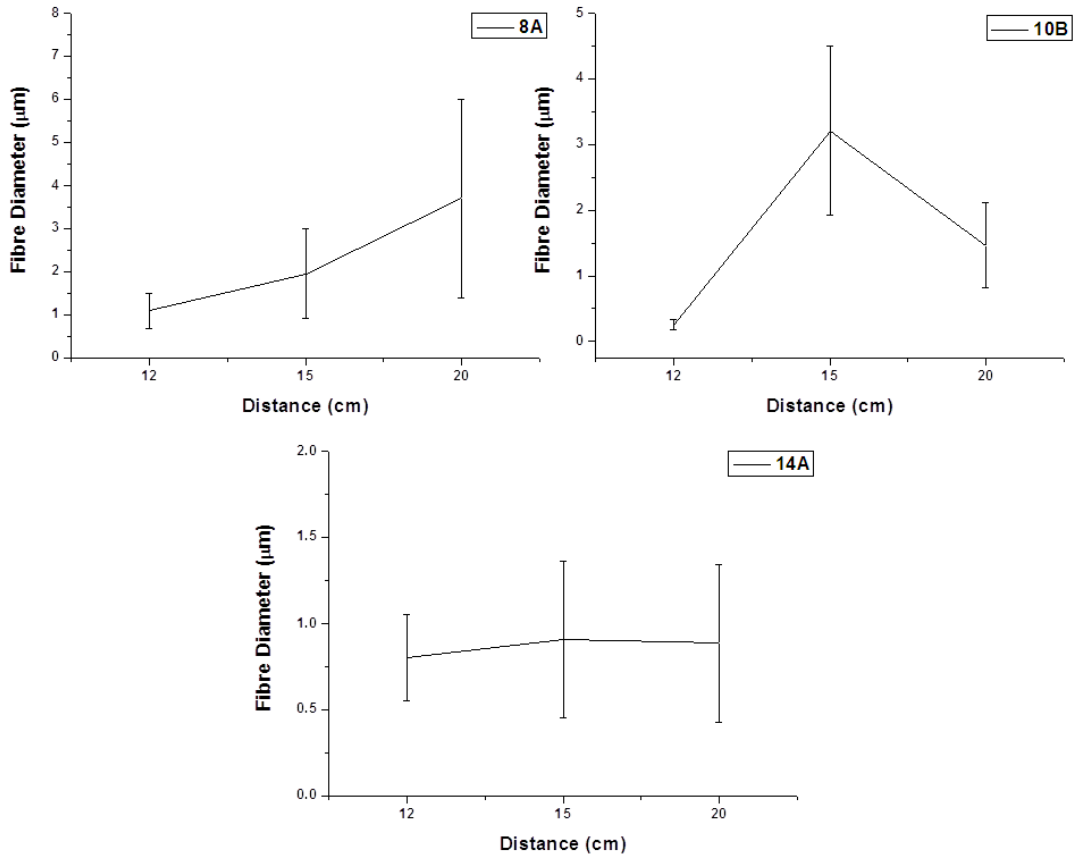

Figure 4.11. Influence of the distance on the fibre diameter of different copolymers

What is quite clear form these results is that there are big differences between the individual copolymers with respect the effect of varying the spinning conditions. The difference between these copolymers is their molecular weight, comonomer content and crystallinity. These results indicate that those factors play a very important role in the electrospinning process. Nevertheless, we were able to electrospin the crystalline, high molecular weight propylene copolymers.

4.3.6 Influence of different collectors

All the samples above were spun unto metal foil. Fibre morphology could be changed by using different collectors; therefore, water, ice and a rotating collector were also investigated as possible collectors. The idea behind the water and ice was that when the fibres were collected on a colder

surface, the polymer might crystallize more rapidly, preventing the collapsing of the fibres. In the example in Figure 4.12 below, polymer 8A were used in a 0.5 wt% solution. The flow rate was 0.05 ml/min, voltage 10 kV and the distance 20 cm.

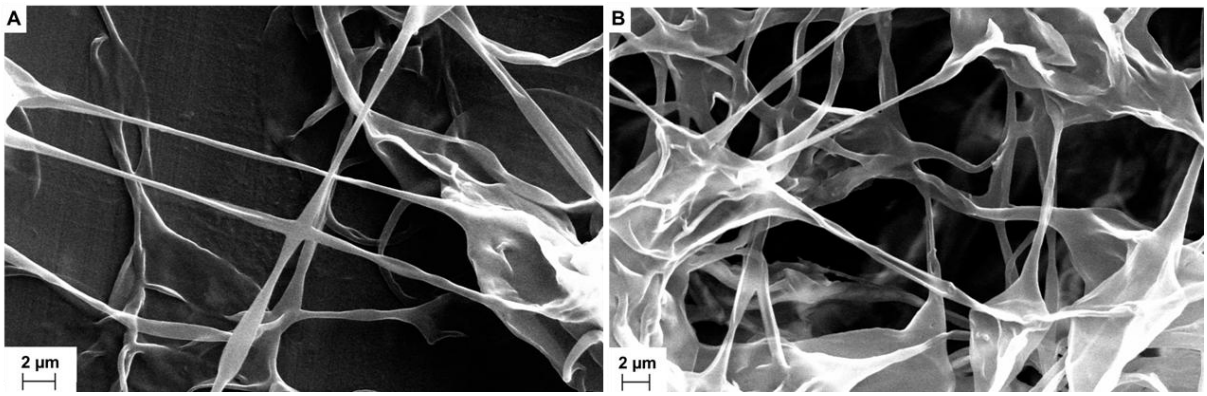

Figure 4.12. SEM images of polymer 8A. A) Spun unto foil and B) spun unto water

When comparing the two samples (Figure 4.12), not much difference was seen when spinning unto foil. The fibre morphology still appeared to be collapsed and beaded.

It was concluded that foil is still a better collector than the water, since it was a struggle to collect the fibres from the water and the fibres had to be dried to get rid of the water. In the next experiment the foil was placed on ice with salt, to try and cool the collector surface even more. The foil needed to cover the ice, otherwise the polymer tended to spin towards the ice and not the foil. Lastly the fibres were directly spun unto the ice and scooped off the water, when the ice had melted. As with spinning onto water, the fibres were dried in a vacuum oven. All three these samples (Figure 4.13) were spun at a flow rate of 0.05 ml/min, 15 kV, at a TCD of 15 cm and a solution concentration of 2wt%.

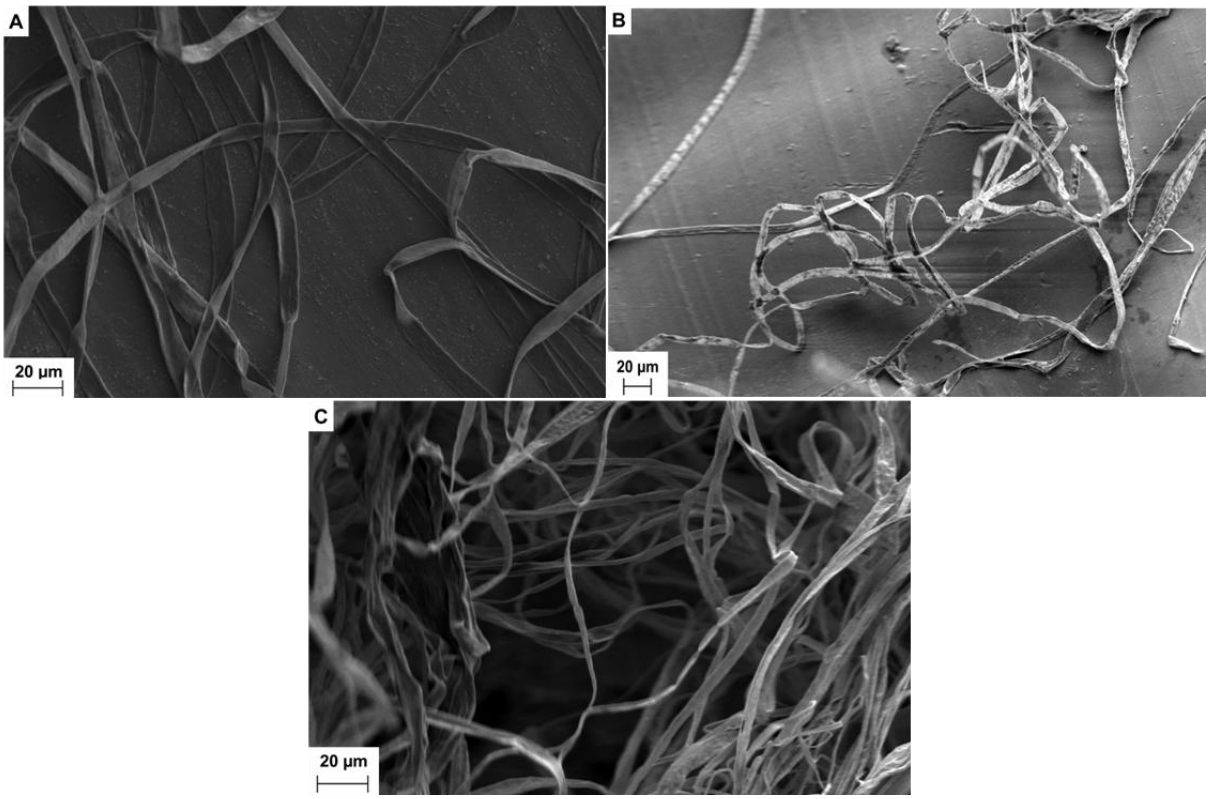

Figure 4.13. SEM images of polymer 10B. Spun unto A) Foil, B) foil on ice and C) ice

Again there was not a considerable difference in the fibre morphology of the polymer when using the different collector surfaces. The only difference could be seen in the fibre diameters, indicated in Table 4.5. Spinning on to ice produced the thinnest fibres, probably due to the fact that the polymer crystallized, producing thinner fibres. This collector, however, was not feasible since the fibres tend to spin to other surfaces as well as the ice. In addition, collection of the few fibres that collected on the ice was quite difficult.

Table 4.5 Fibre diameter on the different collectors

Sample	Fibre Diameter (µm)	STDEV
Foil	6.138	1.88
Foil on ice	6.688	1.93
Ice	4.118	1.79

Experiments were also performed using a rotating collector. In Figure 4.14 the SEM images of polymer 8A spun on to a static and on to a rotating collector can be seen.

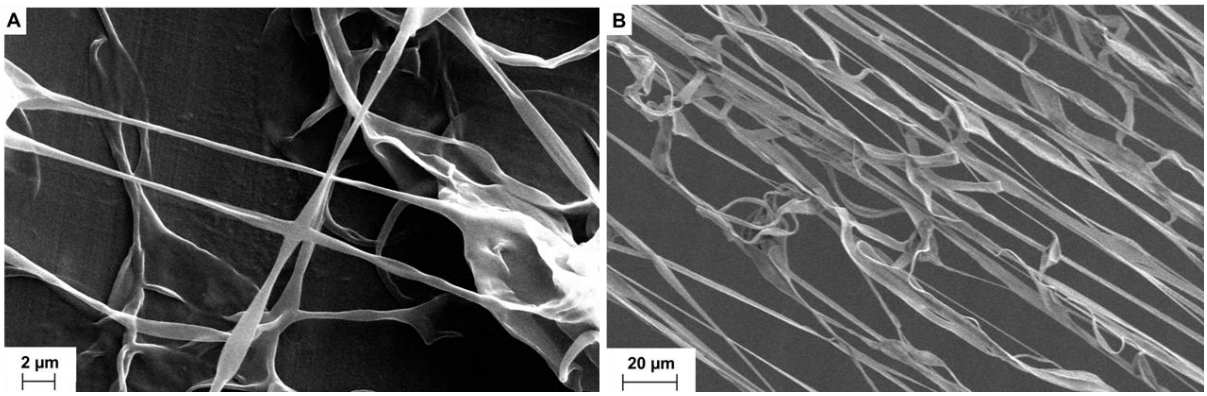

Figure 4.14. SEM images of polymer 8A, 1.5 wt%, TCD of 15cm, 15kV and 0.1 ml/min on A) Static collector and B) Rotating collector

By using the rotating collector the fibres are less beaded. The absence of beads can be attributed to the better stretching of the fibres on the rotating collector. Better solvent evaporation would also lead to a less collapsed structure.

From experimenting with different collectors it could be concluded that a colder surface won't prevent the collapsing of the fibres. However, a rotating collector did produced fibres with a better morphology.

4.3.7 Beaded fibres

Many of the copolymers used in this study showed the occurrence of beads when electrospun. There are a few factors that influence the formation of beads and the most important ones being the solution concentration or the viscosity of the solution, the surface tension of the solution and the net charge density which is carried by the jet. The higher the viscosity the less the chances of bead formation, the same goes for the net charge density. Reducing the surface tension will encourage less bead formation as well [20]. There are also some processing conditions that will influence the bead formation. Below I will only discuss a few factors that tend to influence the formation of beads.

4.3.7.1 Solution concentration and surface tension

Some research has been done on the formation of beads by changing the concentration of the solution or the solvent [21]. Fong *et al* [20]. found that with a low solution viscosity you will see the occurrence of beads, as the viscosity of the solution increases the beads becomes elongated and change shape, then at a certain viscosity all beads disappear. Ramakrishna [15] explained it by saying that the surface tension decreases the surface area per unit mass. So when there is a high concentration of free solvent molecules, which is the case with a low solution concentration, the solvent molecules tend to agglomerate and the surface tension will then cause the molecules to

assume a spherical shape. With a higher concentration there is more interaction between the polymer molecules and the solvent molecules. Now when the solution is stretched, the solvent molecules will not agglomerate but rather expand over the entangled polymer molecules. In our case the solution concentration was not very high, but the solution viscosity was. This should lead to more chain entanglements and therefore we could have expected bead-free fibres [22]. This was clearly not the case, indicating that solution concentration or viscosity was not the parameter that was causing the bead formation.

4.3.7.2 Conductivity of the solution

When the solution becomes more conductive, more charges can be carried by the jet. This will increase the stretching of the solution, which in turn will decrease the changes of bead formation [15]. The conductivity of the solution can be increased by using a more conductive solvent or by adding ions to solution. Since the solvent system used in this study was not that conductive, this might be the main reason for the beads that are forming.

4.3.7.3 Voltage

Mixed results have been obtained for the relationship between voltage and bead formation. Jarusuwannapoom *et al* [23]. found that the bead formation decrease with an increase in voltage. When the voltage increases, more stretching of the solution will take place, leading to fewer beads being formed along the fibre axis. Some researchers, however, found that when the voltage increases, the tendency of bead formation also increases[18, 24, 25]. The shape of the beads will also change to a spherical form when the voltage increases. The explanation for this is that at high voltage the Taylor Cone may draw back into the needle, leading to an unstable jet, which in turn will lead to bead formation [15, 18].

In our case changing these factors proved to be quite difficult. Since our polymer required a very specific solvent system and the weight concentration was already low, but an increase was not possible, due to viscosity problems when electrospinning. Some researchers also found that when the solvent evaporation is not sufficient beads will also occur[13]. This might also play a role in the bead formation during the electrospinning of the copolymers. All the solvents used in our solvent system, with the exception of the acetone, have high boiling points and therefore will not evaporate that easily during electrospinning. One way to improve the conductivity of the solvent without changing the solvent or the solvent combination is by adding an ionic salt [26].

Zong *et al* [25]. reported that when adding salt to the solution, the charge density of the surface that is ejected will increase and therefore more electrical charges will be carried by the jet. The electrical field then impose higher elongation forces on the jet and the bead formation is decreased [12].

We therefore tried different types of salt to find one that would dissolve in our solvent combination. Simply mixing the salt with the solvent combination prior to dissolution of the polymer was not successful. None of the salts we tried dissolved. Next the salt was first added to the one solvent, in our case DMF, until it dissolved and then the polymer and the other solvents were then added.

Table 4.6. Solubility of salts in different solvents

Salt	Weight %	Solvent	Dissolved
KCl	1	Cyclohexane/ Acetone/DMF	×
NaCl	1	Cyclohexane/ Acetone/DMF	×
$CaCl_2$	1	Cyclohexane	×
$CaCl_2$	0.5	Cyclohexane	×
$CaCl_2$	0.5	DMF	Dissolved until other solvents were added
LiCl	0.5	DMF	✓

LiCl was the only salt that worked with our solvent system. LiCl is also one of the salts used the most to enhance the conductivity of a solution for electrospinning [21, 26, 27].

In this section we will only show the results obtained by using one polymer of the poly(propylene-co-1-octene) range, 8B.

The initial electrospinning, in cyclohexane/acetone/DMF, did not work that well. The fibres were beaded and seemed wet, indicating bad solvent evaporation. LiCl was then added to the polymer solution.

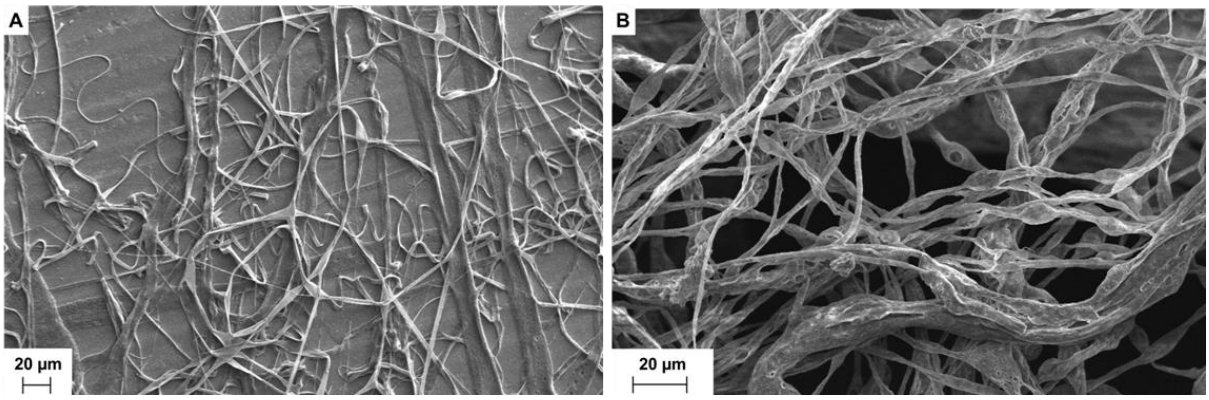

Figure 4.15. SEM images of polymer 8B A) spun without salt and B) spun with 2 wt% LiCl

Looking at Figure 4.15 it is clear that by adding the salt there is definitely change in the morphology of the fibres. They are still beaded, but the solvent evaporation seems better, since the

fibres are not that wet. The addition of salt may change some aspects of the fibre morphology. Some researchers found, that by adding salt, the diameter of the fibres might increase [26, 28]. The explanation for this is that with the addition of salt the net charge density increases and this will lead to more polymer moving towards the collector, producing thicker fibres. Looking at the two samples in Figure 4.15 sample A has a fibre diameter average of 4.02 μm and the sample B a diameter average of 2.64 μm. So for this sample the addition of salt decreased the fibre diameter of the electrospun polymer. Articles also have been published where it was shown that the addition of salts did decrease the fibre diameter[19, 29]. Since the salt increases the conductivity of the solution, it means that the solution will undergo more stretching and the jet will also be whipped more, leading to fibres with a smaller diameter. However, too much salt may also cause the uniformity of the fibres to decrease and may cause bead formation. There are three forces present while electrospinning, viscoelastic, surface tension and electrostatic force. If too much salt is added, the ionic strength will be increased and this could cause an imbalance in the three forces, which in turn will lead to an unstable jet causing non uniform fibres [19].

Since the polymer seemed to spin more easily when adding the salt, it was thought that a different solvent combination could be used, with solvents in which our polymer will dissolve easier. Figure 4.16 shows fibres produced where only cyclohexane and DMF (80/20) were used, since acetone was added to the previous solvent system to increase the conductivity. The salt will, therefore, take over the role of the acetone, which is a non-solvent for the polypropylene copolymers. The different solvent system did not work since it seemed the fibres tended to agglomerate together. So it would seem that 3-solvent system is still the best to use.

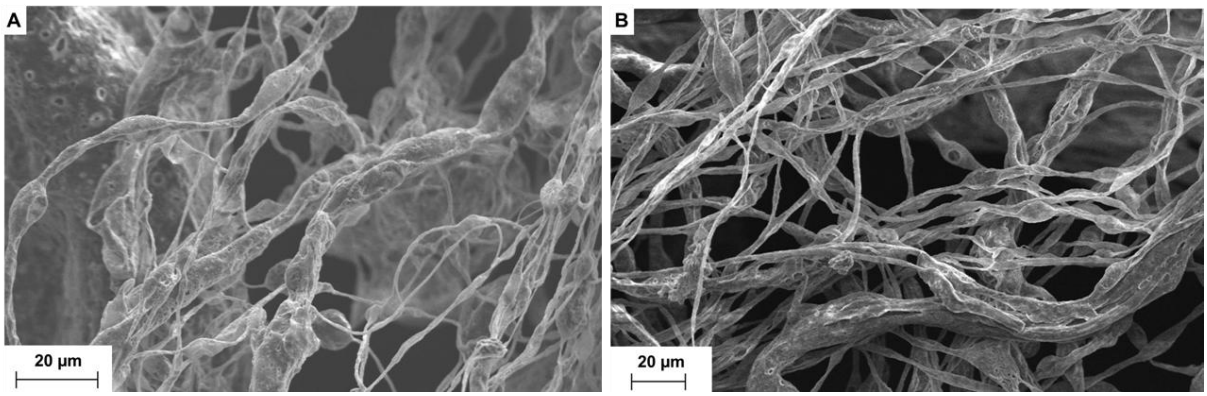

Figure 4.16. Polymer 8B in cyclohexane/DMF (80/20) with A) 2 wt % LiCl and B) 1 wt% salt

The next objective was to find the optimum amount of salt to use, since the salt did influence the fibre morphology it would be better to add the least amount as possible.

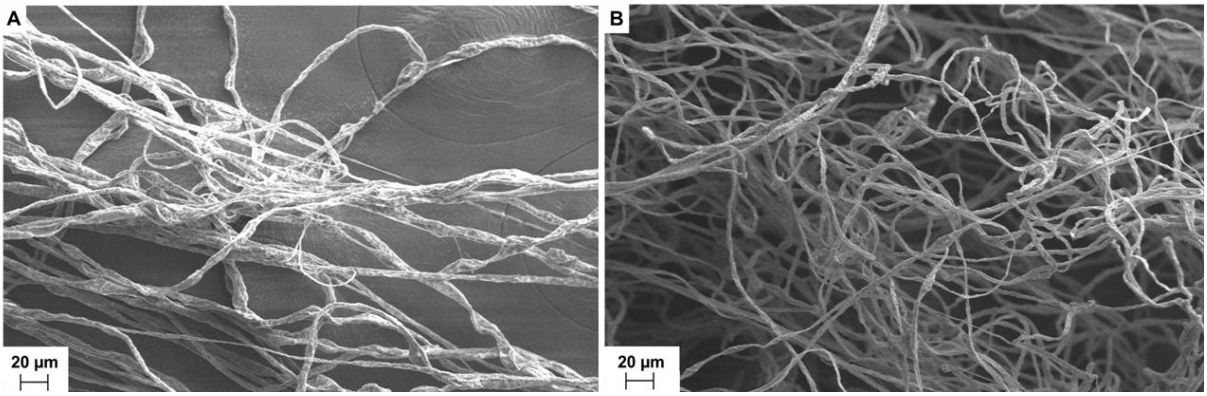

Figure 4.17. Polymer 8B A) 1 wt% LiCl and B) 0.2 wt% LiCl

The morphology of the fibres looks smoother and beadles with the addition of the salt and even with only just 0.2 wt% salt the fibres still seem bead free. The fibre morphology also seemed smoother when less salt added. The LiCl improved the fibre morphology leading to smooth, bead-free fibres with the addition of only 0.2 wt% salt.

4.3.8 Melting and crystallinity differences

One of the aspects of using fibres is how their crystallinity and thermal properties differ from the original polymer. Some articles have been published regarding the crystallinity of the fibres. It is said that as the fibre forms, a small part will crystallize to form lamella and the rest of the material will be amorphous. When the fibres are subjected to the shear forces during electrospinning, the lamella will form fibrils and the tie-molecules will go through the adjacent crystals and small bundles will be formed. Konkhlang *et al* [30]. found that the nanofibre comprise of nanofibrils that are lined up parallel to the fibre axis [14]. In this study WAXD and DSC was done to look at the difference between the melting and crystallinity properties of the fibres and the pure polymers. The data differed for the different copolymers.

WAXD analysis was done to investigate the influence of electrospinning on the type of crystal structure in the material. For a poly(propylene-1-octene) copolymer (8B) the WAXD spectra of the polymer and the fibre are shown in Figure 4.18.

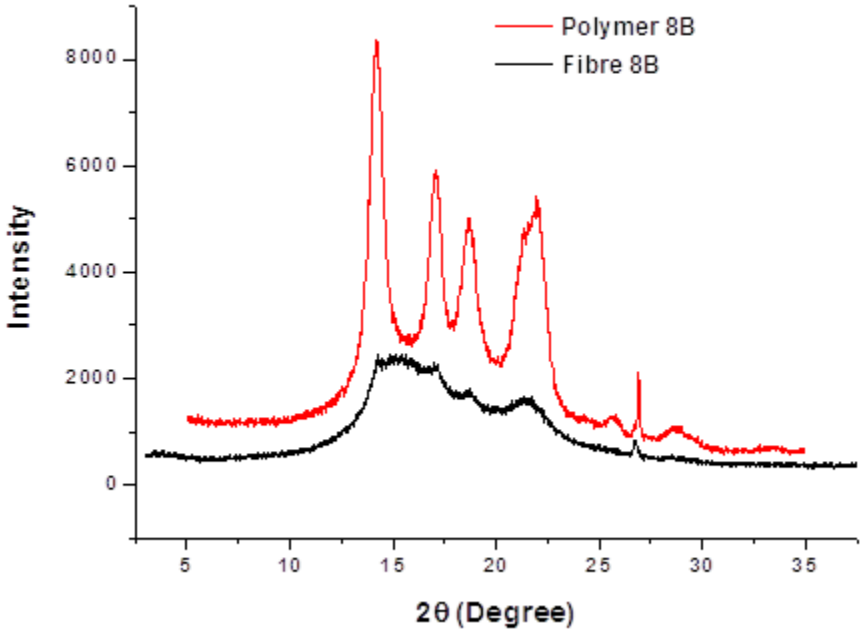

Figure 4.18. WAXD spectrum of polymer 8B

It seems that the same crystal structure is present in the fibre as in the polymer powder for polymer 8B (Figure 4.18. WAXD spectrum of polymer 8B). However, the peaks of the powder are much sharper and more defined, where as those of the fibre are much broader. This is an indication that the crystalline order in the fibre was reduced [18]. There are 4 defined peaks present in the powder sample. All these peaks are an indication of the alpha phase crystal form present in the polymer powder. It seems that mostly alpha phase crystals are present in the fibre. The broad peak of the fibre at about 15-16° may indicate the presence of beta phase crystals.

For polymer 14A (Figure 4.19), we can see the disappearance of peaks, indicating that the crystal structure of this polymer did change. Again the peaks for the fibres are much broader that those of the powder, indicating the decrease in the crystalline order. Again the 4 alpha phase crystal form peaks are quite clear in the polymer powder, but not as clear in the fibres.

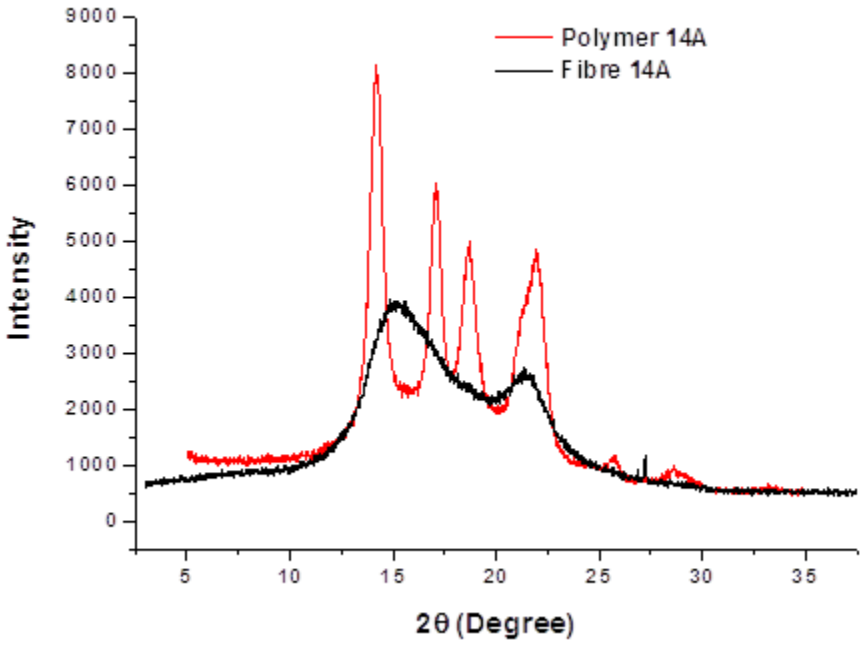

Figure 4.19. WAXD spectrum of polymer 14B

Polymer 10B behaved quite different from the other two copolymers. No conclusions could be made from the WAXD spectra of this polymer.

The crystallinity was calculated by using the following equation

$$D_{Crystallization} = \left(\frac{Area\ crystallization\ peaks}{Area\ crystallization\ peaks + Amorphous\ area}\right) \times 100 \quad 4.1$$

The crystallinity difference between the powder and fibre is reflected in Figure 4.20.

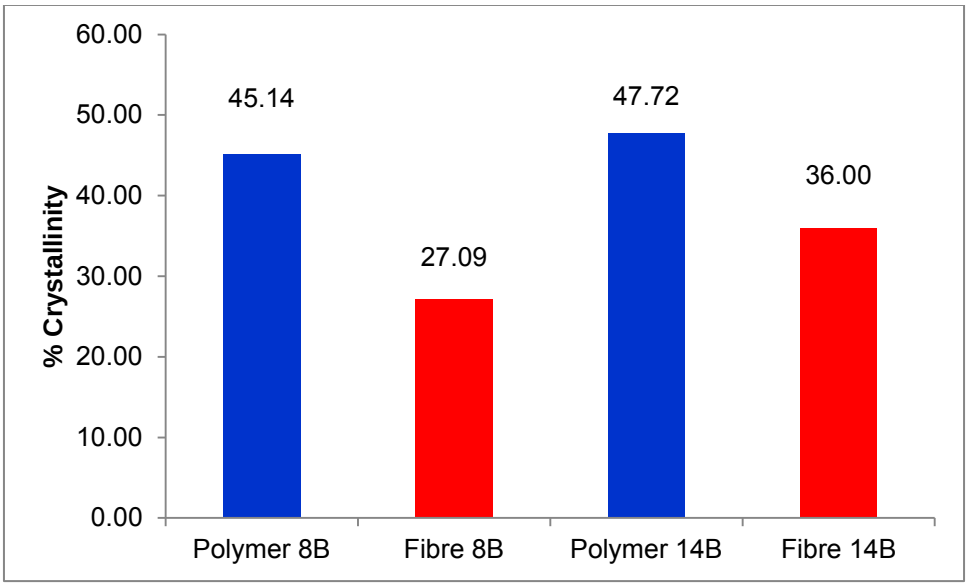

Figure 4.20. Difference in crystallinity between the polymer powder and fibre for polymer 8B and 14B

For both these samples the crystallinity decreased notably when in fibre form. The reason for this is that even though the polymer under goes stretching during the electrospinning process, the distance in which it travels is too short for the crystals to align before it reaches the collector plate and dries. The solvent evaporation usually takes place so quickly that the polymer does not get time to form crystals. This leads to the fibres having a decreased crystallinity compared to the pure polymer[14,31]. This phenomenon has been observed by other researchers as well [14, 18]. The length of the side chains of the copolymer could also prevent rapid crystallization during electrospinning. The DSC melting peaks (first scan) for the powders and the fibres were also obtained. These are shown in Figure 4.21.

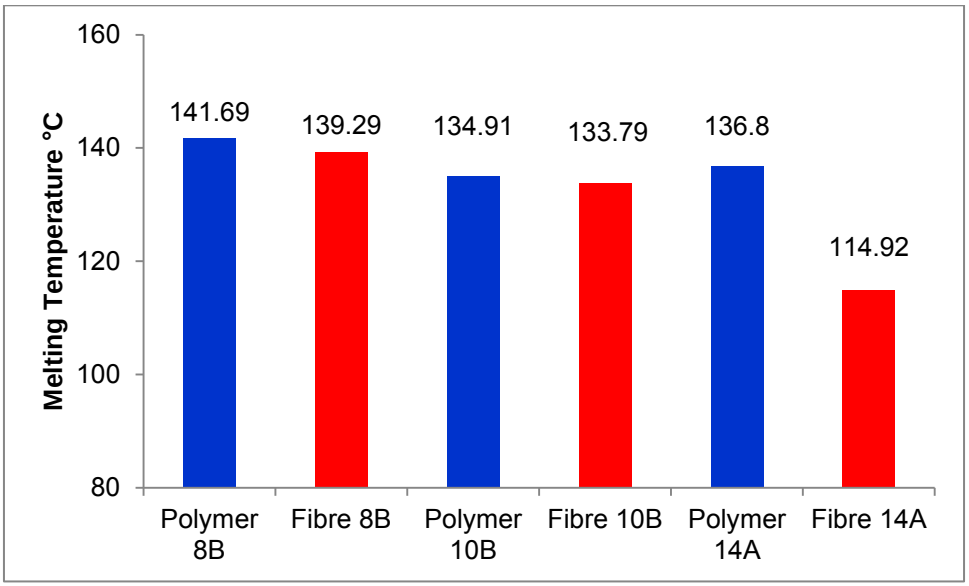

Figure 4.21. Difference in melting temperature between polymer powder and fibre

The melting temperatures of the powders and fibres were determined by DSC. When considering the melting temperature difference between the powders and fibres, there is not a noticeable difference for polymer 8B and 10B. However, Polymer 14A exhibits a noticeable drop in the melting temperature between the powder and fibre. The length of the comonomer could play an important role regards to how the polymer crystallize during electrospinning which in the end can influence the melting temperature.

4.3.9 Solution melting temperature

As can be seen from the results, these polymers could be electrospun quite successfully when using the cyclohexane/DMF/acetone solvent system. A commercial isotactic PP could, however, not be electrospun from this solvent system, under the conditions that we used.

To try and explain why the copolymers worked and not the isotactic polypropylene, the crystallinity, molecular weight, comonomer content and solution melting temperatures of each polymer were examined. In Table 4.7, data relating to copolymers of propylene and 1-alkenes and isotactic polypropylenes are given. Note that PPC8 relates to sample 8B, PPC10 is sample 10B. Samples PPC14 and PPC18 were not electrospun during this study. These samples are merely listed here to point out an interesting phenomenon.

Table 4.7. Molecular weight, thermal and comonomer data for the different copolymers

Polymer	Comonomer (mole%)	Mw[a)]	PD[b)]	Tm[0c)] °C	Tm[d)] °C	Xc[e)] %
PPC8	1-Octene (0.9)	506700	2.4	139.8	87.7	25.4
PPC10	1-Decene (1.0)	467300	2.3	138.6	85.4	28.4
PPC14	1-Tetradecene (0.9)	639200	2.5	134.1	82.3	26.5
PPC18	1-Octadecene (1.0)	631000	2.3	131.4	80.3	35
iPP 1		420500	4.8	161.4	106.3	51.1
iPP 2		468000	2.4	145.6	N/D	41.1

a) Molecular weight determined from SEC; b) Polydispersity index; c) Melting temperature determined from DSC; d) Solution melting temperature determined using SCALLS; e) Crystallinity determined by DSC

The molecular weight of the samples are all in the same range (400 000 – 650 000 g/mole). The DSC crystallinity of the iPP samples is slightly higher than for the copolymers, yet copolymers with similar crystallinity were electrospun. What is significant here is the “solution melting temperature” of the copolymer. This was determined by solution crystallization analysis by laser light scattering (SCALLS) [32]. This is the temperature at which a crystalline structure, formed by crystallization from solution, will melt/dissolve upon re-heating. It is clear that, for copolymers with similar molecular weight, and similar comonomer content, solution melting temperature in a given solvent (in this case, 1,2 4 trichlorobenzene) decreases as the comonomer type changes, with the comonomers with the longer alkane side-chain leading to copolymers that melts more easily in solution. This indicates that the solubility is influenced by the type of comonomer. This can be illustrated further by considering the Flory theory and the use thereof to study the melting point depression of polyolefins as a function of copolymer composition.

The Flory-Huggins equation for the free energy of mixing was initially developed for concentrated polymer solutions, as was pointed out in the 2005 review on Crystaf and Tref by Soares et al [33]. The equation below was in fact developed to describe the melting point depression in the presence of a diluent (solvent), with T_m being the “solution melting” temperature of the polymer.

$$\frac{1}{T_m} - \frac{1}{T_m^0} = \frac{R}{\Delta H_u}\left(\frac{V_u}{V_1}\right)\left[-\frac{\ln v_2}{x} + \left(1 - \frac{1}{x}\right)v_1 - \chi_1 v_1^2\right]_2 \qquad (4.2)$$

Here where T_m^0 is the melting temperature of the pure polymer, T_m is the equilibrium melting temperature of the polymer in solution, ΔH_u is the heat of fusion per repeating unit, V_u and V_1 are the molar volumes of the polymer repeating unit and diluent, respectively, υ_1 and υ_2 are the volume fractions of the diluent and polymer, respectively, x is the number of segments, and χ_1 is the Flory–Huggins thermodynamic interaction parameter.

In techniques like TREF, CRYSTAF (and SCALLS), the crystallization step occurs in dilute solution, which complicates things as we have a non-uniform distribution of the polymer segments in the solvent. Whilst it is therefore strictly speaking not possible to apply equation 4.2 for dilute solutions, Mandelkern [34] states that the change in chemical potential with increasing dilution is so small that equation 1 is obeyed even in dilute solutions. We can therefore rearrange Equation 4.2 as follows, whilst substituting the number of repeat units (r) for the number of segments (x). This yields equation 4.3:

$$\frac{1}{T_m} - \frac{1}{T_m^0} = \left(\frac{R}{\Delta H_u}\right)\left(\frac{V_u}{V_1}\right)(v_1 - \chi_1 v_1^2) - \frac{R}{\Delta H_u}\left[\frac{ln(v_2)}{r} + \frac{v_1}{r}\right] \quad (4.3)$$

The term on the right-hand side approaches zero if the molecular weight is large, and for polymeric systems we can therefore rewrite equation 4.3 as

$$\frac{1}{T_m} - \frac{1}{T_m^0} = \left(\frac{R}{\Delta H_u}\right)\left(\frac{V_u}{V_1}\right)(v_1 - \chi_1 v_1^2) \quad (4.4)$$

In the case of dilute solutions of copolymers, we need to rewrite the interaction parameter to reflect the contribution of both monomers.

$$\chi_1 = \upsilon_A \chi_{1A} - \upsilon_A \upsilon_B \chi_{AB} \ (4.5)$$

In this case χ_1 is the interaction parameter of the binary copolymer with pure solvent, while χ_{1A} and χ_{1B} are the interaction parameters of the corresponding homopolymers with the same solvent. If the chemical nature of the comonomers is very similar, then one could simply use equation 4.2 (or the derived form thereof).

Alamo and Mandelkern [35] in their discussion of ethylene/1-alkene copolymers specified that the melting temperature of a copolymer can be described by the relationship

$$\frac{1}{T_m} - \frac{1}{T_m^0} = -\frac{R}{\Delta H_u} \ln p \ (4.6)$$

Here Tm is regarded as being the melting temperature of the copolymer, and T_m^0 is the melting temperature of the pure homopolymer and ΔH_u is the heat of fusion of the crystallizable unit, and p is the sequence propagation probability of the crystallizable monomer. In an attempt to relate the Flory theory to crystallization results obtained (in solution) by Crystaf, first Monrabal et al[36]., and then followed by Brull et al [37]. made some assumptions which allowed for the simplification of Equation 1 to:

$$\frac{1}{T_m} - \frac{1}{T_m^0} = \frac{R}{\Delta H_u} \ln[1 - N_2] \ (4.7)$$

Here N_2 is the molar fraction of the copolymer that is included, and since ln[1-N_2] ≈ -N_2 for low values of comonomer the above can be rearranged to:

$$\frac{1}{T_m} - \frac{1}{T_m^0} = -\frac{R}{\Delta H_u} N_2 \quad (4.8)$$

or

$$T_m = T_m^0 - \frac{R[T_m^0]^2}{\Delta H_u} N_2 \quad (4.9)$$

The above (equation 4.9) can be derived if it is assumed that $T_m.T_m^0 \approx [T_m^0]^2$

We are therefore left with two equations that could be applied, i.e. equations 4.4 and 4.9. If the latter is applicable, plotting comonomer content (N_2) against $\frac{1}{T_m} - \frac{1}{T_m^0}$ should lead to a straight line, with the slope not affected by the type of comonomer. This would then mean we assume that the nature of the comonomer does not affect the solubility of the polymer in a given solvent. In other words, the right-hand term of equation 4.4 would only be influenced by amount of comonomer, and not the interaction parameter. Recently Brand [38] showed quite clearly that for a whole range of C_3/C_8, C_3/C_{10}, C_3/C_{14} and C_3/C_{18} copolymers plotting N_2 against $\frac{1}{T_m} - \frac{1}{T_m^0}$ does not yield a straight line if all the copolymers are plotted on the same graph (in fact a second order polynomial fit was much better). For the individual copolymers, and for low comonomer content, the plots of N_2 vs $\frac{1}{T_m} - \frac{1}{T_m^0}$ did yield straight lines, but the slopes of the lines differed for the copolymer types.

From this study it was concluded that the net interaction parameter in the Flory Huggins equation cannot be ignored for these specific polymers. The fact that type of comonomer content had an influence on the solubility of the polymer, explained in our case why these copolymers behave so differently in solution, even though all of them had more or less the same amount of comonomer. This also serves to explain the ease with which these copolymers could be electrospun, compared to the commercial isotactic polypropylenes.

4.3.10 Conclusion

The use of propylene copolymers and more specifically the propylene-higher 1-alkene copolymers is a facile way of producing high-melting polyolefin micro-and nanofibres by solution electrospinning. A solvent system that allows electrospinning at ambient temperature was developed for these copolymers. It was shown that the same system did not work for iPP, at least not in our hands.

4.4. References

1. Larrondo, L.; St. John Manley, R. *Journal of Polymer Science. Polymer Physics Edition* **1981,** 19 (6), 909-920.

2. Larrondo, L.; St. John Manley, R. *Journal of Polymer Science. Polymer Physics Edition* **1981,** 19 (6), 921-932.

3. Larrondo, L.; St. John Manley, R. *Journal of Polymer Science. Polymer Physics Edition* **1981,** 19 (6), 933-940.

4. Givens, S. R.; Gardner, K. H.; Rabolt, J. F.; Chase, D. B. *Macromolecules* **2007,** 40 , 608-610.

5. Rein, D. M.; Cohen, Y.; Ronen, A.; Zussman, E.; Shuster, K. *Materials Research Society Symposium Porceedings* **2008,** 1083E (Coupled Mechanical, Electrical and Thermal Behaviors of Nanomaterials), No pp. given, Paper #: 1083-R03-03.

6. Lee, K.; Ohsawa, O.; Watanabe, K.; Kim, I.; Givens, S. R.; Chase, B.; Rabolt, J. F. *Macromolecules* **2009,** 42 (14), 5215-5218.

7. Son, W. K.; Youk, J. H.; Lee, T. S.; Park, W. H. *Polymer* **2004,** 45 (9), 2959-2966.

8. Lee, C. K.; Kim, S. I.; Kim, S. J. *Synthetic Methods* **2005,** 154 , 209-212.

9. Lee, K. H.; Kim, H. Y.; Khil, M. S.; Ra, Y. M.; Lee, D. R. *Polymer* **2003,** 44 (4), 1287-1294.

10. Rabolt, J. F.; Lee, K. H.; Givens, S. R. United States of America Patent , 2007.

11. Baumgarten, P. K. *Journal of Colloid and Interface Science* **1971,** 36 (1), 71-79.

12. Garg, K.; Bowlin, G. L. *Biomicrofluidics* **2011,** 5 (1), 013403/1-013403/19.

13. Hsu, C. -.; Shivkumar, S. *Journal of Materials Science* **2004,** 39 , 3003-3013.

14. Baji, A.; Mai, Y.; Wong, S.; Abtahi, M.; Chen, P. *Composites Science and Technology* **2010,** 70 (5), 703-718.

15. Ramakriskna, S.; Fujihara, K.; Teo, W. E.; Lim, T. C.; Ma, Z. *An Introduction to Electrospinning and Nanofibers;* World Scientific Publishing Co. Pte. Ltd: Singapore, 2005; .

16. Frenot, A.; Chronakis, I. S. *Current Opinion in Colloid and Interface Science* **2003,** 8 , 64-75.

17. Greiner, A.; Wendorff, J. H. *Aangewandte Chemie International Edition* **2007,** 46 , 5670-5703.

18. Deitzel, J. M.; Kleinmeyer, J.; Harris, D.; Beck Tan, N. C. *Polymer* **2001,** 42 (1), 261-272.

19. Ding, W.; Wei, S.; Zhu, J.; Chen, X.; Rutman, D.; Guo, Z. *Macromolecular Materials and Engineering* **2010,** 295 (10), 958-965.

20. Fong, H.; Chun, I.; Reneker, D. H. *Polymer* **1999,** 40 , 4585-4592.

21. Liu, Y.; He, J.; Yu, J.; Zeng, H. *Polym.Int.* **2008,** 57 (4), 632-636.

22. Eda, G.; Shivkumar, S. *Journal of Material Science* **2006,** 41 (17), 5704-5708.

23. Jarusuwannapoom, T.; Hongrojjanawiwat, W.; Jitjaicham, S.; Wannatong, L.; Nithitanakul, M.; Pattamaprom, C.; Koombhongse, P.; Rangkupan, R.; Supaphol, P. *European Polymer Journal* **2005,** 41 (3), 409-421.

24. Demir, M. M.; Yilgor, I.; Yilgor, E.; Erman, B. *Polymer* **2002,** 43 (11), 3303-3309.

25. Zong, X.; Kim, K.; Fang, D.; Ran, S.; Hsiao, B. S.; Chu, B. *Polymer* **2002,** 43 (16), 4403-4412.

26. Fallahi, D.; Rafizadeh, M.; Mohammadi, N.; Vahidi, B. *e-Polymers* **2008,** No pp. given.

27. Qin, X.; Yang, E.; Li, N.; Wang, S. *Journal of Applied Polymer Science* **2007,** 103 (6), 3865-3870.

28. Arumugam, G. K.; Khan, S.; Heiden, P. A. *Macromolecular Materials and Engineering* **2009,** 294 (1), 45-53.

29. Choi, J. S.; Lee, S. W.; Jeong, L.; Bae, S.; Min, B. C.; Youk, J. H.; Park, W. H. *International Journal of Biological Macromolecules* **2004,** 34 (4), 249-256.

30. Kongkhlang, T.; Tashiro, K.; Kotaki, M.; Chirachanchai, S. *Journal of the American Chemical Society* **2008,** 130 (46), 15460-15466.

31. Duzyer, S.; Hockenberger, A.; Zussman, E. *Journal of Applied Polymer Science* **2011,** 120 (2), 759-769.

32. Brand, M. Investigation of molecular weight effects during the solution crystallisation of polyolefins, Thesis (MSc)--University of Stellenbosch, 2008, 2008.

33. Soares, J. B. P.; Anantawaraskul, S. *Journal of Polymer Science Part B: Polymer Physics* **2005,** 43 (13), 1557-1570.

34. Mandelkern, L. *Crystallization of polymers;* Cambridge University Press: Cambridge, U.K: New York, 2002; .

35. Alamo, R. G.; Mandelkern, L. *Thermochimica Acta* **1994,** 238 (0), 155-201.

36. Monrabal, B.; Blanco, J.; Nieto, J.; Soares, J. B. P. *Journal of Polymer Science Part A: Polymer Chemistry* **1999,** 37 (1), 89-93.

37. Brüll, R.; Pasch, H.; Raubenheimer, H. G.; Sanderson, R.; van Reenen, A. J.; Wahner, U. M. *Macromolecular Chemistry and Physics* **2001,** 202 (8), 1281-1288.

38. Brand, M. The use of laser light scattering to study solution crystallization phenomena in polyolefins, Thesis (PhD)--University of Stellenbosch, 2012, 2012.

Chapter 5

Electrospinning of poly(ethylene-co-vinyl alcohol)

5.1 Solution electrospinning of poly(ethylene-co-vinyl alcohol) (EVOH)

Poly(ethylene-co-vinyl alcohol) (EVOH) is a polymer that has been used in various solution electrospinning experiments. One of the main reasons for that is that the polymer can dissolve quite easily in a number of conductive solvents, which is ideal for electrospinning. Nanofibres can be used in a wide variety of applications, due their high surface area, the ease at which modification of their surface can take place as well as the better mechanical properties these material exhibits[1, 2]. EVOH is a polymer that is hydrophilic yet insoluble in water, biocompatible, does not degrade easily and has excellent barrier properties[2, 3]. EVOH also contains a hydroxyl group, which will react with numerous other monomers or polymers[4, 5]. Combine these excellent properties of EVOH with those of nanofibres, and it is definitely advantageous to obtain EVOH nanofibres.

5.1.1 The use of different solvents

5.1.1.1 Isopropanol/water

The polymer we used was a commercial EVOH copolymer containing 44 % ethylene. What was initially attractive about this polymer as a candidate for electrospinning is the fact that it was soluble in solvents with high dielectric constants. Kenaway *et al* [6]. published an article where it was reported that EVOH copolymers with 56 - 71wt% vinyl alcohol, were electrospun from a 2-propanol/water solution (70% 2-propanol). The polymers were dissolved at 80 °C and when cooled to room temperature, stayed in solution for a few hours before precipitating. In many cases EVOH fibres were used in biomedical applications, making the water/2-propanol system quite popular[7, 8].
The first attempts at solution electrospinning of the EVOH copolymer, a 12 wt% solution was prepared. Since dissolving of EVOH was much easier than the propylene copolymers, higher solution concentrations could be obtained without viscosity becoming a problem. Figure 5.1 shows the SEM micrographs of the microfibers obtained by this means.

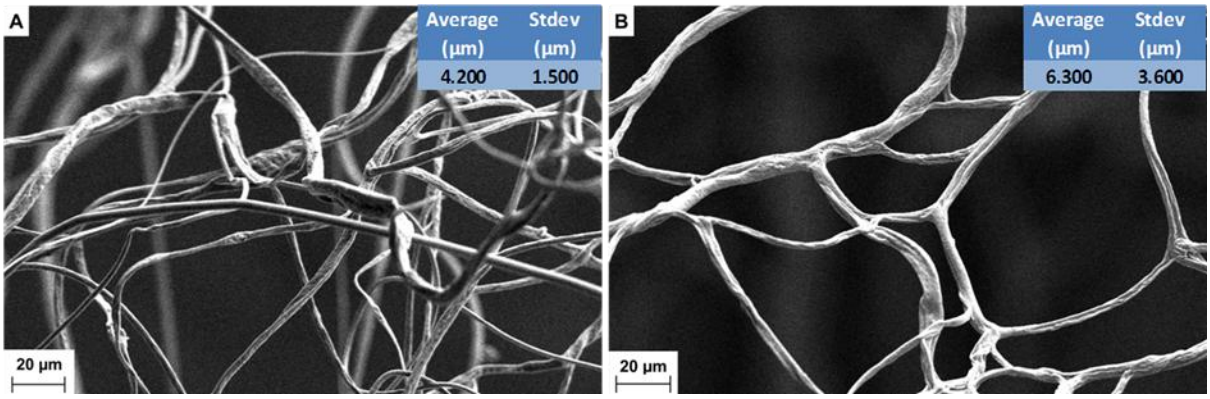

Figure 5.1. SEM images of EVOH nanofibres produced from 2-propanol/H_2O solution (12 wt%) spun at TCD of 15 cm, flow rate of 0.05 ml/min and A) 15 kV and B) 20 kV

From Figure 5Figure 5.1 it was already clear that these fibres had a different morphology than that of the polypropylene copolymers. In this case micro- instead of nanofibres were obtained. From what was reported in literature, we expected to obtain nanofibres. It should be taken into account that in this study we used an EVOH copolymer with different ethylene content to those reported previously [6-8]. When keeping the TCD and flow rate constant and changing the voltage, the higher voltage increased the fibre diameter by about 2 µm as can be seen from the example in Figure 5.1.

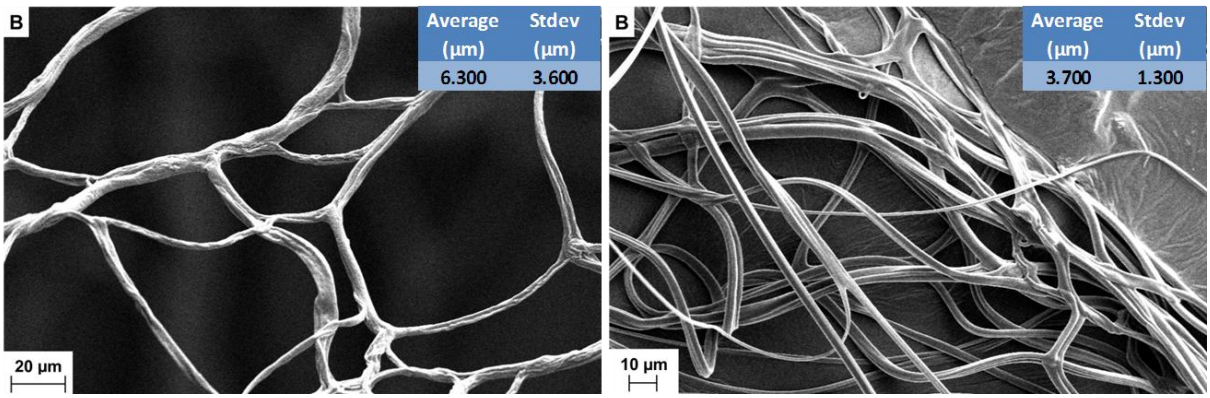

Figure 5.2. SEM images of EVOH nanofibres produced from 2-propanol/H_2O solution (12 wt%) spun at a flow rate of 0.05 ml/min, 20 kV and TCD of A) 15 cm and B) 20 cm

When comparing the effect of the TCD, the larger TCD (Figure 5.2) still resulted in thinner fibres. Using a TCD of 15 cm, a voltage of 15 kV and a flow rate of 0.025 ml/min, the thinnest fibres were obtained, as shown in Figure 5.3, although the fibre diameter was still in the micrometre range. The morphology of these fibres was not very smooth and elongated beads could be observed in some of the samples.

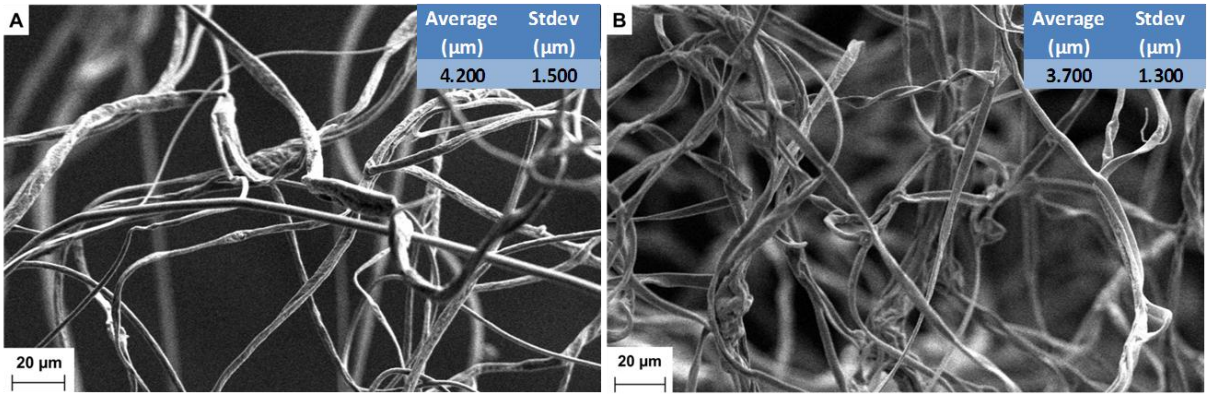

Figure 5.3. SEM images of EVOH nanofibres produced from 2-propanol/H_2O solution (12 wt%) spun at 15 kV, TCD 15 cm and flow rate a) 0.05 ml/min and b) 0.025 ml/min

The addition of salt was thought to be a way of improving the morphology of the fibres, but when adding salt, the 12 wt% solution could not be electrospun. The solution was too viscous at 12 wt% and the addition of salt appeared to have increased the viscosity. It also appeared as if the solution became too conductive and the jet receded into the needle. The solution concentration was reduced to 10 wt% and 0.2 wt% salt (LiCl) was added. The fibres obtained were not smoother and the electrospinning remained difficult. The morphology indicated that insufficient stretching of the solution took place. This was attributed to the fact that solution was too viscous and dried at the tip of the needle, making electrospinning difficult, even impossible. The next solution to be prepared was an 8 wt% solution and 0.2 wt% LiCl was added. The average diameter of the fibres decreased significantly when decreasing the solution concentration, with fibres in the 1 – 2 µm range being produced. A feed rate of 0.025 ml/min produced the thinnest fibres (see Figure 5.4).

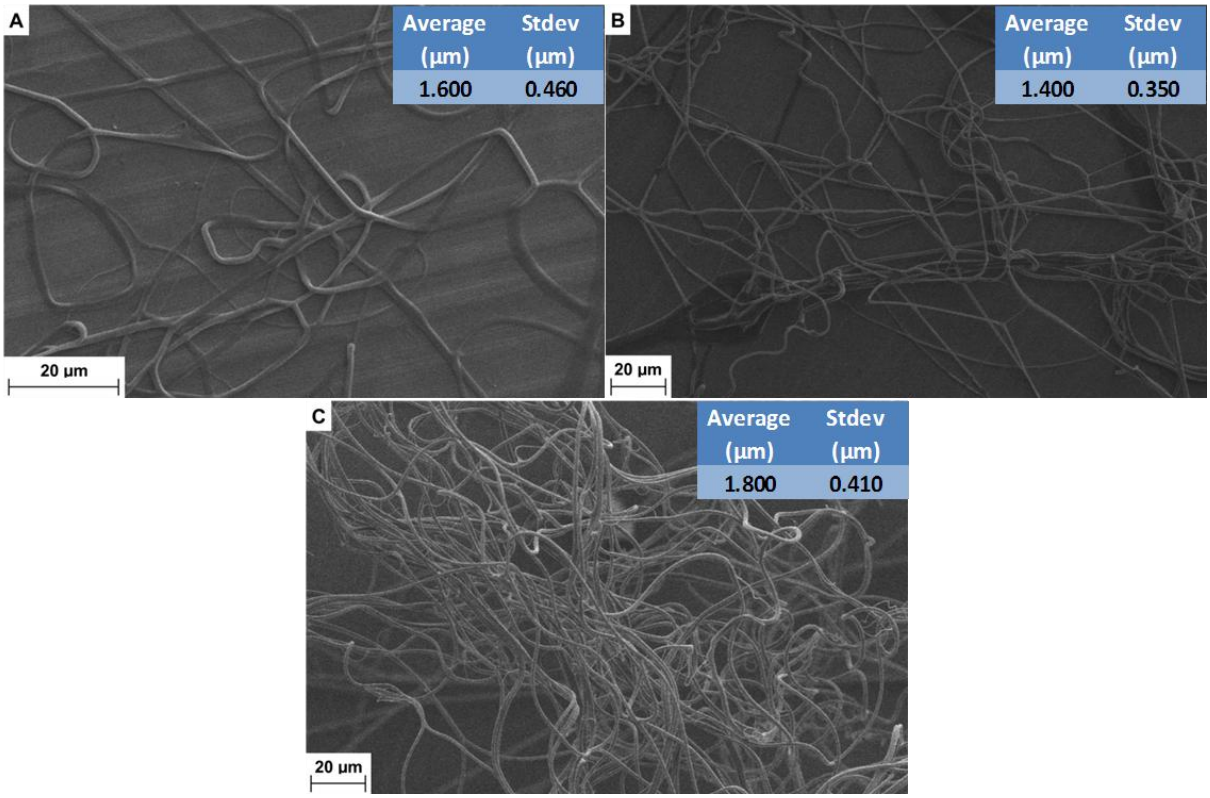

Figure 5.4. SEM images of EVOH nanofibres produced from 2-propanol/H_2O solution (8 wt%), spun at 10 kV, TCD of 15 cm and flow rate of A) 0.05 ml/min, B) 0.025 ml/min and C) 0.01 ml/min

All the samples were spun at 10 kV. When we used a higher voltage, the fibres were difficult to collect. The use of a TCD of 20 cm resulted in thinner fibres, but the fibres did not seem to be that uniform and even appeared swollen. Those spun at a TCD of 15 cm did, however, have more beads.

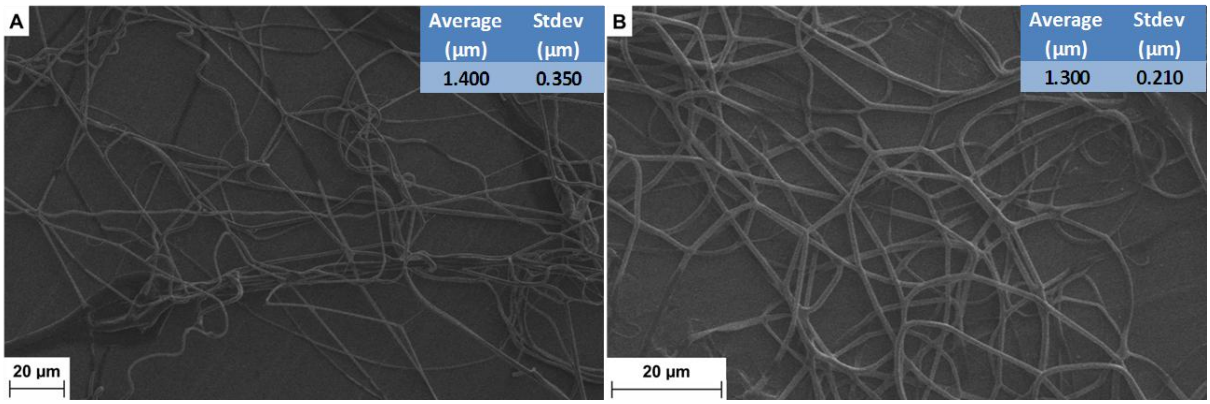

Figure 5.5. SEM images of EVOH nanofibres produced from 2-propanol/H_2O solution (8 wt%), spun at 10 kV, flow rate of 0.025 ml/min and a TCD of A) 15 cm and B) 20 cm

The problems we encountered with the 2-propanol/water mixture lead us to try other solvents.

5.1.1.2 DMF

In this study it was decided to rather use a more conductive system, since our aim was not produce nanofibres for medical/biological applications. EVOH dissolves readily in N,N, dimethylformamide (DMF), which is a very conductive solvent, ideal for electrospinning. The first step in the electrospinning process was to determine the optimum solution concentration to achieve the required fibre morphology.

It was first attempted to prepare a 10 wt% solution at 100 °C. Even at 10 wt % polymer in DMF, electrospinning did not happen. At low solution viscosity the jet is unstable and Rayleigh instability will occur. What this implies is that the jet will break-up into droplets, but in long chain molecules the complete break-up will not always occur and beaded fibres will rather be formed [9, 10]. Increasing the concentration to 12 wt% solution resulted in the formation of fibres. At a concentration of 20 wt% the solution concentration was too high and caused the needle to become blocked. From Figure 5.6 it can be seen that that higher solution concentration gave more uniform and beadless fibres. EVOH dissolves quite easily in DMF, therefore the lower the solution concentration, the less viscous the solution will be (Table 5.1). The viscosity was determined on a Brookfield viscometer.

Table 5.1 Solution viscosity of different wt% solutions

Solution	Viscosity (CPS)
12 wt%	182.5
13 wt%	254.5
14 wt%	328.0
15 wt%	437.0

The solution viscosity can be related to the molecular entanglements in the solution, the higher the viscosity the more molecular entanglements in the solution. The molecular entanglements play an important role in the solution electrospinning process. For beadless fibres to be produced the jet must be quite stable and continuous. As soon as the jet loses its stability, the fibres that are formed will not be uniform and beaded fibres may be formed [9, 11]. The tendency is for the fibres to become thinner and more uniform with an increase in the solution concentration, which is shown in Figure 5.6.

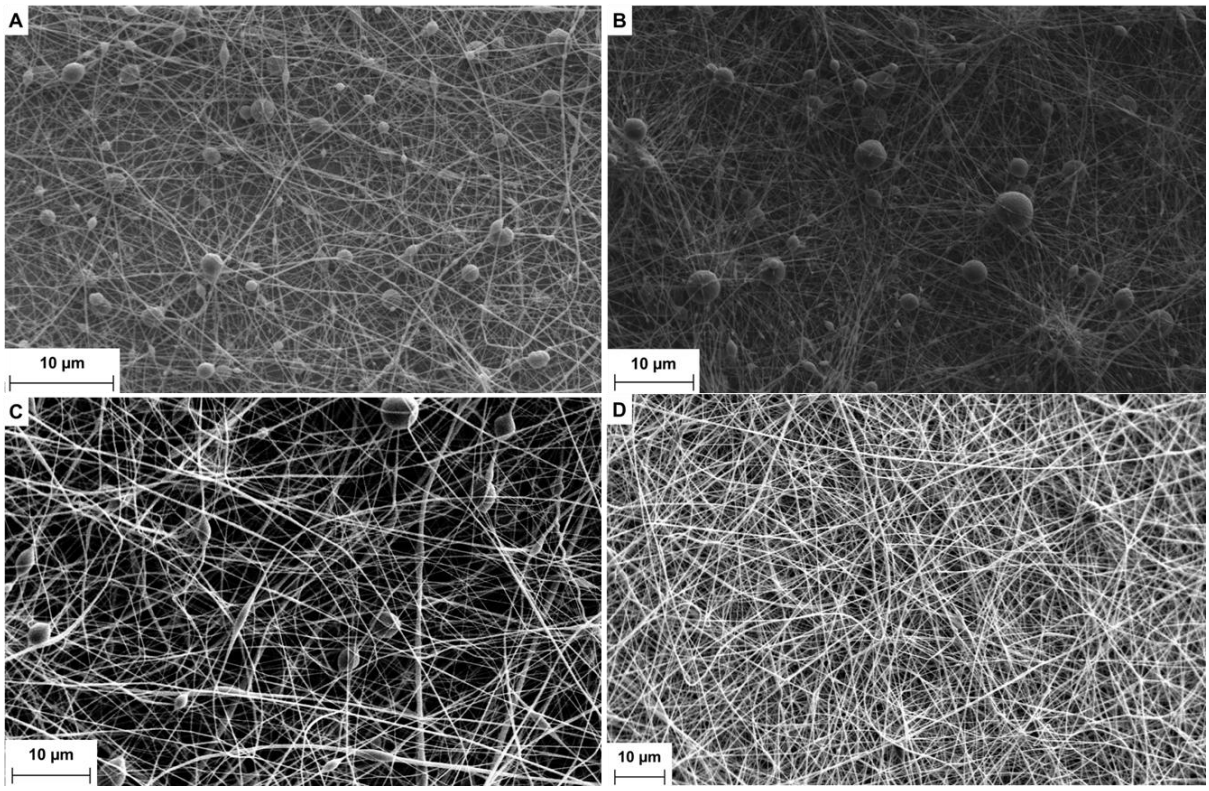

Figure 5.6. SEM images of EVOH nanofibres (44 wt% ethylene) produced from A) 12 w/w % solution, B) 13 w/w % solution, C) 14 w/w % solution, D) 15 w/w % solution (DMF as solvent)

The next step was to compare the flow rate, tip-to-collector distance (TCD) and voltage.

In the first experiments the flow rate was kept constant at 0.05 ml/min and the tip to collector distance (TCD) at 15 cm and the voltage varied between 10 – 20 kV.

In Figure 5.7 the SEM images of the EVOH spun at the various voltages can be seen. The sample spun at 15 kV produced the thinnest fibres. A higher voltage usually produces thinner fibres, since the more charges carried by the jet, the more the jet can be stretched and elongated, favouring the production of thin fibres [9]. This explains the reduction in the fibre diameter between Samples A and B shown in Figure 5.7. The increase in the fibre diameter between Sample B and C can be explained by the fact that with higher voltage more solution gets drawn out of the needle and thicker fibres are formed. Baumgarten [12] showed that with an increase in the voltage the fibre diameter will decrease until a minimum is reached, and then increase again. What should also be noted here that without the addition of salt, the EVOH fibres produced semi-beadless fibres at a voltage as low as 10 kV which was not the case with the polypropylene copolymers. The use of a more conductive solvent explains this phenomenon. DMF has a very high dielectric constant (38) and is very conductive. The more conductive the solution, the more charges are carried by the jet, the more charges carried by the jet the more it will undergo stretching. Since DMF already supplies charges to the jet, the formation of thin and beadless fibres should be possible at lower voltage [9, 13-15].

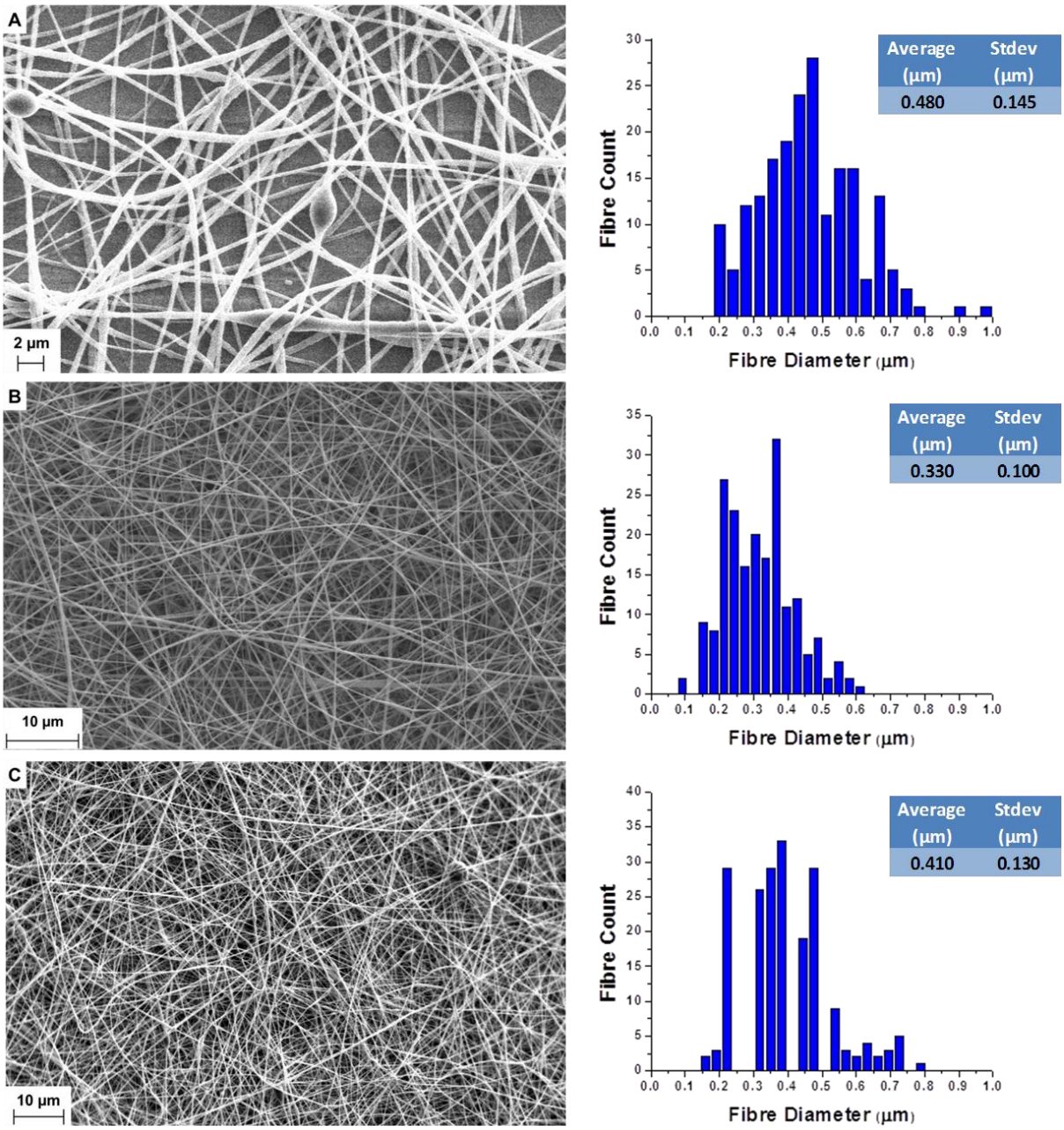

Figure 5.7. SEM images of EVOH fibres. Flow rate: 0.05 ml/min, Distance: 15 cm and A) 10 kV, B) 15 kV and C) 20 kV

For the next example the TCD was kept constant at 15 cm, the voltage at 15 kV and the flow rate varied between 0.05 and 0.01 ml/min (Figure 5.8). Since the EVOH dissolved much easier and stayed in solution at room temperature for a longer time than the polypropylene copolymers, a slower flow rate was possible without the solution drying at the tip of the needle or crystallizing out of solution. However the thinnest fibres were formed using the higher flow rate of 0.05 ml/min. The feed rate determines the amount of solution that will be available to be electrospun. A high feed rate will most often increase the diameter of the fibres, since there is now more solution at the tip of the needle that needs to be drawn away. In our case the higher feed rate encouraged the

formation of thinner fibres. There is a certain point where the amount of the solution supplied at the needle tip will equal the rate at which it is taken away and then the increase in the feed rate will increase the charges on the jet, which in turn will allow the jet to be stretched more and thinner fibres will be obtained [9].

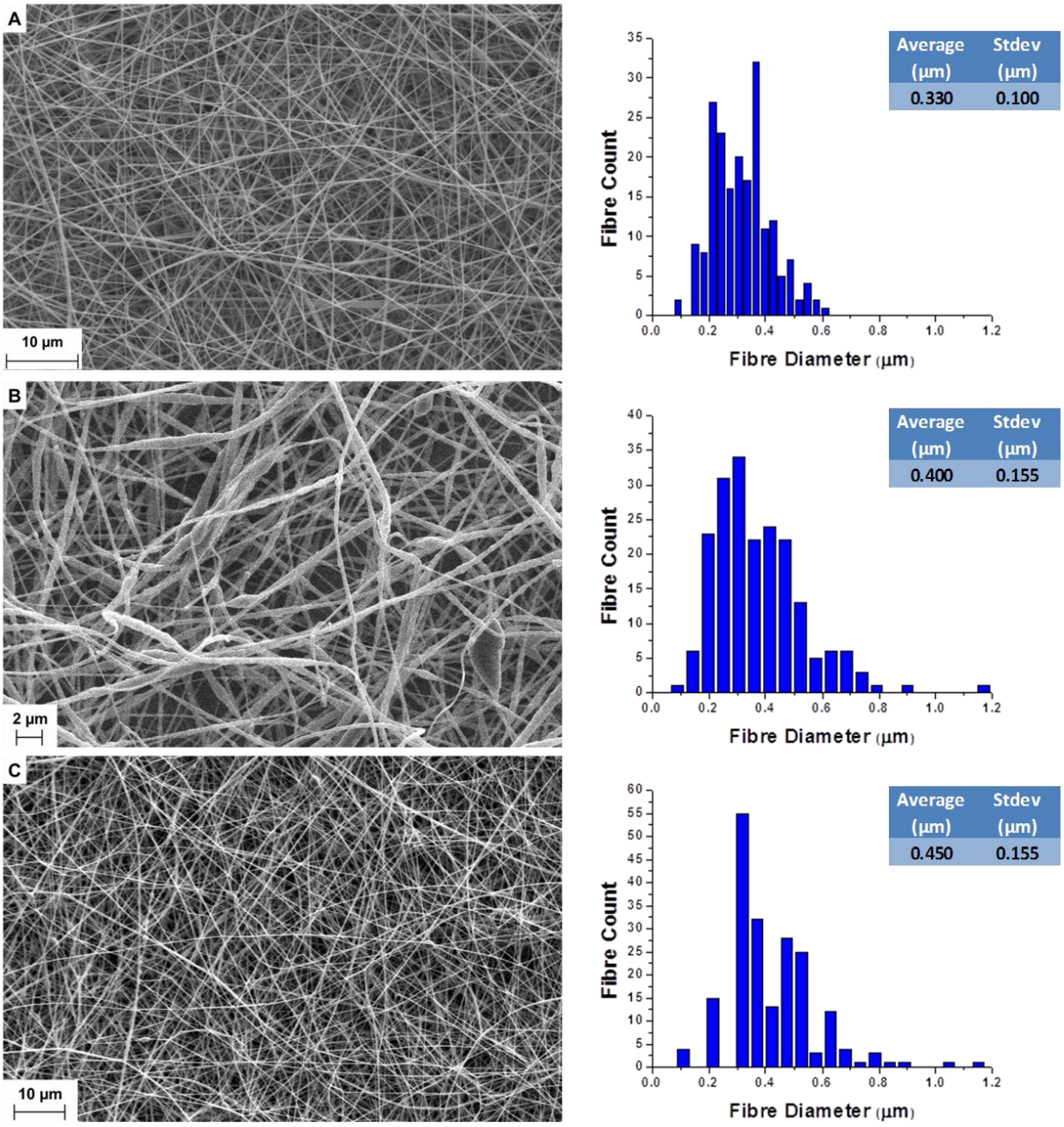

Figure 5.8. SEM images of EVOH fibres produced by electrospinning from DMF solution. Distance and voltage kept constant at 15 cm and 15 kV respectively and a flow rate of A) 0.05 ml/min, B) 0.025 ml/min and C) 0.01 ml/min was used.

The last parameter to change was the tip to collector distance. The voltage was kept constant at 20 kV and the flow rate at 0.01 ml/min and the TCD varied between 15 cm and 20 cm.

In this case, the larger distance produced thinner fibres; beadless fibres were, however, observed for both distances, indicating that the voltage played the biggest role in the formation of beads. One of the effects of a smaller distance is that the jet will accelerate faster, since the electrical field strength is higher. The jet will arrive at the collector plate in a short time and the fibres might not have enough time to be elongated and a fibre mesh can be formed [9, 16]. The fibres in Sample A though does not seem to be sticking together, but at 20 cm the jet can travel further, allowing it to be stretched more and also giving the solvent enough time to be evaporated.

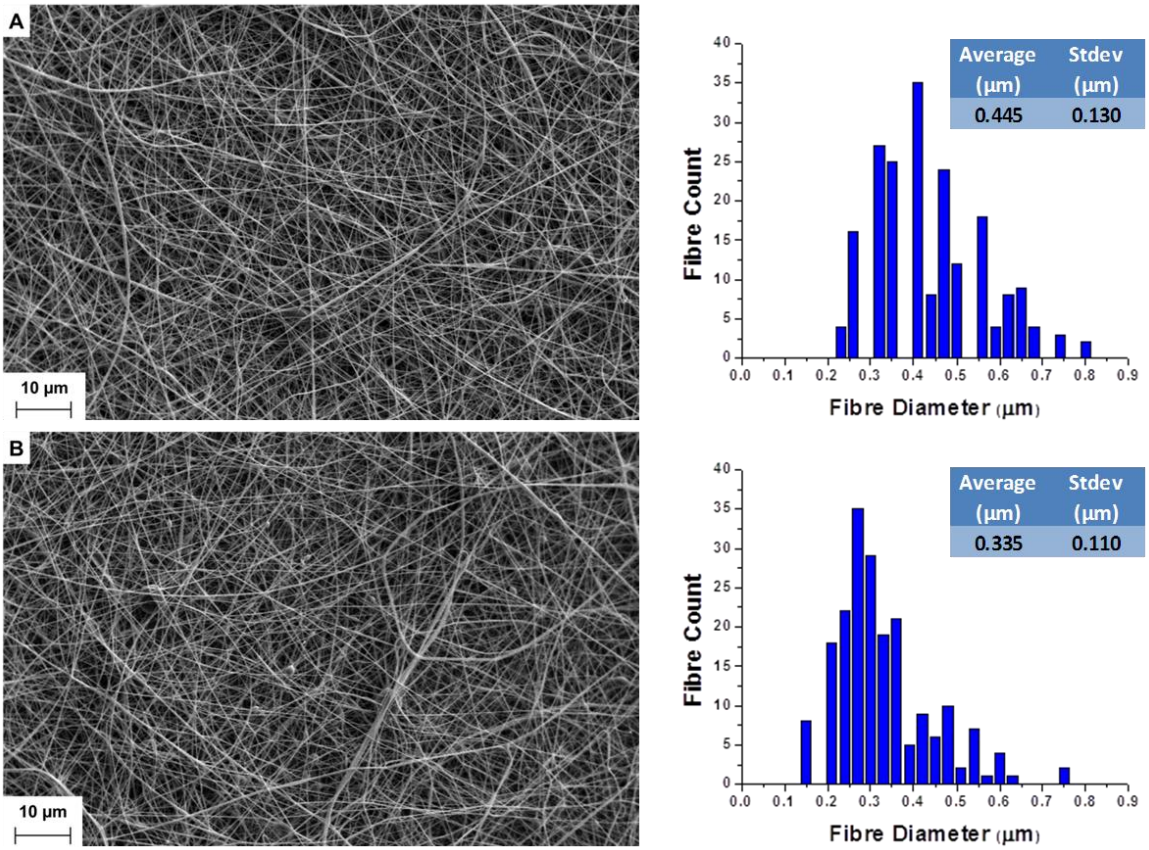

Figure 5.9. SEM images of EVOH nanofibres spun at 20 kV with a flow rate of 0.01 ml/min and at a distance of A) 15 cm and B) 20 cm

The fibres obtained by using DMF were mostly beadless, but in some samples a few beads could still be observed. Since we saw that with the polyolefins the addition of salt encourages the formation of beadless fibres, LiCl was added to the EVOH solution.

The LiCl dissolves quite easily in DMF, and 0.2 wt% LiCl was added to the EVOH solution and positive results (less beading) were obtained. The viscosity of the solution increased noticeably with the addition of the salt. The higher viscosity of the solution may also be part of the reason why beadless fibres were obtained.

Table 5.2. Viscosity of the solutions with and without salt

Solution	Viscosity (CPS)
15 wt%	437
15 wt% (Salt)	508

When spinning the solution at 10 kV, beaded fibres were usually obtained. The addition of the LiCl resulted in the production of uniform and smooth fibres.

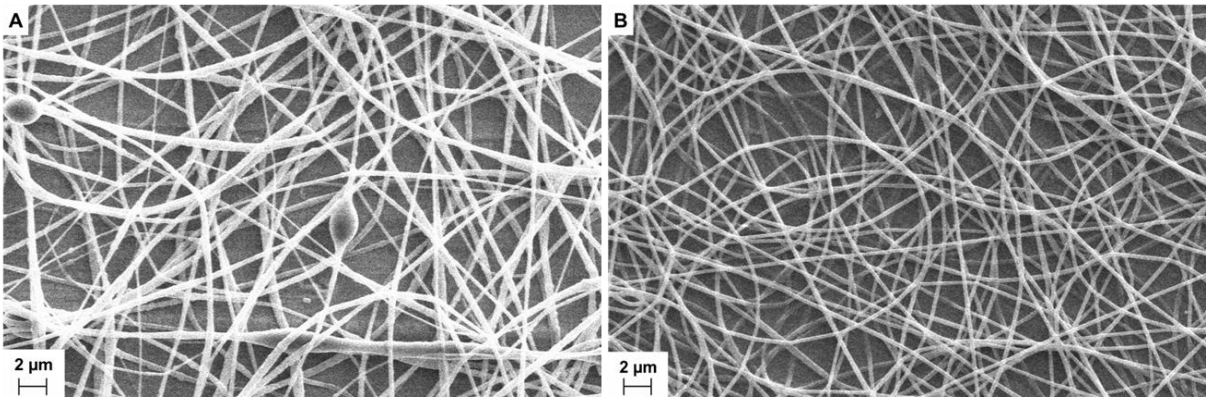

Figure 5.10. SEM images of EVOH nanofibres spun A) without LiCl and B) with 0.2 wt% LiCl at a TCD of 15 cm, 10 kV and a flow rate of 0.05 ml/min

New spinning conditions needed to be determined for the solutions containing LiCl.

Figure 5.11 illustrates the influence of the voltage on the fibre diameter. Higher voltage did produce the thinner fibres, but it can be seen that there are beads present in some of the fibres. At the higher voltage more stretching of the fibres do take place, but the Taylor cone can become unstable or the jet may even recede into the needle, causing the formation of beads [9].

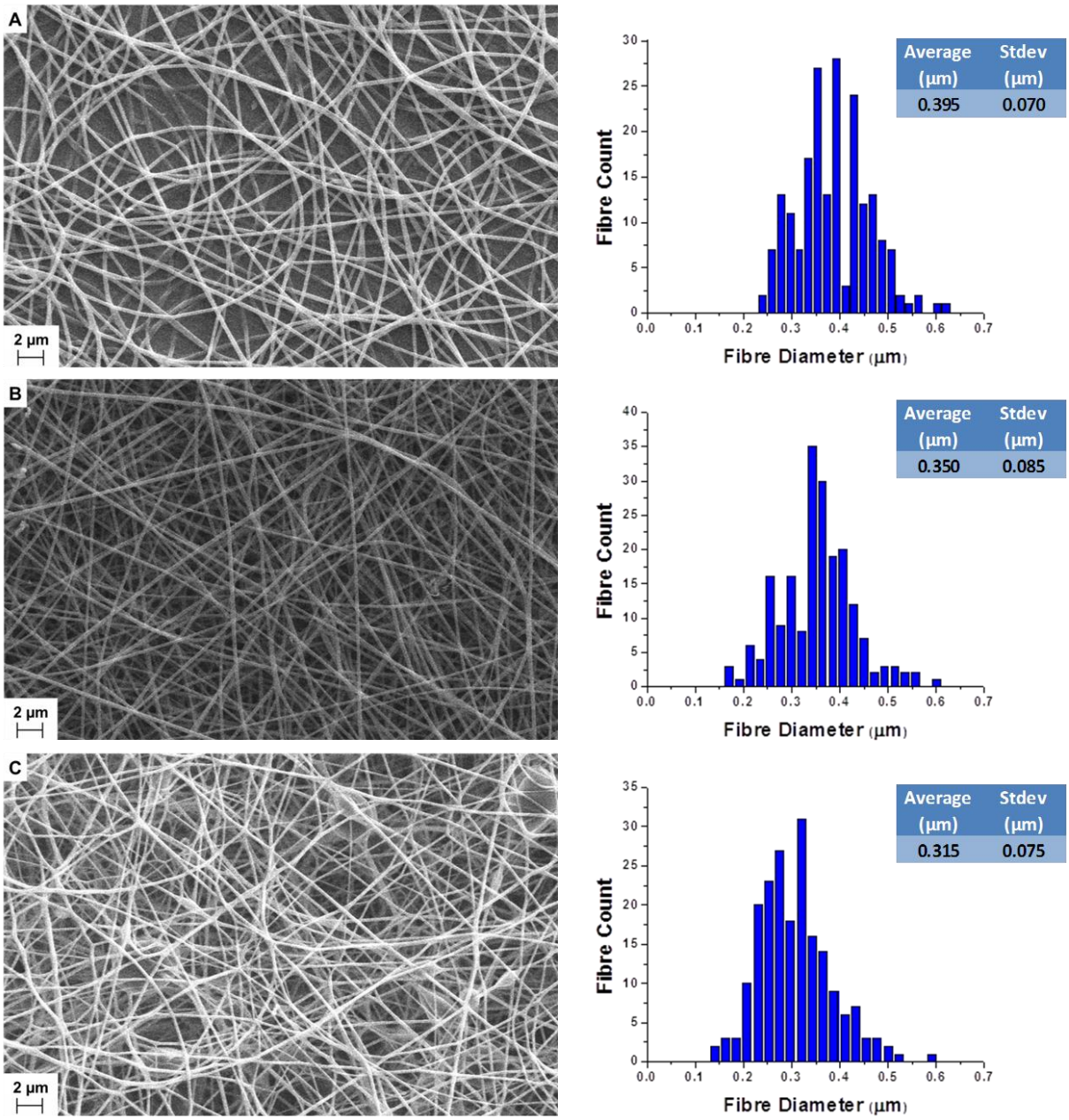

Figure 5.11. SEM images of EVOH nanofibres produced with 0.2 wt% LiCl. Distance and flow rate kept constant at 15 cm and 0.05 ml/min. The voltage varied, A) 10 kV, B) 15 kV and C) 20 kV

For the next example the flow rate was varied between 0.05 ml/min and 0.01 ml/min, the TCD was and voltage was kept constant at 15 kV and 15 cm respectively. The lower flow rate did seem to produce thinner fibres; but once again the difference between the different flow rates was very small and can even be regarded as insignificant. The fibre distribution for the 0.01 ml/min did seem to be better, since more fibres were obtained at more or less the same diameter.

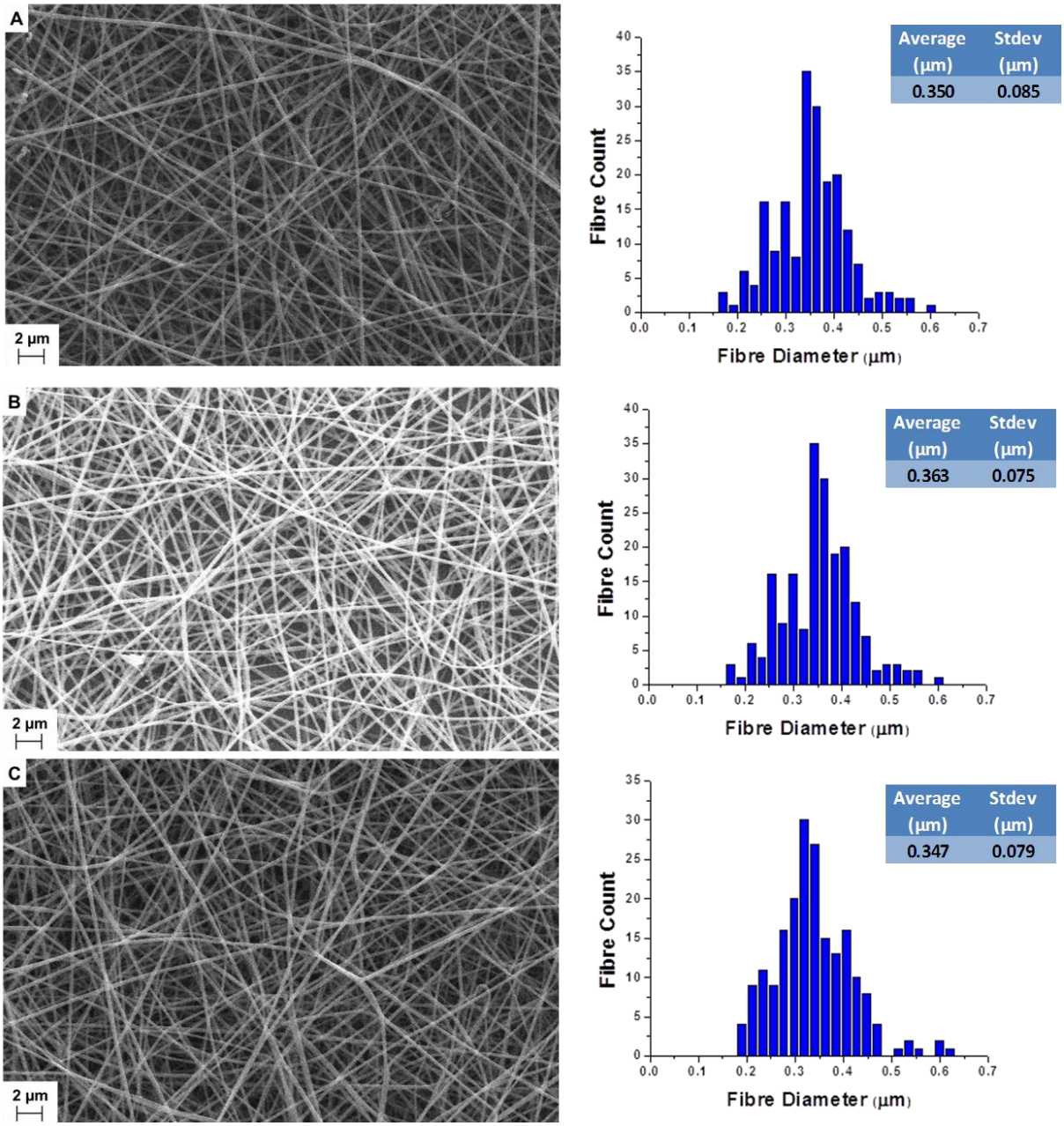

Figure 5.12. SEM images of EVOH nanofibres produced with 0.2 wt% LiCl, spun at 15 kV with TCD of 15 cm and a flow rate of A) 0.05 ml/min, B) 0.025 ml/min and C) 0.01 ml/min

For the next example the voltage was kept constant at 15 kV and flow rate at 0.05 ml/min. The TCD was varied between 12 and 20 cm. The greater distance did produce the thinner fibres, which can attributed to the fact that the jet has a longer time to travel before reaching the collector plate giving it more time to be elongated as well as for the solvent to be evaporated.

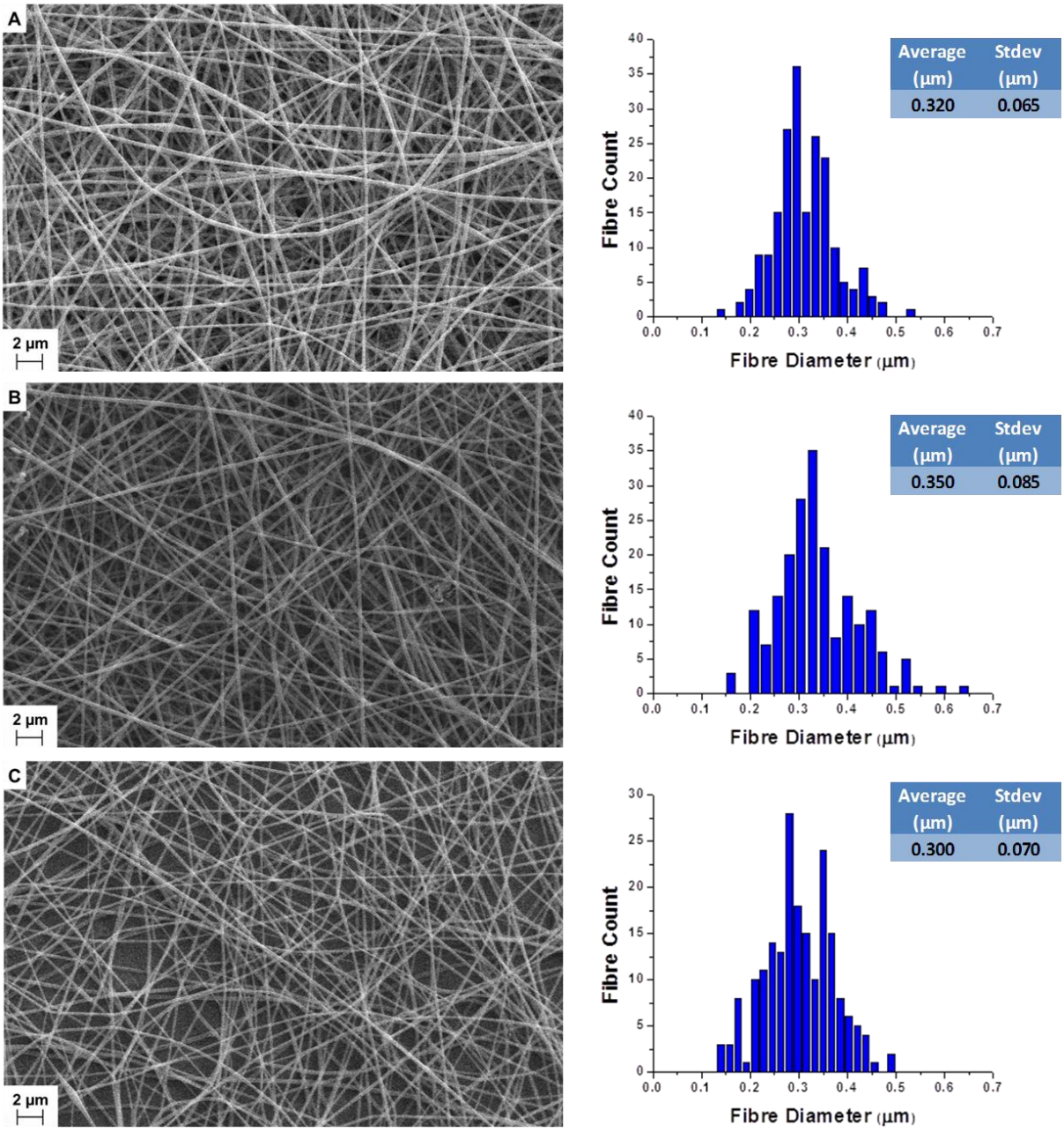

Figure 5.13. SEM images of EVOH nanofibres produced with 0.2 wt% LiCl spun at 15 kV, flow rate of 0.05 ml/min and a TCD of A) 12 cm, B) 15 cm and C) 20 cm.

The results of varying the different parameters are summarized in Figure 5.14. To test the influence of each parameter, the other two parameters were kept constant and the third parameter was varied.

The fibre diameter did decrease with an increase in voltage, although the decrease between 15 kV and 20 kV is very small. The sample at 20 kV however did also produce beaded fibres, whereas at 15 kV, smooth fibres were obtained. When higher voltage is applied, there are more charges on the jet and will lead to thinner fibres, which is the case between the 10 kV and 15 kV sample. The

beaded fibres could be due to the fact that at high voltage the jet might become unstable at certain stages and then beads could be formed. The difference between the flow rates did not seem to influence the fibre diameter too much. The smallest fibres were produced at the highest TCD.. At 12 cm we did observe in decrease in fibre diameter when comparing it with the 15 cm, which can be attributed to the fact that the electrical field strength is very high at short distance, and could also lead to an increasing in the elongation of the jet [16-20].

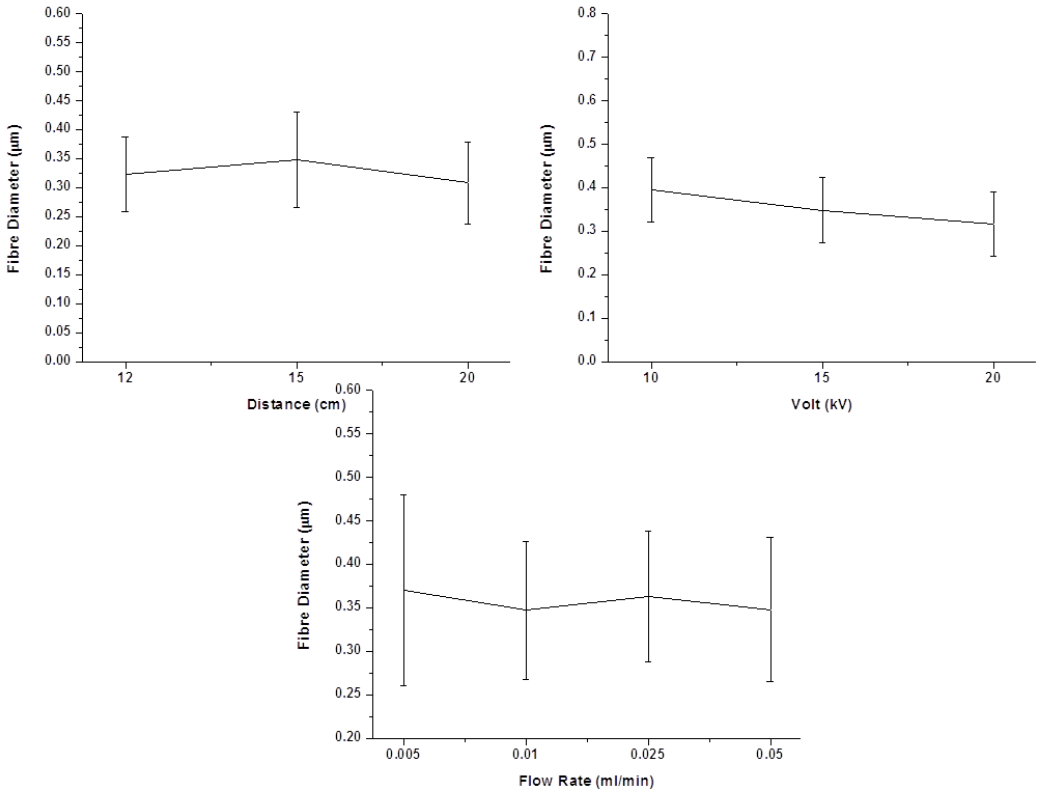

Figure 5.14. Summary of the influence of each parameter on the fibre diameter

5.1.1.3 DMSO

It was observed with the DMF solutions of EVOH that the polymer starts crystallizing from solution on standing. This was not observed with the isopropanol/water system but the fibres obtained with that solvent system were not uniform and definitely not in the nanometre range. DMSO was chosen as the next solvent since it has a high dielectric constant as well and is a good solvent for EVOH. DMSO is also somewhat less toxic than DMF and EVOH fibres obtained from DMSO have also been used in medical applications.

The DMSO seemed to be a very good electrospinning solvent and we could even decrease the flow rate even more, even though the viscosity of the solution was higher. At the lower flow rate the fibre morphology was also more uniform.

Table 5.3. Viscosity of the solutions in DMF and DMSO

Solution	Viscosity (CPS)
15 wt% (Salt) in DMF	508
15 wt% (Salt) in DMSO	655

The results obtained with electrospinning using a 15 wt% EVOH (with 0.2 wt% LiCl) solution in DMSO are shown in Figure 5.15.

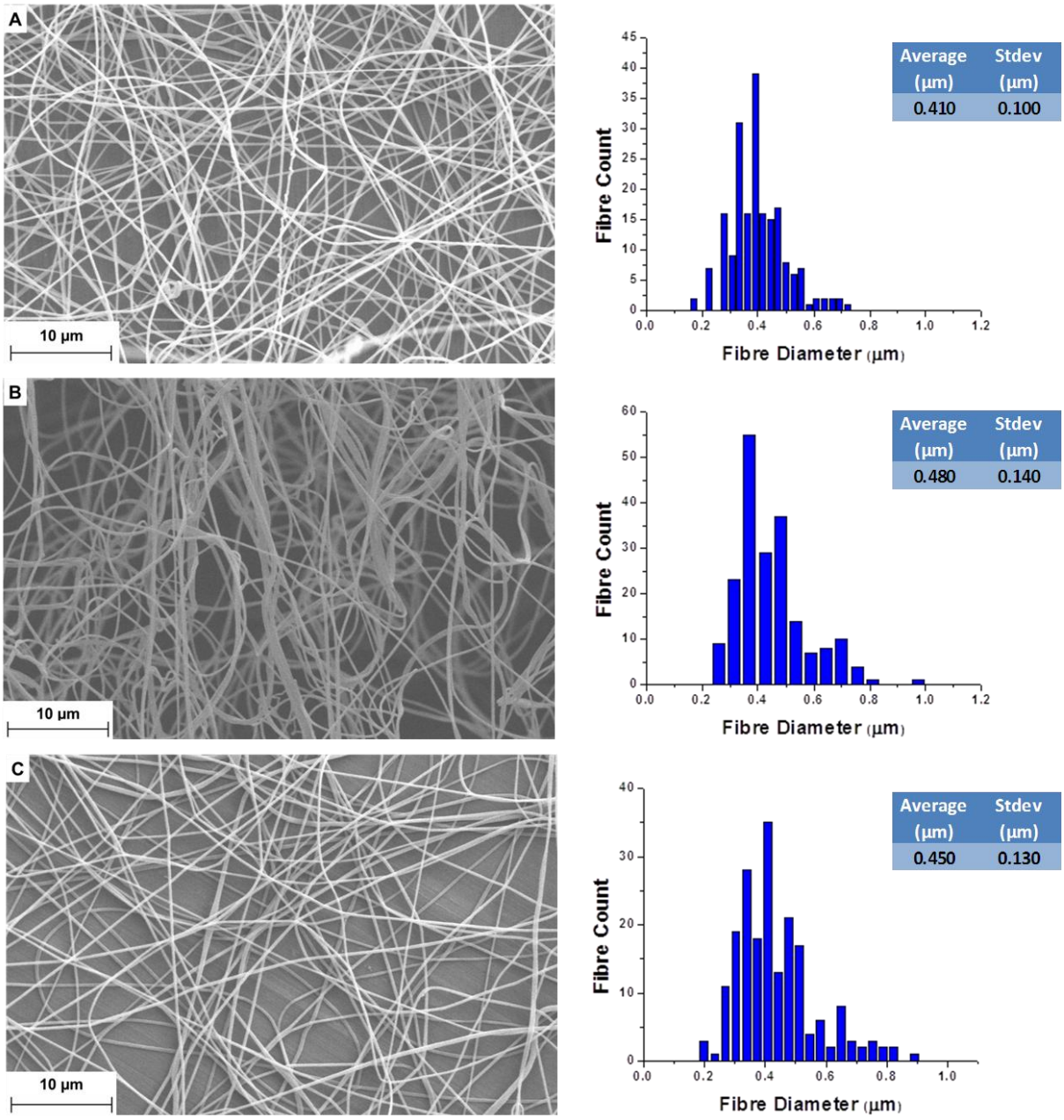

Figure 5.15. SEM images of EVOH nanofibres produced from DMSO solution (15 wt%) with 0.2 wt% LiCl, spun at 15 kV, TCD of 25 cm and a flow rate of A) 0.025 ml/min, B) 0.01 ml/min and C) 0.008 ml/min

It is clear that smooth, thin fibres were obtained, with excellent results obtained with most sets of experimental parameters. The results obtained at a voltage of 10 kV are shown in Figure 5.16. The lower voltage did seem to favour smaller diameters; however, the fibre mat is thicker at 15 kV than that at 10 kV as can be seen in Figure 5.16.

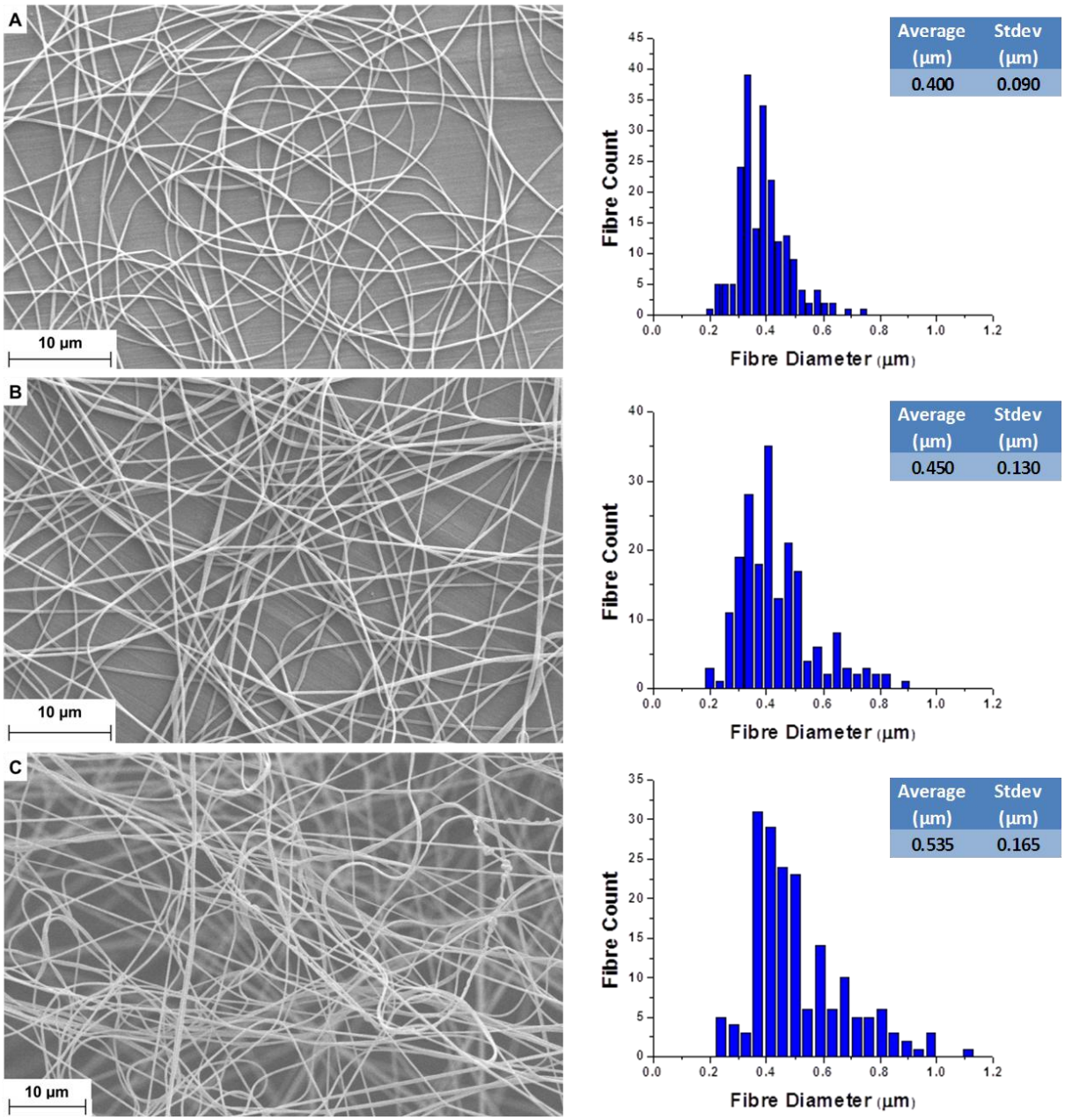

Figure 5.16. SEM images of EVOH nanofibres produced from DMSO solution (15 wt%) with 0.2 wt% LiCl, spun at TCD of 25 cm, a flow rate of 0.008 ml/min and A) 10 kV, B) 15 kV and C) 20 kV

DMSO does have a high boiling point and the solvent will not evaporate that easily. It can be seen when looking at the influence of the distance. At 25 cm the thinnest fibres were obtained and this is

possibly due to the solvent having more time to evaporate and the jet being able to undergo more stretching. This is illustrated in the SEM micrographs shown in Figure 5.17.

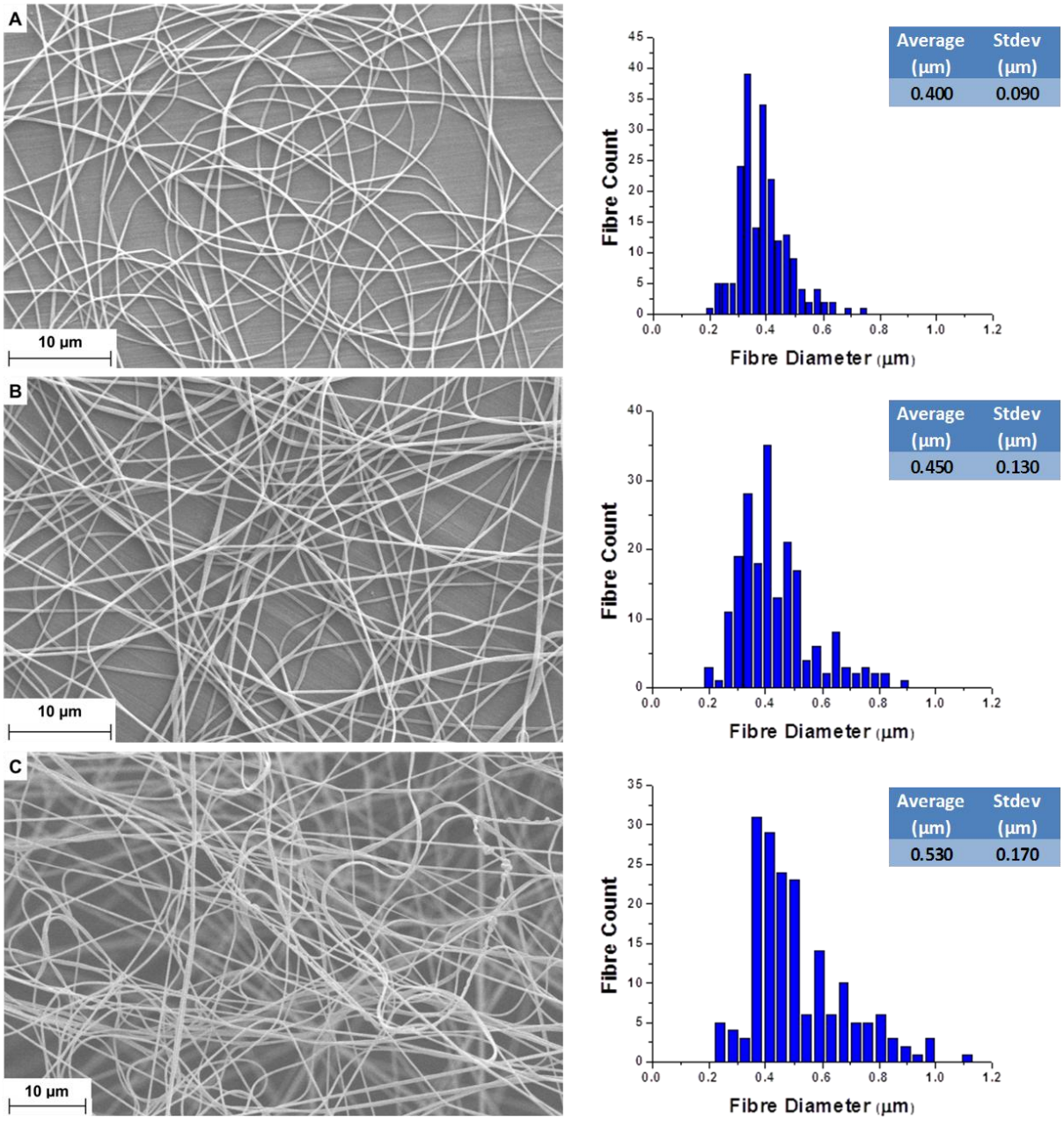

Figure 5.17. SEM images of EVOH nanofibres produced from DMSO solution (15 wt%) with 0.2 wt% LiCl, spun at a flow rate of 0.008 ml/min, 15 kV and TCD of A) 15 cm, B) 20 cm and C) 25 cm

The influence of the parameters is summarized in Figure 5.18. Again for these experiments, two parameters were kept constant while the third parameter was varied. The spinning parameters did seem to have a greater influence when using DMSO, than when using DMF.

In the case of the voltage, the fibre diameter increased with an increase in the voltage. It is reported that in some cases, if the voltage is too high, the jet becomes unstable, leading to

insufficient stretching of the solution [9, 16, 17]. This will then lead again to the formation of thicker fibres. DMSO is already very conductive, and adding more charges to the solution the electrical field will be very strong, leading to the unstable jet. The thinnest fibres were obtained at the greatest distance. At higher distance the solution will be stretched more and the longer path travelled will give the solvent more time to evaporate. The flow rate had the least influence on the fibre diameter, and although the slower feed rate did produce the thinnest fibres, the difference between the fibre diameters were not that significant, given the standard deviation. What was observed for these samples was that the polymer did stay in solution for a substantial time and there were no problems with the polymer crystallizing out as was the case with DMF.

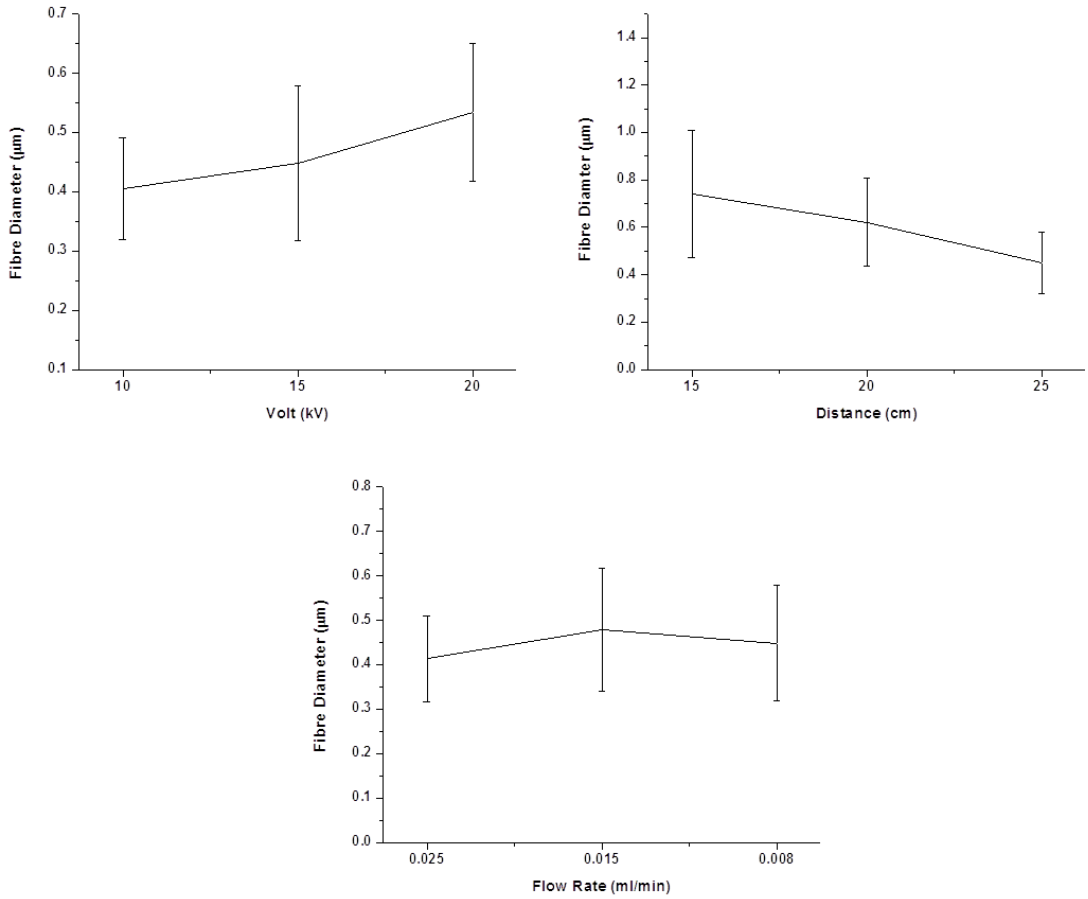

Figure 5.18. Summary of the influence of each parameter on the fibre diameter of EVOH spun from DMSO solution.

5.1.2 Melting and crystallinity

The way the polymer molecules are packed during electrospinning was discussed in Chapter 4. According to papers by Liu *et al* [21, 22]. a small part of the fibre will crystallize and the rest will be

amorphous. It is also known that the fibres consist of nanofibrils that are lined up parallel to the fibre axis [23, 24]. DSC was done on the EVOH, as well as the 13 wt% and 15 wt% polymer fibres. When looking at the 1st heating scan in Figure 5.19, we can see that the EVOH and nanofibres produced from a 13 wt% solution still has more or less the same melting temperature, the difference being about 2 °C between the two, with the fibres melting at a lower temperature. The melting temperature of the fibres produced from a 15 wt% solution shifted to a significantly lower value (about 5 °C lower).

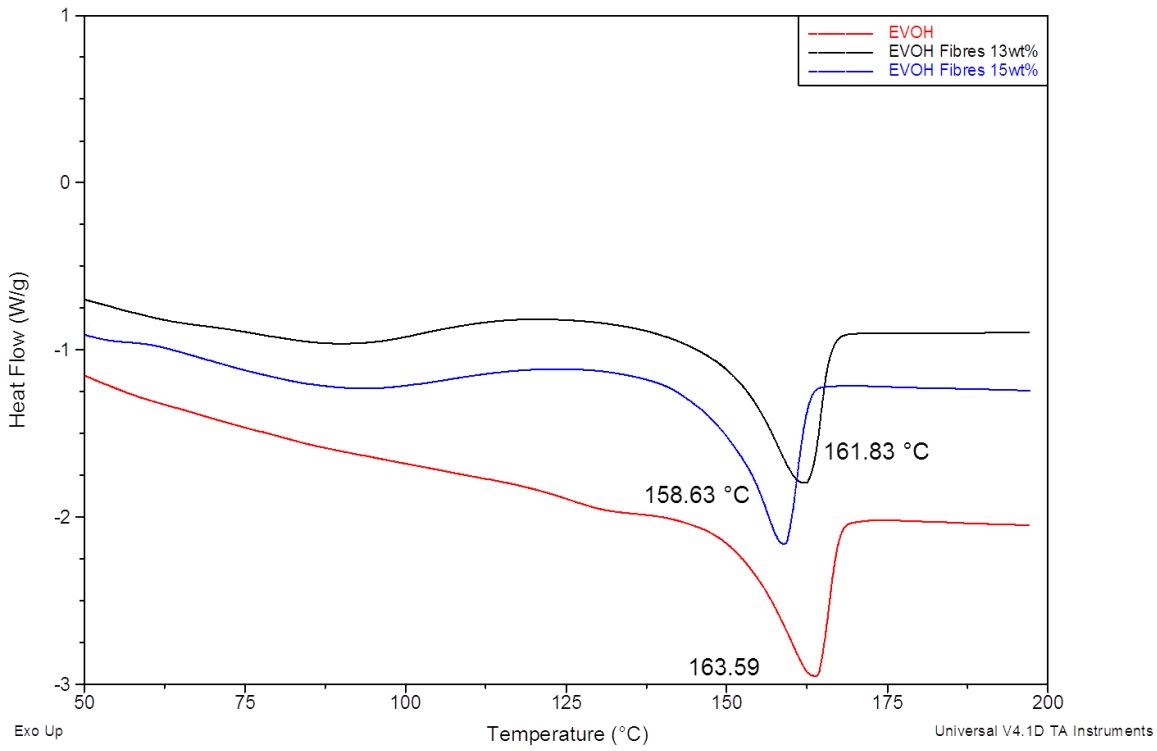

Figure 5.19. DSC thermogram of the 1st heating of the bulk EVOH and EVOH fibres produced from 13 wt% and 15 wt% solutions.

Liu *et al* [21, 22]. discussed the influence of the fibre diameter on the melting temperature. Usually with a decrease in crystallinity we would find a decrease in the melting temperature. In Table 5.4 it is seen that the area under peak increases for the fibres compared to the pure polymer. No value for the heat of fusion of 100 % crystalline EVOH could be found in literature. Therefore, it is difficult to make conclusion whether there is a definite increase in the crystallinity. Liu also found that when the fibre diameter is broader, the melting temperature and crystallinity tend to increase. This could be a possible explanation for the difference between the melting temperature of the fibres produced from 13 and 15 wt% solutions. The fibres produced from the 15 wt% solution have a fibre diameter average of 330 nm (± 100 nm) and the 13 wt % an average diameter of 460 nm (±130

nm). The difference however is not that large, but the difference of 130 nm in the diameter may be the reason for the increase in melting temperature for the fibres produced from the 13 wt% solution.

The decrease in melting temperature between the fibres produced from a 15 wt% solution and the (bulk) EVOH can be due to the way the polymer crystallizes during the electrospinning process. When a polymer is electrospun, the speed at which the jet is whipped, which is dependent on the voltage applied, and the distance the jet travels influences the crystallinity of the fibres. In other words, the formation of the crystals in governed by the stretching of the solution and the solvent evaporation. If not enough time is given for crystallization, the formation of smaller crystallites with defects will take place, leading to a lower crystallinity [25].

Table 5.4. Melting temperature and area under the melting peak for EVOH, 13 wt% EVOH fibres and 15 wt% EVOH fibres

Sample	Tm (°C)	Heat of fusion (J/g) (Area under peak)
EVOH	165. 71	63.47
EVOH Fibres (13 wt% solution)	163.03	72.01
EVOH Fibres (15 wt% solution)	158.63	64.25

For the composite formation, both aligned and non-aligned fibre mats were to be used. To align the fibres, the fibres were collected on a rotating drum. A piece of aluminium foil is placed on the drum to collect the fibres. As the drum rotates, the fibres will be aligned. Therefore it was necessary to investigate the crystallinity and melting of the aligned and non-aligned fibres. The fibres were spun from a 15 wt% DMSO solution, at 0.008 ml/min, 15 kV and a TCD of 20 cm.

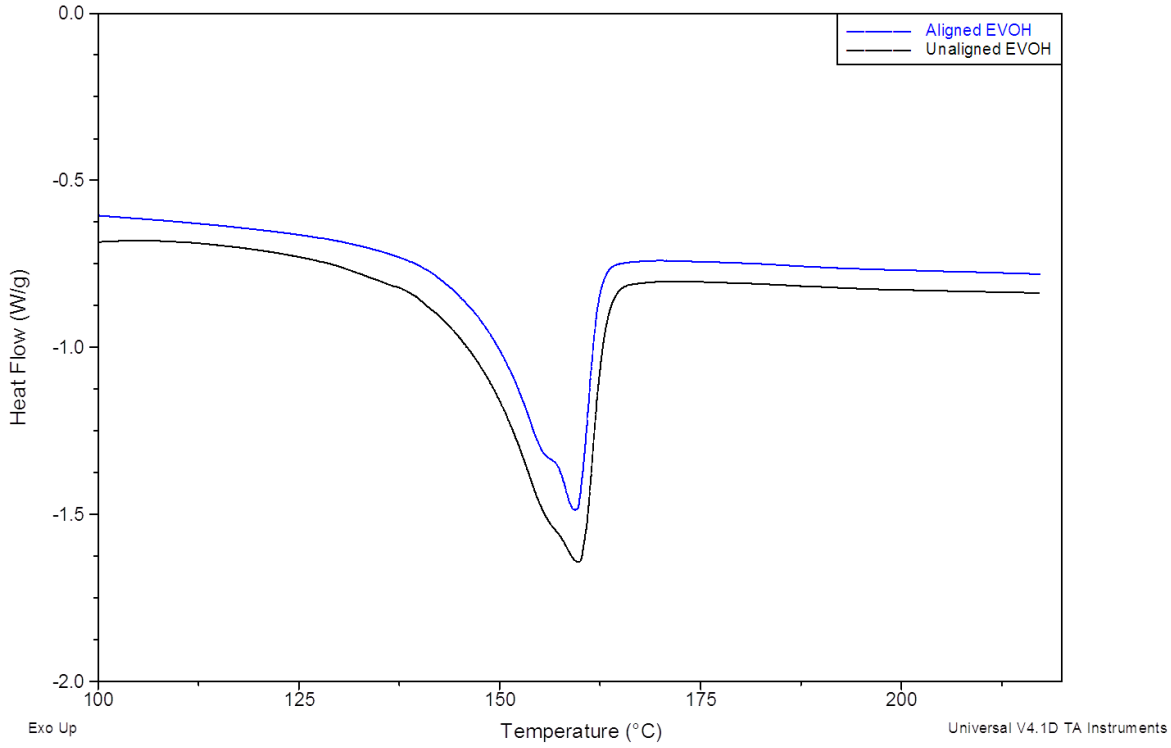

Figure 5.20. Melting endotherm (1st heating scan) of aligned and unaligned EVOH fibres

From Figure 5.20 it is clear that the alignment of the fibres has no influence on the melting temperature of the fibres.

There was also no difference between the crystallization temperatures of the two types of fibres; however there was a difference in the percentage crystallinity as can be seen from the area underneath the melting peak (Figure 5.20) and the heat of fusion (Table 5.5).

The unaligned fibres had a greater heat of fusion, indicating the unaligned fibres are more crystalline than the aligned fibres. It would be expected that it will the other way around, since the aligned fibre collection take place on a rotating collector. When collecting fibres on a moving collector, the fibres will be stretched as it is collected. Although the fibres were stretched more by the rotating collector, it might be possible the molecules did not have enough time to align or the fibre were already dry when reaching the collector and no further stretching took place. It should also be taken into a count that the rotating collector does align the fibres somewhat, but not a great deal of alignment could be seen in the SEM images.

Table 5.5. Thermal properties of the non-woven and aligned fibres

Sample	Tm (°C)	Heat of fusion (J/g)
EVOH Fibres (Non-Woven)	159.54	78.73
EVOH Fibres (Aligned)	159.09	67.87

5.2 Composite formation

For a filler to be used as reinforcement in a polymer matrix it must possess certain properties, which include high surface area, good adhesion between the filler and the matrix, proper mechanical properties, high aspect ratio and good dispersion inside the matrix to name a few. Nanofibres meet most of the criteria mentioned here and therefore it is no surprise that these materials are popular to be used as nanofillers inside a polymer matrix. In this study the aim was to use the EVOH nanofibres as reinforcement in a LDPE matrix.

5.2.1 Melting experiments on the fibres

Work has been done regarding the compatibility of the LDPE and EVOH [26], concluding that these two polymers are quite compatible. This was shown by Shebani [26] by the use of DSC. He proved that that EVOH can be used as a compatibilizer for LLDPE/wood composites. Many papers discuss the reinforcement function fibres will have when added to polymer matrix [27-30]. In most cases the fibres will increase the strength of the material, since the stress applied to the material will be transferred to the fibres. Low density polyethylene melts at about 120 °C, so when reinforcing this material with polymeric fibres, the fibres should not melt, but remain in fibre form to react as reinforcement. EVOH has a significantly higher melting temperature than LDPE, thus making it a candidate for fibrous reinforcement. Initially it had to established that when the LDPE was melted (at 140 °C), with the EVOH fibres, that the fibres would retain their original form. The first task would be to test if and when the fibres melt when subjected to heat for a certain time. The fibres were placed on glass slides in a press, the press were heated till 140 °C and the fibres kept there for different times. The result of these experiments can be seen in Figure 5.21. From the SEM images it was quite clear that the fibres initially did not melt at 140 °C. It was only after 20 minutes at 140 °C that some of the fibres started to fuse together. This, however, was not a problem, since the melting of LDPE at 140 °C will only take at the most 10 minutes.

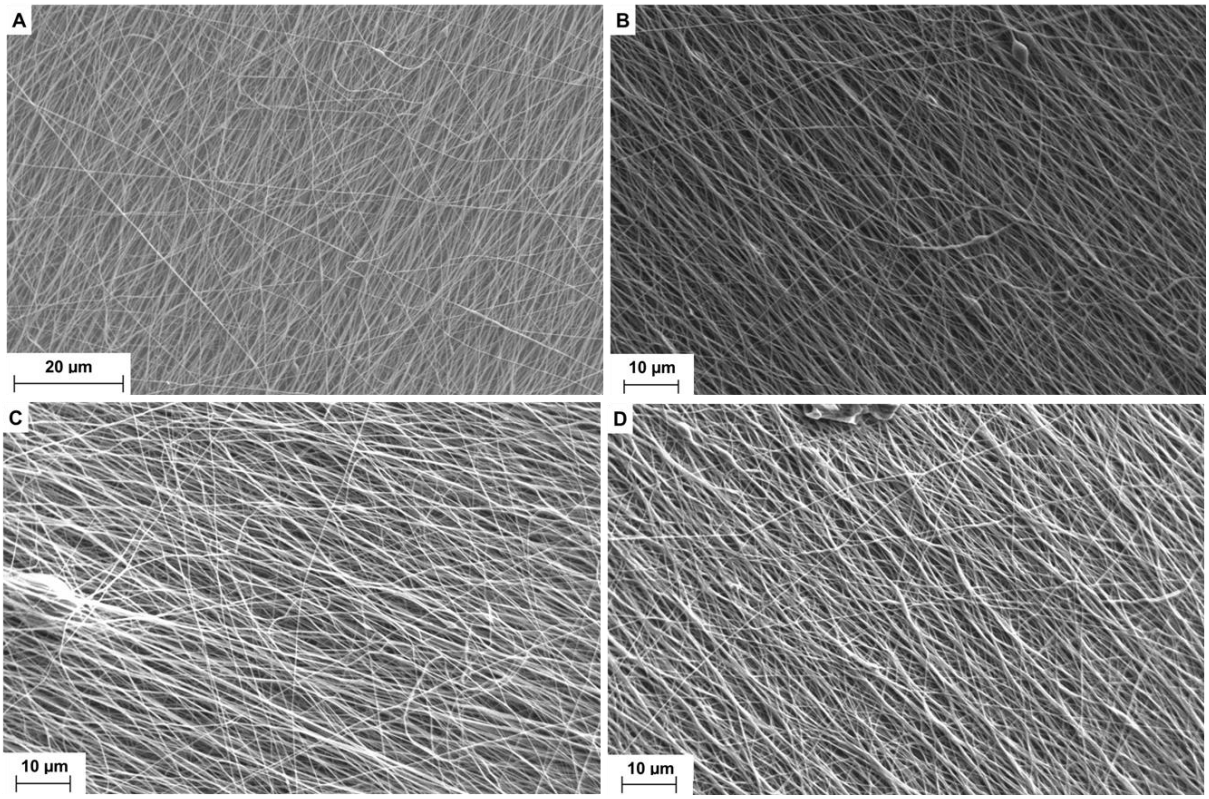

Figure 5.21. Melt experiments of 15 wt% EVOH fibres kept at 140 °C for A) 5 min, B) 10 min, C) 15min and D) 20 min

5.2.2 Incorporation of EVOH fibres in a LDPE matrix

The next step was trying to incorporate the fibres into the matrix. This proved to be much more difficult than anticipated. The easiest way seemed to be by using injection moulding. But due to the viscosity effects, the polymer tended to flow into the mould and the fibres did not flow that readily, leaving the fibres concentrated in one area and not distributed throughout the moulding at all. The second way was by adding polymer pellets and fibres to the mould and then heating the mould and pressing films. It was discovered that the pellets melted, but the fibres floated on top, so the fibres were only on the surface of the material and not incorporated throughout the LDPE.

The next method we tried was to press two LDPE films, place a fibre mat in between the two films and then melt press the two films together, with the fibre mat in between. There were some difficulties with this as well, with the films not always melting together and becoming separated afterwards, due to the fibre mat in between. If too much pressure was applied during the pressing process, the fibres got pushed out to the side. Eventually some composites were formed that could be used for mechanical testing. A cross section was taken of some of the composites before tensile testing, to determine the adhesion between the polymer and the fibres as well as if to see if the fibre form was not compromised. Figure 5.22 (SEM image) shows that the adhesion between the polymer matrix and the fibres is very good and the fibres are imbedded in the polymer matrix and not separate. The fibre form is also retained.

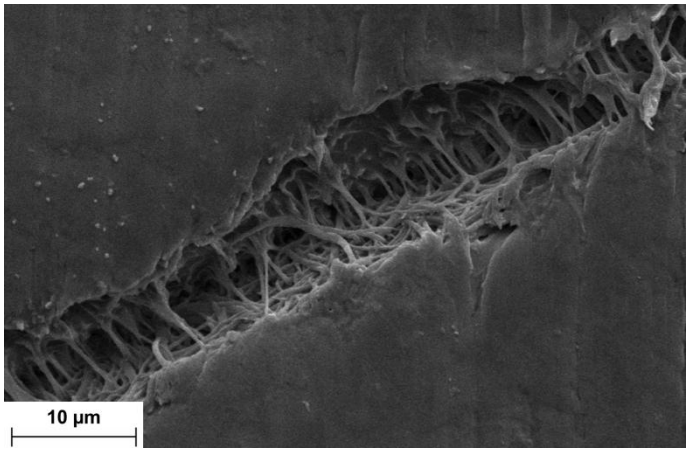

Figure 5.22. Cross section of a LDPE/Non-woven fibres/LDPE film before tensile testing

The amount of fibre and polymer was very difficult to calculate and this factor must be taken in to account when observing the tensile properties of these materials.

5.2.3 Tensile properties

Nanofibres are supposed to show an increase in elastic modulus as well as tensile strength, over the parent polymer, due to the aligned molecular structure inside the fibre. During electrospinning the molecular chains should align along the fibre axis, resulting in fibres comprising of aligned molecular chains, which should enhance their mechanical properties [23, 24].

The EVOH fibres were pressed between LDPE films and tensile testing was performed on these samples. The nanofibres clearly had an influence on the mechanical properties of the composites compared to pure LDPE (Figure 5.23). Fibres tend to be better reinforcing nanofillers than whiskers or short fibres; this being is ascribed to their high aspect ratio [31]. When using shorter fibres, the stress transfer from the matrix to the fibres is very poor, shorter fibres tend not to overlap, so they do not strengthen the material and the edges can act as stress initiators, implying that it will be the origin of the crack [32].

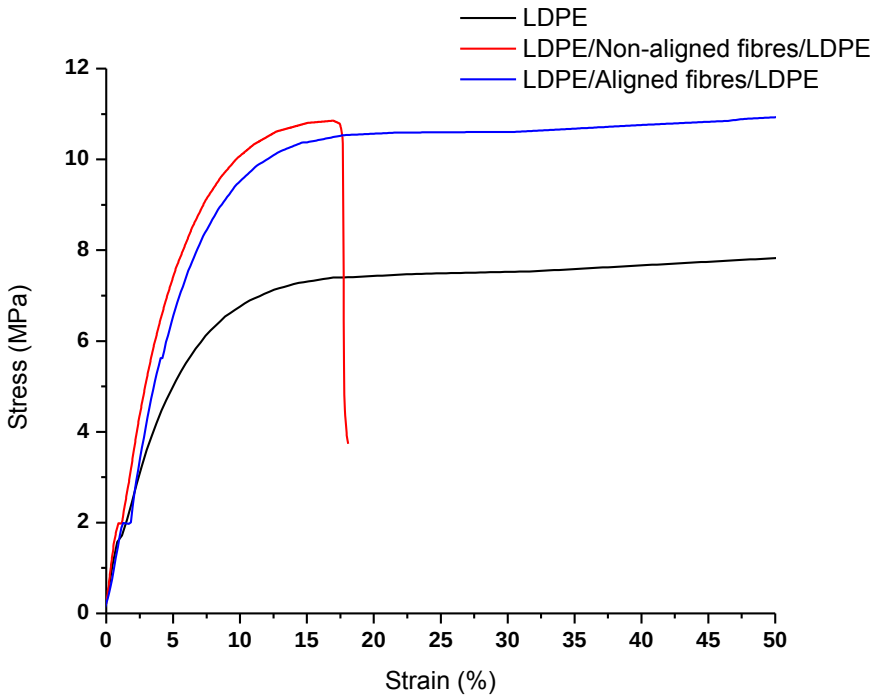

Figure 5.23. Stress-strain curve of LDPE en LDPE/EVOH Fibres composites

The improvement of the material with the fibres indicates that the nanofibres acted as an effective reinforcing filler and there appeared to be good adhesion between the fibres and the polymer matrix. The high surface ratio of the fibres also allowed good stress transfer from the polymer matrix to the fibre and thus increasing the stiffness of the material, which is indicated by the Young's modulus (Figure 5.24).

The only property showing no improvement was the elongation at break. This can be ascribed to the morphology and molecular orientation differences between the two samples [33]. LDPE is a material with low crystallinity and the polymer extends quite easily when a force is applied. By adding the fibres, which have higher crystallinity, the mobility of the composite is decreased. Therefore the composite will not undergo as much elongation during the tensile test. The decrease in the elongation at break has been seen by various researchers [30, 33, 34]. Cracks and voids may also form in the material; this decreases the stress transfer and then eventually the elongation at break. The composite material also experiences a great deal of stress at certain strains than the pure polymer. This is ascribed to the fibres pre-existing molecular orientation due to the electrospinning process [33].

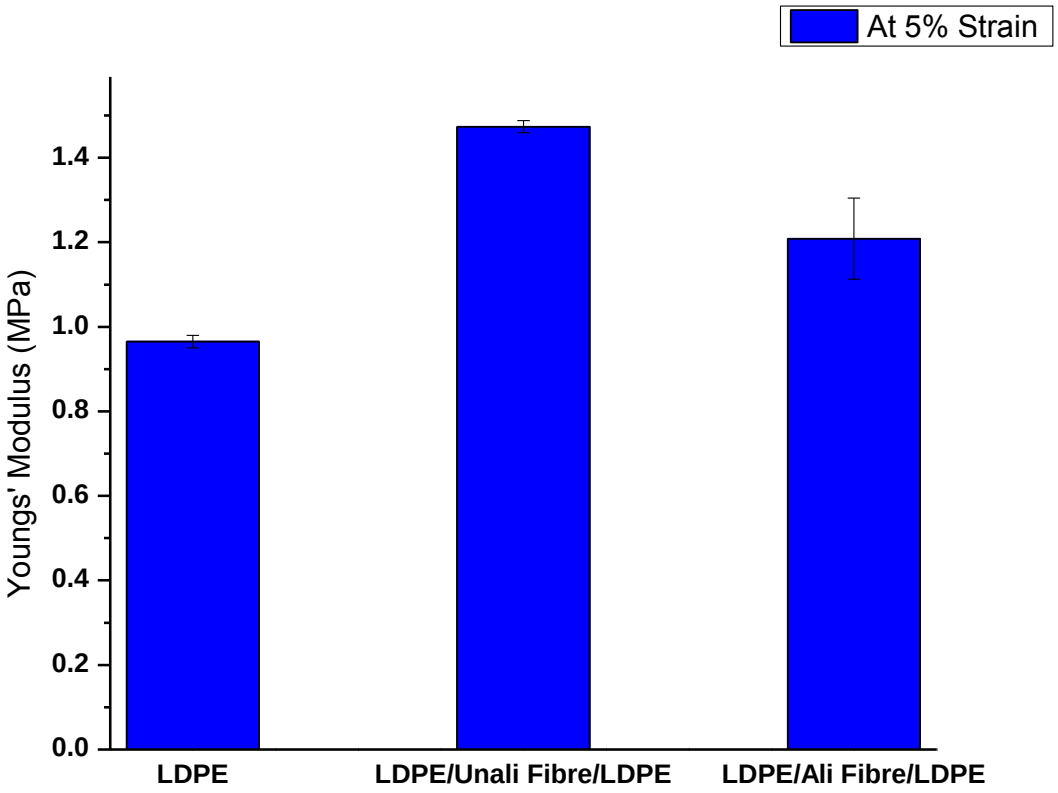

Figure 5.24. Elastic modulus (5% strain) of pure LDPE and LDPE/EVOH Fibre (non-woven and aligned) filled composites

The unaligned fibres had a greater effect on the stiffness of the material, than the aligned fibres. We would expect to see a greater enhancement of the stiffness of the material when using aligned fibres, since the load transfer between the fibres will be better. It is well known that fibres exhibit better strength when aligned parallel to the fibre axis, but perpendicular to it, they exhibit very weak tensile strength [35]. When comparing the crystallinity of the aligned and unaligned fibres (Table 5.5) it can be seen that the unaligned fibres are more crystalline than the aligned ones. The crystallinity of the fibres plays an important role in the reinforcement effect of the fibres. The higher the crystallinity, the higher the modulus will be, the crystalline material will make the material stronger. Another explanation for the trend in Figure 5.24 is that the dispersion of the non-aligned fibre mat may be better than that of the aligned mat. When placing the fibre mat between the two films, the aligned fibre mat may bundle and therefore lead to a worse dispersion of the fibres in the polymer matrix. Although the same size fibre mat was used each time the weight of the fibre mat may differ, this implies that in some samples there are more fibres than in others. The stress-strain curve in Figure 5.23 indicates this better. The red curve is that of the composite containing the non-aligned fibre mat and it can be seen that the curve differs from that of the pure LDPE and the

LDPE/aligned fibre composite. From stress-strain curve of the composite containing the aligned fibre mat it seems as if the stress transfer takes place up until a certain point, but then the matrix elongates normally, like it would for LDPE. This may indicate that there are big parts of the matrix that are not in contact with fibres and, therefore, the influence of the fibres inside the matrix will not be as effective for the aligned fibres. What should also be taken note of is that due to way the composites is prepared, it was difficult to calculate the precise amount of fibre present, this may also lead to differences in the way the composites behave under applied stress.

Table 5.6. Comparison of the modulus for different composites

Sample	Modulus	% Increase
LDPE	0.96	
LDPE/Unali Fibre/LDPE	1.47	51
LDPE/Ali Fibre/LDPE	1.21	26

The difference between the aligned and non-aligned mats is not that significant when comparing the tensile strength as can be seen in Figure 5.25. What is more noticeable is the increase in tensile strength of the material when adding the fibres. LDPE is known for its low tensile strength. LDPE has many branches present inside the polymer, this makes it less crystalline and therefore its tensile strength will not be that high. When adding fibres (well dispersed), the mobility of the chains will be restricted. The stress that is applied to the polymer matrix will be transferred to the fibres and this leads to the material having better tensile strength.

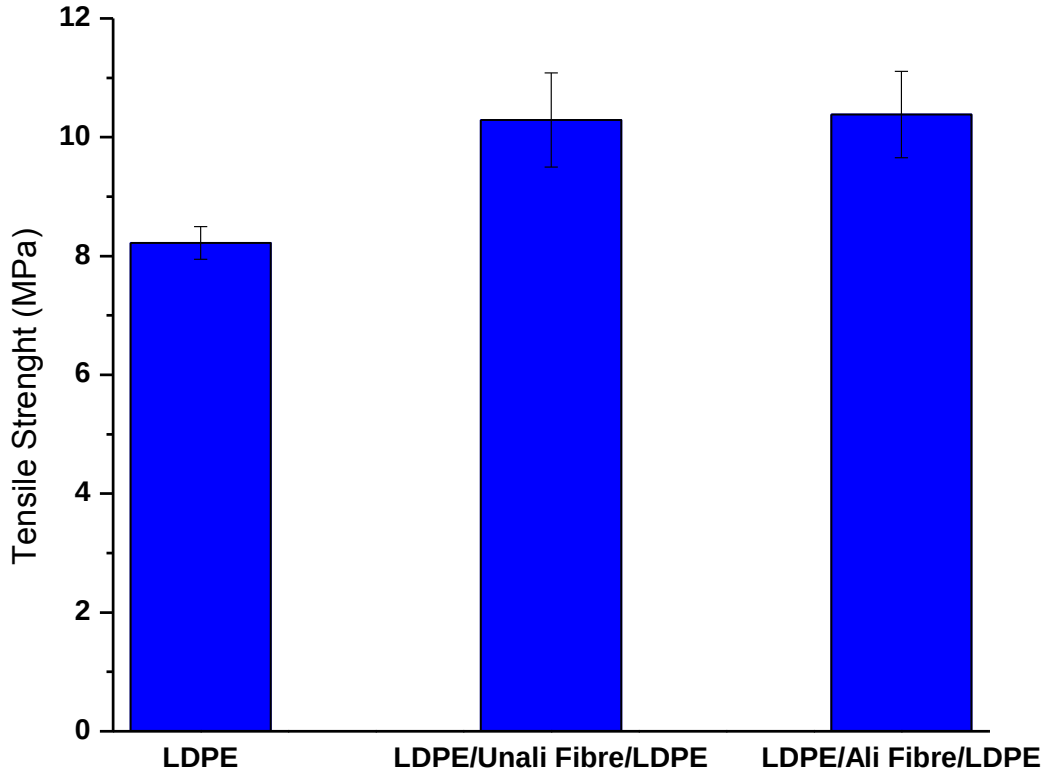

Figure 5.25. Tensile strength of pure LDPE and LDPE/EVOH Fibre (non-aligned and aligned) filled composites

All these above-mentioned results were the average of 5 tests. There was a variety in the results obtained, although more or less in the same range. We can, however, see that the standard deviation for the composites is quite large. These variations in the results can be explained by the defects introduced by both the sample preparation methods as well as the inherent defects in the fibres. Some of the fibres incorporated in the matrix may have fibre defects which will influence the tensile properties. The fibres may also form a porous structure during electrospinning and these pores may lead to stress concentration sites, initiating breakage. The molecular arrangement may also differ from fibre to fibre [36].

In conclusion, though it is quite clear that the addition of EVOH nanofibres lead to a significant change in the mechanical properties of LDPE (Table 5.7)

Table 5.7. Mechanical properties of LDPE and LDPE composites

Sample	Yield strength (at 0.2 % strain offset)	Elongation at break (mm)	Stress at break (MPa)	Ultimate Tensile Strength (MPa)
LDPE	6.71	117.91	8.19	8.22
LDPE/Unali Fibre/LDPE	9.31	45.06	10.51	10.29
LDPE/Ali Fibre/LDPE	7.82	56.25	10.22	10.38

5.3 Electrospinning of EVOH with MWCNT

Another way of reinforcing a polymer matrix is by adding carbon nanotubes. The main attraction of these materials is the enhancement they bring to the modulus and the tensile strength of the material. It has been measured that the nanotubes itself has an elastic modulus of 1-2 TPa [37]. They have excellent mechanical, thermal and electrical properties and due to their small size they have a very high aspect ratio and can be used in polymer materials to form nanocomposites [38, 39]. One of the main problems with incorporating MWCNT in a polymer matrix is the dispersion of the carbon nanotubes throughout the matrix. One method used is electrospinning a polymer solution containing carbon nanotubes and then incorporating the fibres in a polymer matrix. This method provides a way to incorporate nanotubes in a polymer matrix, without influencing or changing the structural integrity of the nanotubes[40]. During electrospinning the MWCNT will be distributed throughout the fibres and aligned with the fibre axis and it is found that the nanotubes tend to align better, maybe due to the spatial confinement of the fibres. Aligned CNT will enhance the area to which the polymer matrix will bond and the aspect ratio will be higher for better reinforcement. When incorporating the fibres into the polymer matrix and melting the fibres, we are left with the carbon nanotubes inside fibres [37].

5.3.1 Electrospun EVOH fibres with MWCNT

Functionalized MWCNTs were used in all experiments. By functionalising the surface of the CNT better interaction between the nanotubes and the polymer matrix is ensured and therefore better reinforcement will take place. The first experiments done for the electrospinning of EVOH with MWCNT were done in DMF. At first only 5 wt% MWCNT was added to the electrospinning solution and no salt was used. The MWCNT did not seem to influence the morphology of the fibre too much, although some beading could be seen. Some examples are show in Figure 5.26.

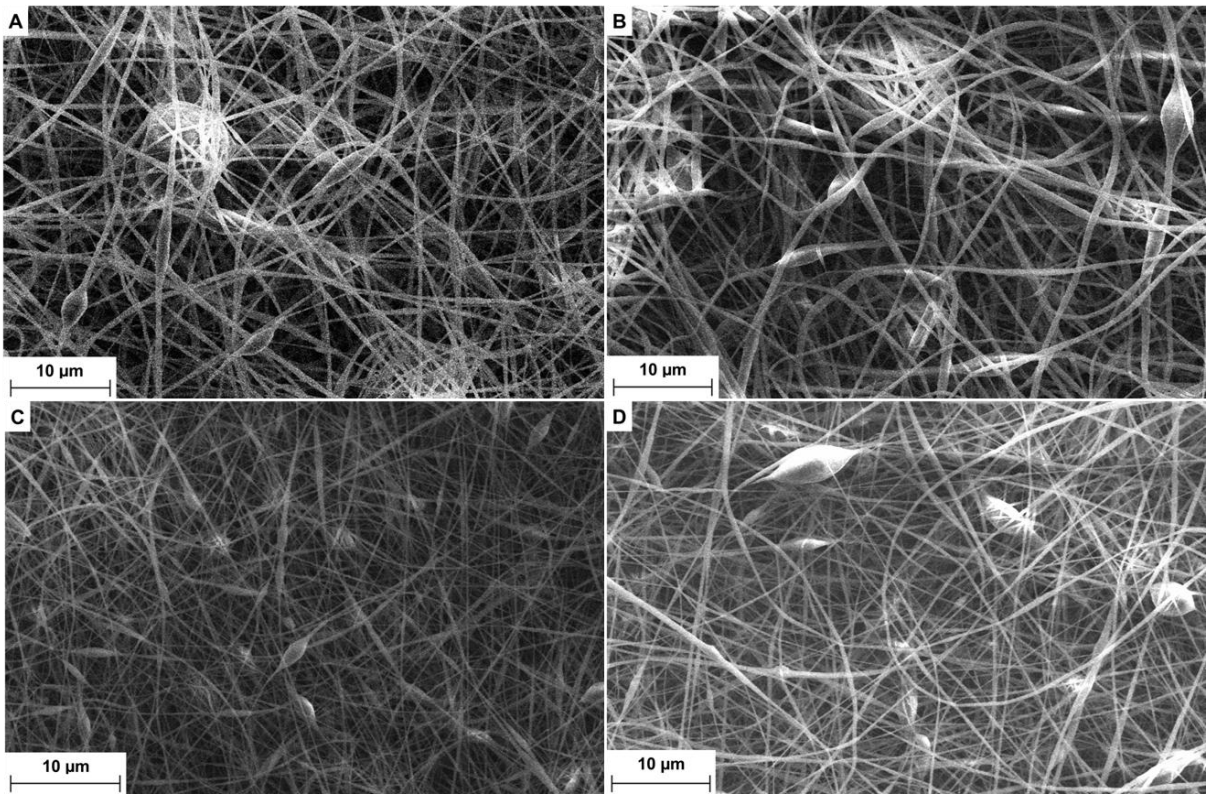

Figure 5.26. SEM images of EVOH nanofibres produced from DMF solution with 5 wt% MWCNT spun at different parameters A) 0.05 ml/min, 15 kV and 20 cm, B) 0.05 ml/min, 20 kV and 20 cm, C) 0.01 ml/min, 20 kV and 20 cm and D) 0.01 ml/min, 15 kV and 15 cm

LiCl was added to the electrospinning solution and immediately beaded fibres could no longer be detected (Figure 5.27). The average fibre diameter of the samples containing MWCNT was 540 nm (±140 nm). This was thicker compared to the 380 nm (± 90 nm) of the EVOH fibres without MWCNT. The nanotubes may influence the fibre diameter due to agglomeration inside the fibre. It was suspected that the nanotubes may not be aligned inside the fibre and some may even protrude through the walls of the fibres, leading to thicker fibres.

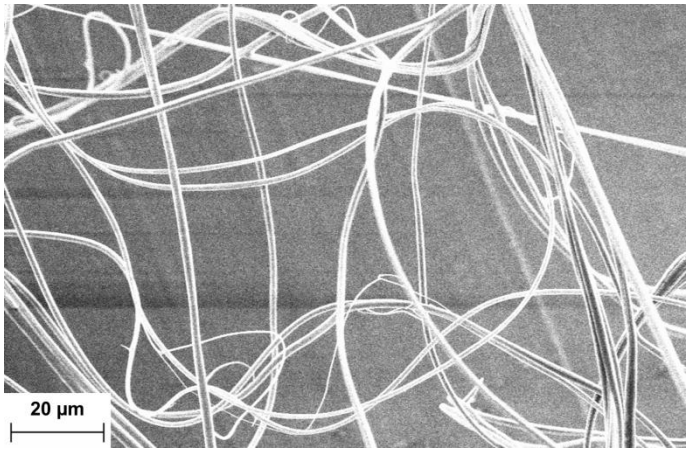

Figure 5.27. SEM image of EVOH nanofibres with 10 wt% MWCNT and 0.2 wt% LiCl

DSC was performed on sample without MWCNT and containing 10 wt% MWCNT to determine the influence of the MWCNT on the crystallinity and melting temperatures of EVOH. There is a slight decrease in the melting temperature of the fibres containing MWCNT. This can maybe be due to the influence the nanotubes have on the way the polymer is electrospun. The crystallization temperature is the same for both samples. It should be noted that the melting temperatures were obtained with the first heating scan and the crystallization after the first heating scan. Thus we are comparing the crystallization from the melt resulting from the heating of the original artefacts.

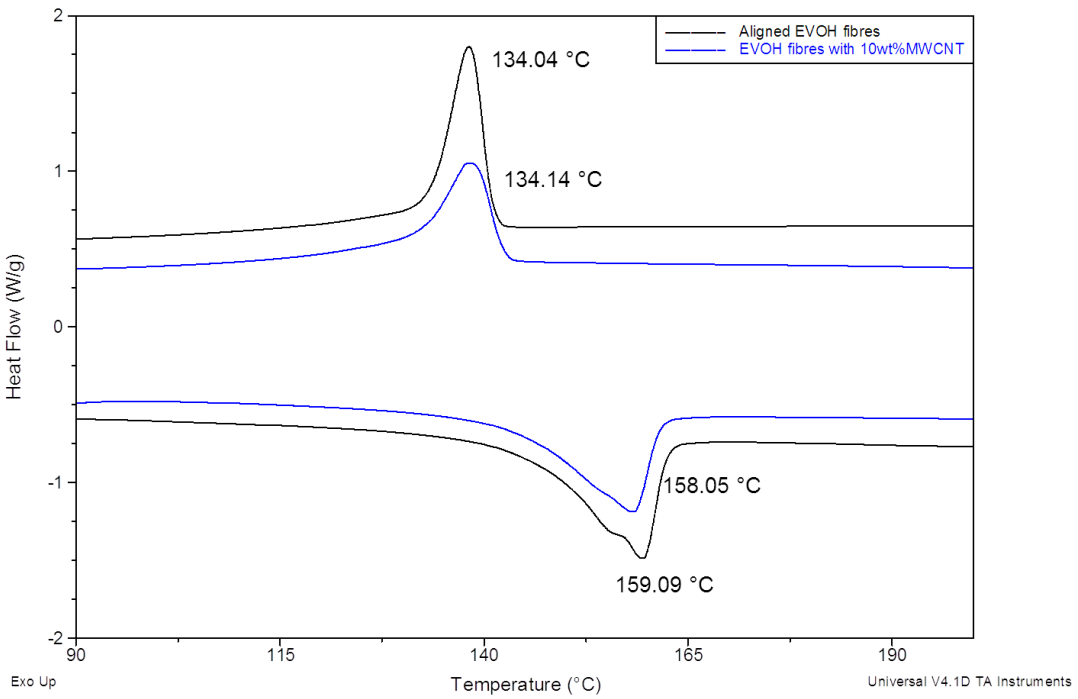

Figure 5.28. DSC Thermogram of EVOH and EVOH containing MWCNT

The crystallinity of the fibres containing nanotubes was also lower than the fibres without nanotubes (Table 5.8). The nanotubes inside the fibres might prevent the orientation of the molecules inside the fibres during electrospinning and this will lower the crystallinity of the fibres containing nanotubes.

Table 5.8. Thermal properties of EVOH fibres with and without CNT

Sample	Tm (°C)	Heat of fusion (J/g)	Crystallization peak (°C)
EVOH Fibres (Aligned)	159.09	67.87	138.04
EVOH Fibres with 10% MWCNT (Aligned)	158.05	56.08	138.14

Transmission electron microscopy was used to visualize the MWCNT and functionalized MWCNT. TEM was also done on the fibres to observe the presence and orientation of the nanotubes inside the fibres. The multi-walled nature of the carbon nanotubes can clearly be seen in Figure 5.29.

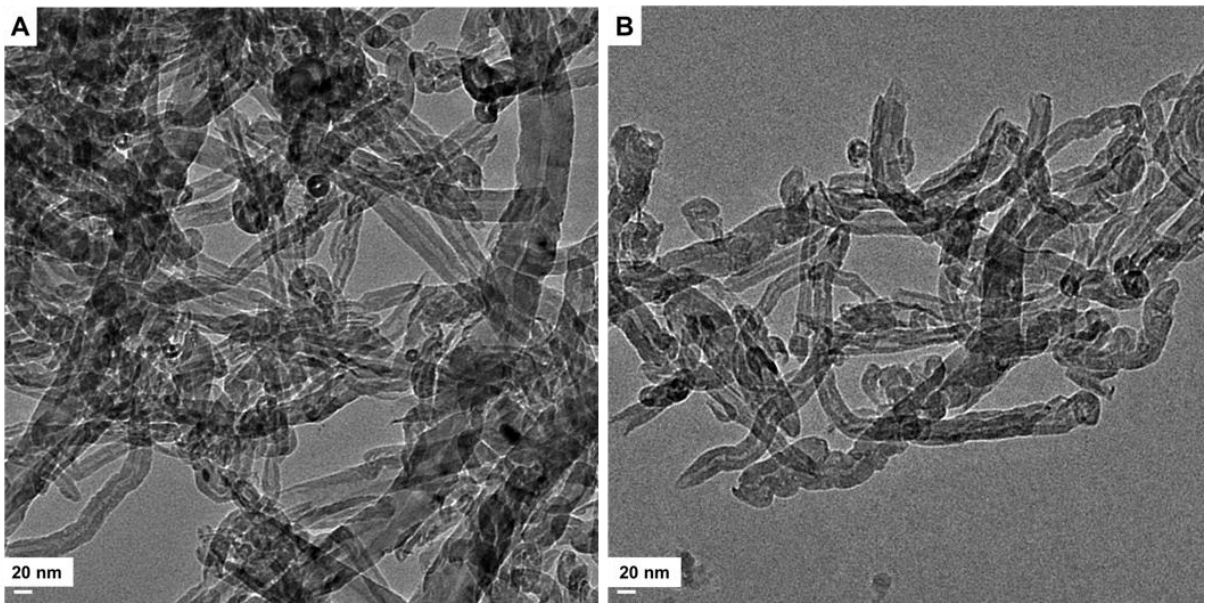

Figure 5.29. TEM images of A) MWCNT and B) Functionalized MWCNT

Finding the nanotubes inside the fibres turned out to be very difficult. This could possibly be due to the fact that the nanotubes were not that well dispersed, and another problem was that the fibre mat was very thick and it was difficult to see inside the fibres with the transmission microscope. Embedding it in resin was problematic, since the fibres float on top. However, the presence of the

nanotubes was confirmed inside the fibre as can be seen in Figure 5.30. In this sample only 5 wt% nanotubes were added.

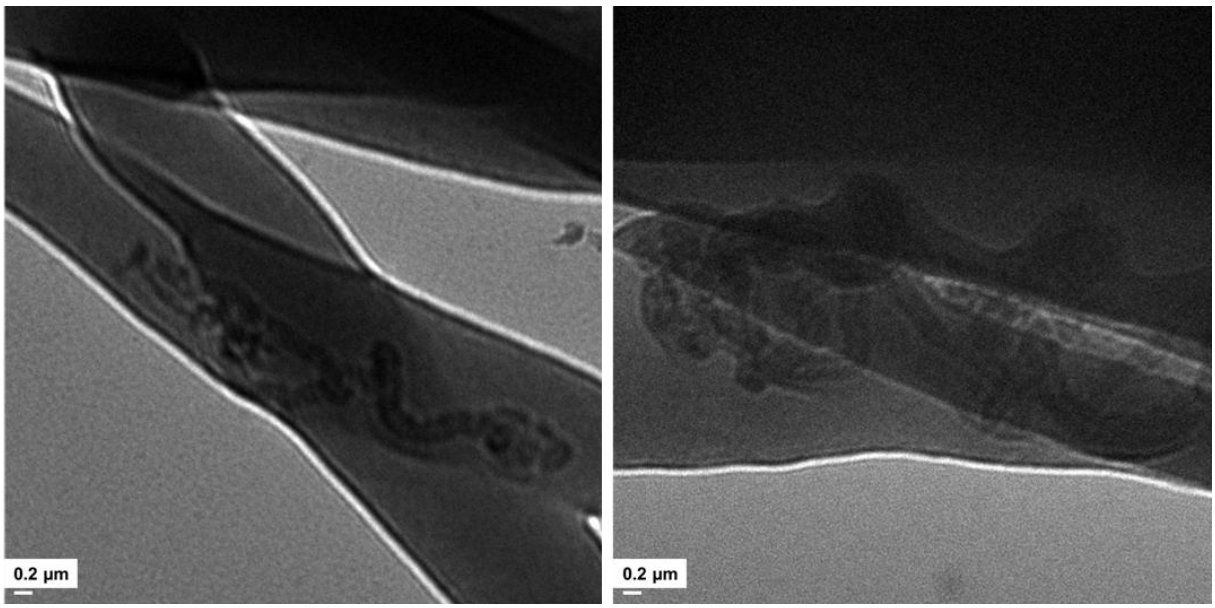

Figure 5.30. TEM images of 5 wt% MWCNT inside EVOH fibres

TEM images of 10 wt% MWCNT inside EVOH fibres was taken as well. Again the TEM images were not ideal, but there were images in which the nanotubes could be seen. It could be concluded from these images that the nanotubes are not straight, but rather curved. The electrospinning process does not allow the full stretching of the nanotubes.

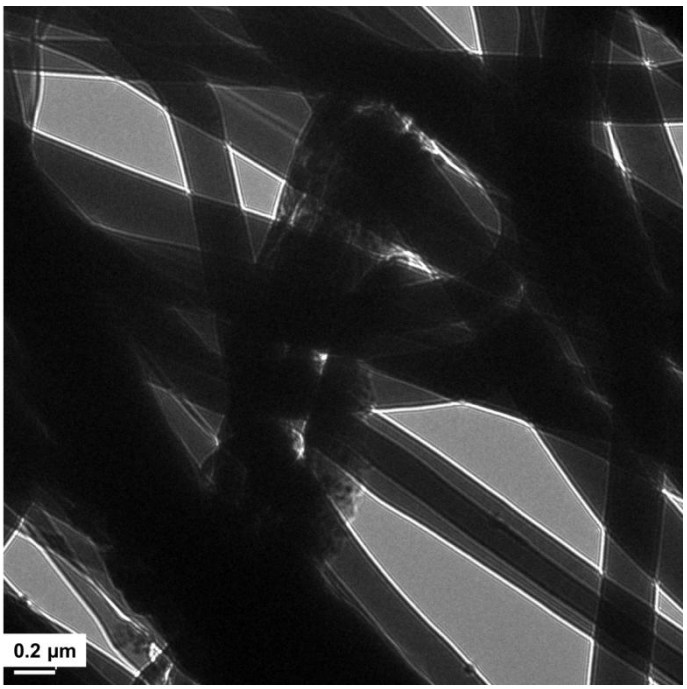

Figure 5.31. TEM image of EVOH fibres with 10 wt% MWCNT

FE-SEM images were taken of the fibres (containing 10 wt% MWCNT) fractured in liquid nitrogen (Figure 5.32. On some of the fibres, artefacts resembling nanotubes could be seen protruding, however, no definite nanotubes could be observed. .

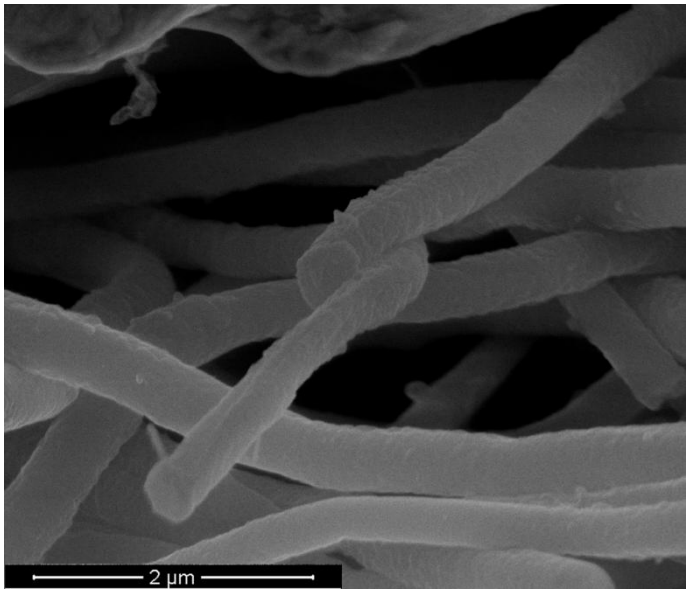

Figure 5.32. FE-SEM images of EVOH fibres containing 10 wt% MWCNT

A paper was published describing a process where electrospun fibres were immersed in a MWCNT solution, kept there for a few minutes and then removed and rinsed [41]. Reportedly, this resulted in MWCNT being adsorbed on the fibres. Subsequently we formed EVOH nanofibres in the absence of MWCNT. We then immersed the fibres in a MWCNT/DMF solution. The sample was then rinsed with water, to get rid of all the unattached MWCNT. The immersing of the fibres into a MWCNT solution did not give the result expected from literature [41]. TEM images (Figure 5.33) indicated that the nanotubes absorb onto the fibre as agglomerates and not evenly spread along the fibres. This indicated that electrospinning EVOH in the presence of MWCNT was the best way of introducing the MWCNT to the polymer.

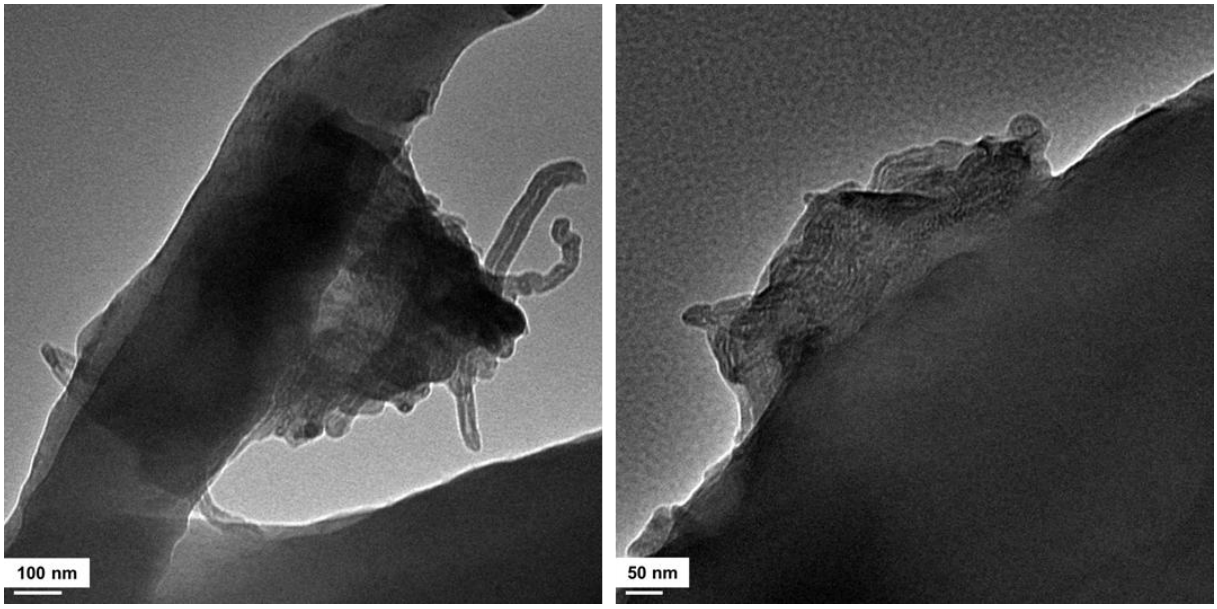

Figure 5.33. TEM images of EVOH fibres immersed in 15 wt% MWCNT solution

Another way to confirm and calculate the amount of nanotubes inside the fibres is by TGA. Since the MWCNT degrade at very high temperature, by looking at the weight loss profile of the fibre/MWCNT we will be able to see if there is any MWCNT present. This will be discussed with the TGA results that follow.

At this stage the solvent was changed for electrospinning to establish if better dispersion of the nanotubes would be possible. Three different solvents were tried: 1) DMF, 2) Isopropanol/H_2O and 3) DMSO. The isopropanol/H_2O did not work, but 15 wt% MWCNT were added to both the other solvent systems for electrospinning. From the TGA curves in Figure 5.34, it is clear that DMSO solvent system worked the best. The weight loss curve indicated that about 12 wt% carbon nanotubes is present whereas with the DMF only 3 wt% MWCNT was present in the fibres. Dispersion of the carbon nanotubes is clearly better in DMSO.

The TGA shows two definite weight loss steps for all the samples. Alvarez *et al* [42]. described this two-step degradation by saying that the first step might be due the degradation of the vinyl alcohol part of the copolymer and the later step is that of the of the ethylene sequences degrading. Chain scission starts to happen at the parts of the chains consisting of the vinyl alcohol units, this will take place until there is no vinyl alcohol units left where chain scission can occur. The last step in the degradation occurs when chain scission starts in the ethylene-containing chain segments. Both weight loss steps can be seen in all the samples. For the samples with the MWCNT, however, the onset of the first degradation step was delayed. This implies that the carbon nanotubes improve the thermal stability of the fibres. The onset of the second degradation however was earlier, so it seems that nanotubes influence the degradation of the polyethylene segments in some way that will cause that part to degrade more rapidly.

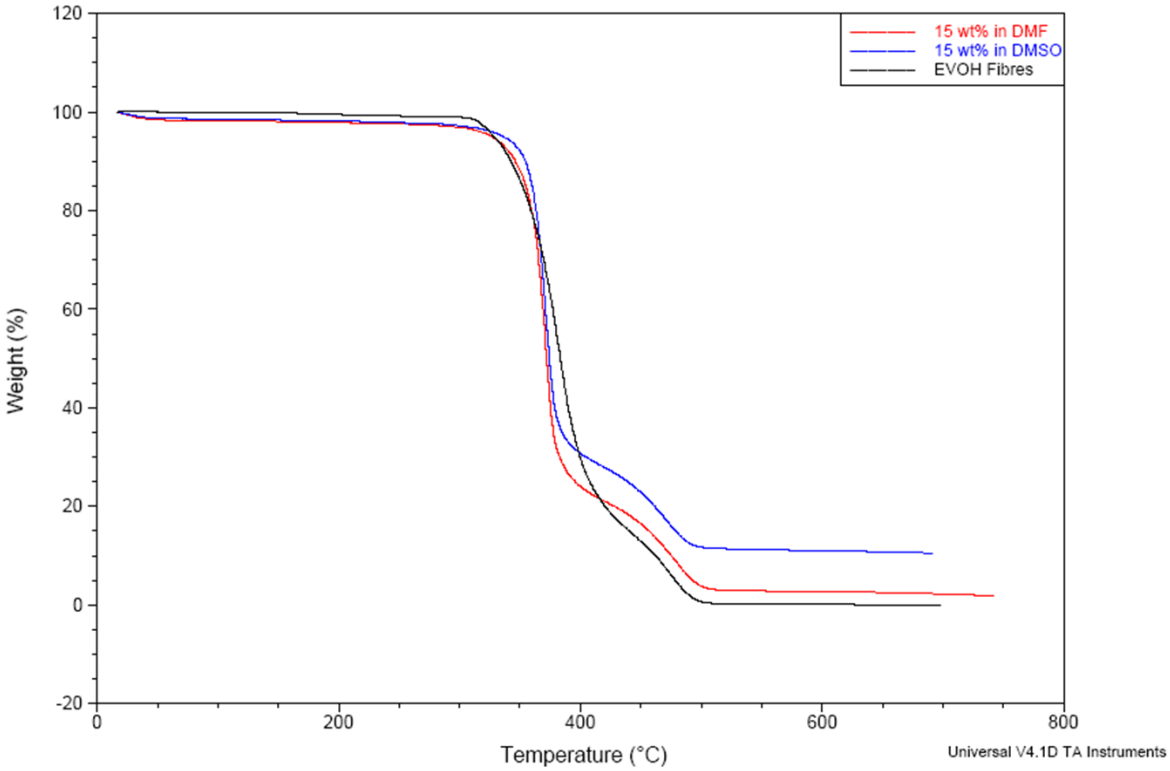

Figure 5.34. TGA thermogram of EVOH fibres and fibres containing MWCNT

5.3.2 EVOH/CNT nanocomposites

The nanocomposite samples were prepared in the same manner as the LDPE/EVOH nanofibre composites. In this case, however, the temperature was increased to the point where the EVOH fibres would also melt, leaving the MWCNT dispersed in the LDPE. For this study only aligned fibres containing MWCNT were used (Figure 5.35). Literature suggested that the better the nanotubes are aligned, the better their reinforcement properties and when aligning the fibres the chances are better for obtaining aligned nanotubes [43]. In the electrospinning process the nanotubes will start off being randomly orientated inside the syringe, the force of the electrospinning jet will orientate them inside the fibre [44].

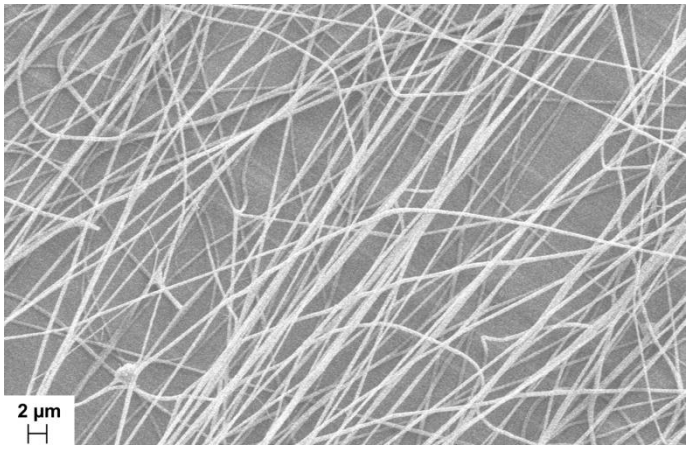

Figure 5.35. SEM images of aligned EVOH fibres filled with MWCNT

A LDPE/MWCNT composite was prepared using EVOH fibres spun with 10 wt% MWCNT. The EVOH/MWCNT fibre mat was placed between two LDPE films. In this case, though, the sample were heated to 160 °C and kept it there for 10 minutes to make sure the EVOH fibres will melt. A cross section image was taken of the composite, both by using SEM and TEM. From the SEM image (Figure 5.36) it was clear that the fibres were definitely melted and the reinforcement of the fibres should play no role when determining the elastic modulus. The crack down the middle of the material is an indication of where to two films overlap, with the melted fibres in-between.

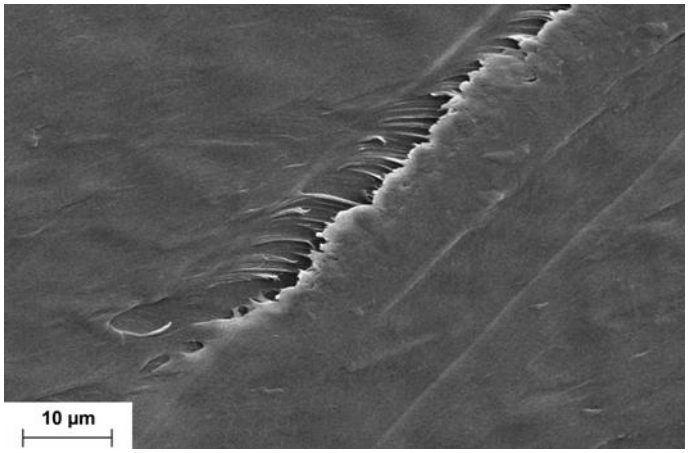

Figure 5.36. SEM image of cross section of LDPE/CNT/LDPE film

In Figure 5.37 the carbon nanotubes inside the film can clearly be seen. The dispersion of the nanotubes does not appear to be satisfactory, however. The TEM image is only a cross section of a small part of the film. The nanotubes though were not always aligned. The lack of alignment can be attributed to the electrospinning conditions. In addition the MWCNT were initially confined to the EVOH fibres, and they maintained this arrangement upon melting. A better strategy would probably have been to remelt and remould the composite, to see if a better dispersion could be obtained.

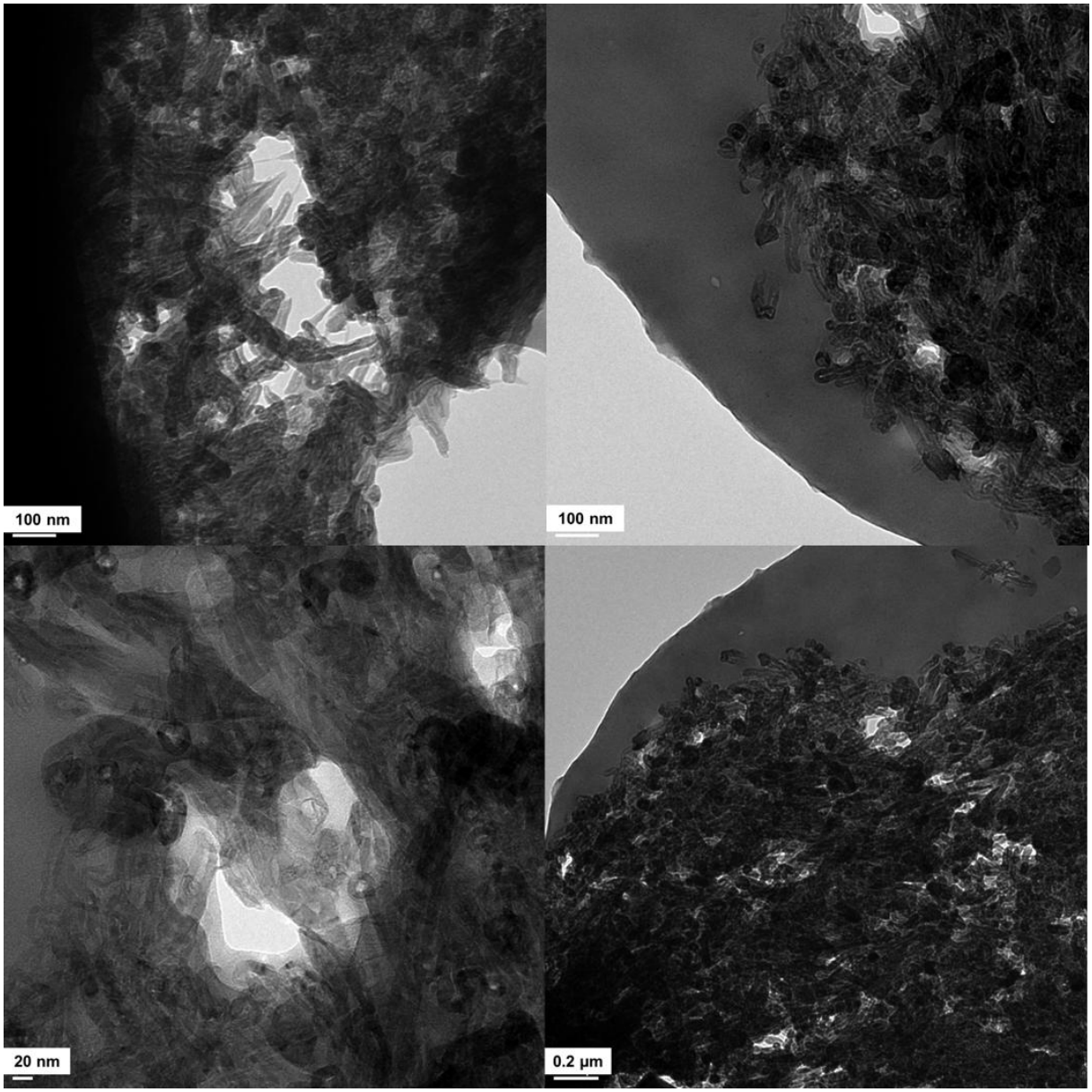

Figure 5.37. TEM images of LDPE/CNT/LDPE composite cross section

Tensile testing was performed on these LDPE/CNT samples and surprising results were obtained. When we compared a sample with melted fibres, without carbon nanotubes, to the other two samples, it appeared as if the presence of EVOH had a greater influence on the polymer matrix than the carbon nanotubes. The preparation of the tensile samples may also play a role in the results; the fibres might shrink during the melting process, leading to uneven dispersion of the carbon nanotubes.

A SEM image of the cross section of a tensile bar after tensile testing was prepared. Tensile tests were performed parallel to the tensile bar and from the images in Figure 5.38 it is evident that the polymer was pulled in the direction of the tensile test, elongating and then eventually broke. The formation of “holes” is clear around the fracture points, indicating the cause of the fracture. The amount of carbon nanotubes inside the film is possibly not enough to have a significant influence

on the mechanical properties. It could, however, be seen that where the polymer broke, there is an indication of molten material, indicating the presence of the molten EVOH inside the LDPE matrix. The presence of the molten EVOH is a possible explanation for formation of the holes in the LDPE matrix during tensile testing, leading to the fracture of the material.

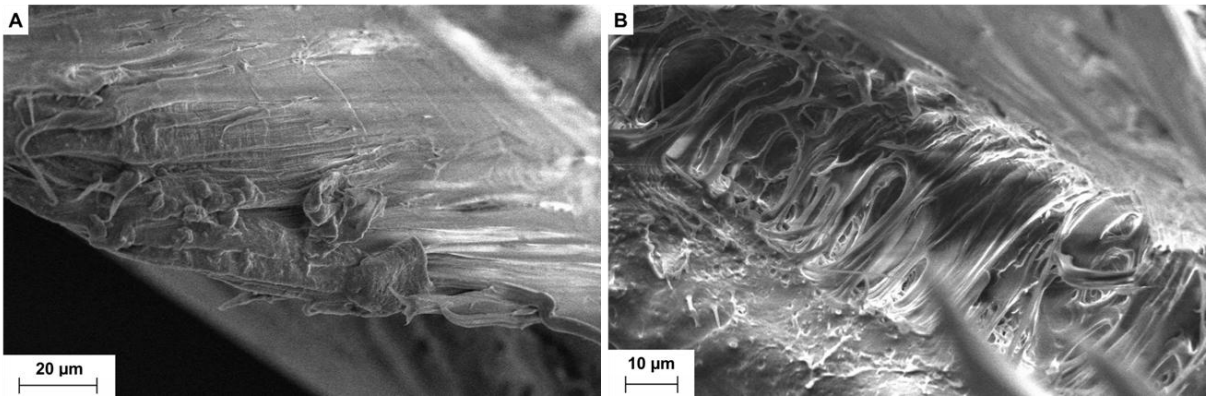

Figure 5.38. SEM images of cross section of surface after tensile testing

The true representation of the effect of the carbon nanotubes on LDPE is not clear, since the presence of the EVOH in the composite seems to be influencing or obscuring the results. It was therefore decided to evaluate the effect of the MWCNT on EVOH as a matrix. The nanotubes which are –COOH functionalized (Chapter 3) should interact well with the EVOH matrix and therefore reinforce the polymer[36]. It has been shown that both functionalized SWCNT and MWCNT significantly affects the modulus, tensile strength and elongation of polyurethane, to a greater extent than the non-functionalized nanotubes [45]. If the nanotubes are strongly bonded or well dispersed inside the matrix, the stress induced by the tensile load on the matrix will be transferred to the nanotubes through interfacial adhesion [46].

A composite of EVOH and MWCNT was prepared by sandwiching a mat of EVOH fibres containing 10 wt% MWCNT between two films of EVOH and melt-compressing the sandwich structure at 160 °C for 10 minutes. The stress-strain curve for the EVOH and the EVOH/MWCNT nanocomposite is shown in Figure 5.39.

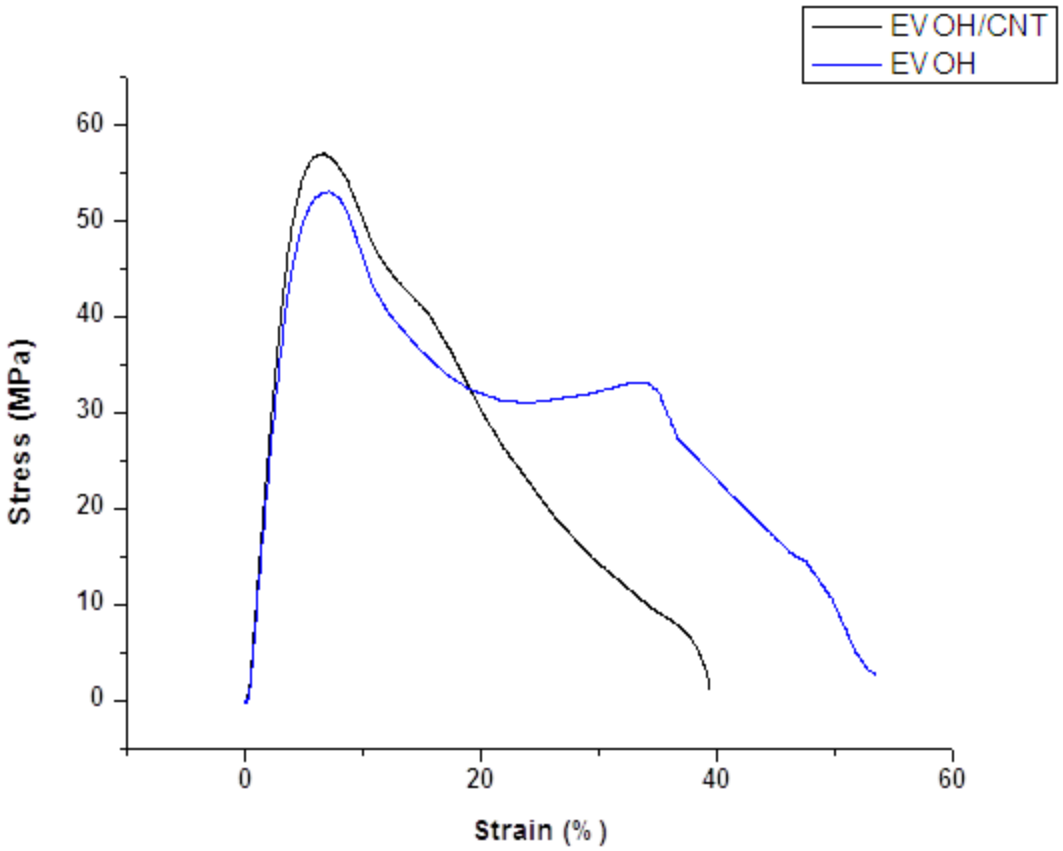

Figure 5.39. Stress/strain curve of EVOH composite with and without CNT

From the stress-strain curve in Figure 5.39, the EVOH sample exhibited better elongation at break than the sample filled with CNT. The decrease in elongation is expected, as the non-deformable MWCNT restrict the ability of the EVOH matrix to elongate after yielding. This effect was also found by Zhao *et al* [47].

The orientation of the nanotubes inside the fibre plays an important role in the properties of these materials. The test is performed parallel to the fibres inside the matrix, however, the nanotubes are not all aligned in the fibre direction, which will lead to the CNT having less of an influence on the mechanical properties than we would expect. The sonication process prior to electrospinning may also damage some nanotubes, leading to less reinforcement [44].

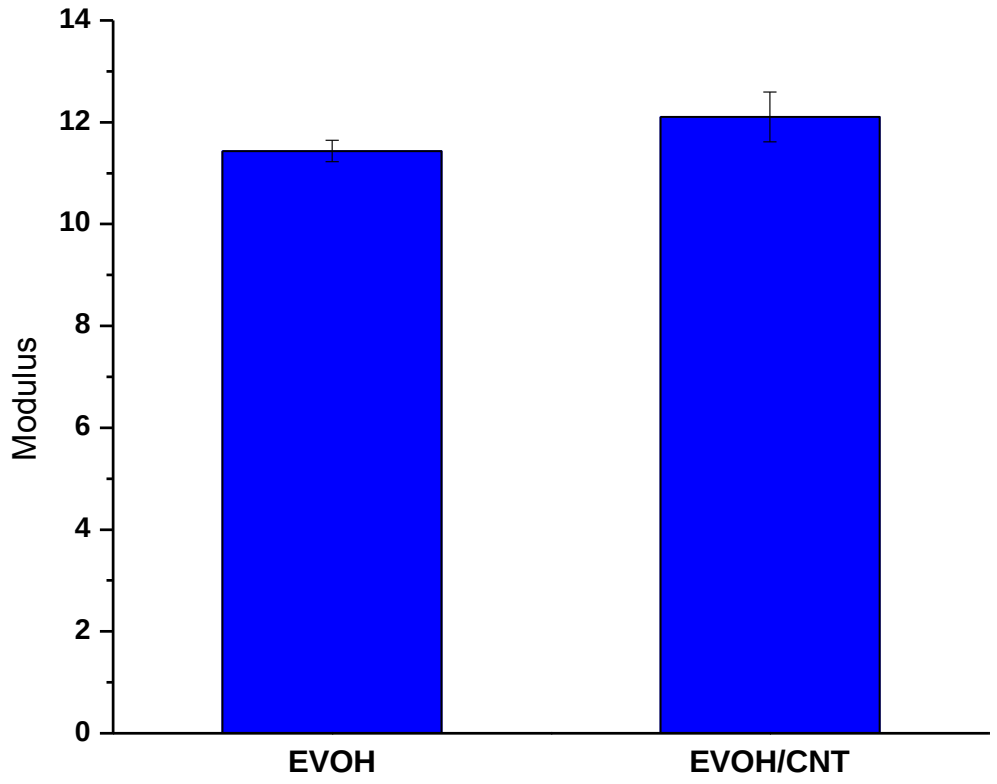

Figure 5.40. Modulus of EVOH and EVOH/CNT taken at 4% strain

From Figure 5.39 is clear that the slope of the elastic portion of the curve is steeper for the MWCNT composite. The elastic modulus was calculated at 4% strain to make a direct comparison between the samples. The elastic modulus of EVOH is already quite high, but it is improved when adding the CNT, an 8.31% increase (Figure 5.40). This increase in modulus again indicates that there good interaction between the CNT and the matrix. Effective stress transfer occurs during tensile testing and therefore the modulus is increased. However the increase is not that significant, which might be indicative of the lack of alignment as well as agglomeration of the MWCNT inside the sample. The total amount of MWCNT in the composite is also fairly low.

The ultimate tensile strength also increased with the incorporation of the MWCNT (Figure 5.41). Overall we can conclude that, as the aggregation of nanotubes will decrease the reinforcing effect[35], and since reinforcement is observed in these examples, that there were enough well dispersed and non-agglomerated nanotubes in the samples.

The mechanism of the deformation of the fibres with carbon nanotubes were discussed by Kim *et al* [48]. They concluded that when stress is applied parallel to the fibre axis the fibre elongates and at a certain length necking starts to occur. They found that the necking usually occurs at the end of

an embedded nanotube. The stress that is applied will reach a certain maximum and then the carbon nanotubes will start to slip inside the material in the direction of the applied stress. This slippage and the effective transfer of the stress inside the fibre to the carbon nanotubes cause the increase in the strain at break as well as the enhanced tensile strength[48]. The two possible fracture mechanisms for nanotubes are that the nanotubes will either break or pull out of the matrix, leading to the failure of the material, since no effective stress transfer between the matrix and the nanotubes will occur [49]. It has been proven that the crack responsible for the failure of the material starts in areas with low nanotube concentration. This then propagates along the areas with weak nanotube loading, at a certain crack opening width the nanotubes will break or pull out of the matrix and then eventually leads to the failure of the material [46].

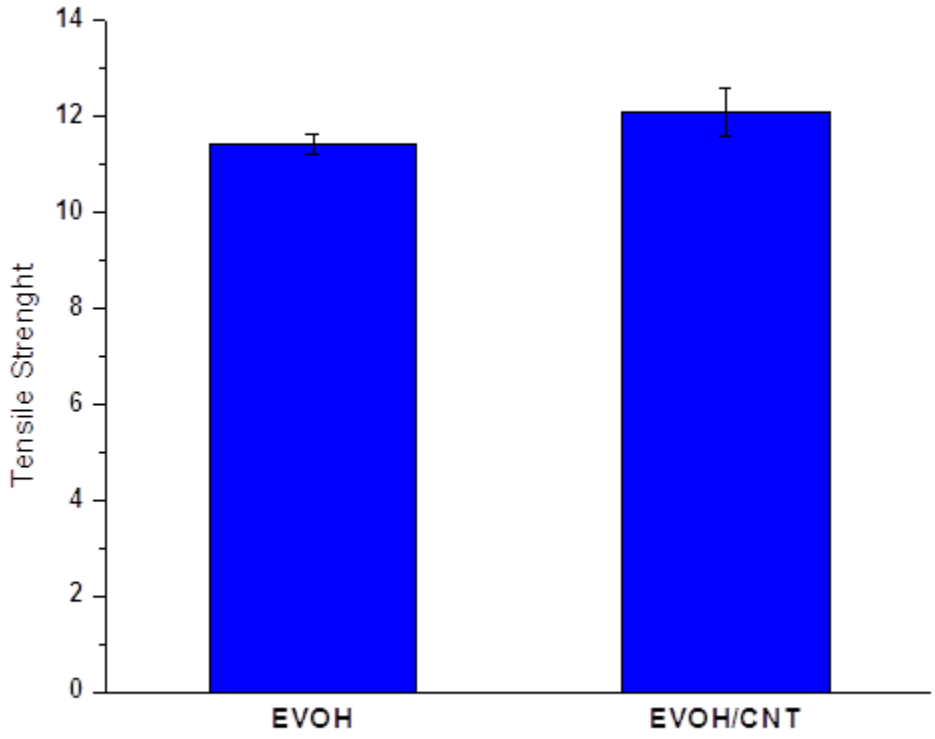

Figure 5.41. Tensile strength of EVOH and EVOH/MWCNT composites

The increase in modulus and tensile strength for the composite over the EVOH was 8.31% and 8.18% respectively. These results were the average of 5 tests that were more or less in the same range. The results did differ a bit between the different samples as can be seen by the error bar indicated on each column. These differences are probably due to the method of sample preparation.

The nanotubes on the other hand may also play a role in influencing the properties. If the nanotubes are not evenly distributed, leading to some same samples containing more nanotubes than others, the results will vary accordingly. The way the nanotubes are distributed in the fibres used to prepare these nanocomposites also differ quite significantly from fibre to fibre, and in some fibres these tubes are more aligned than in others. The adhesion between the nanotubes and the polymer may also vary between samples, as the extent of functionalization might differ between the nanotubes [36].

Table 5.9. Mechanical properties of EVOH and EVOH/MWCNT

Sample	Modulus	Yield strength (at 0.2 % strain offset)	Elongation at break (mm)	Ultimate Tensile Strength (MPa)
EVOH	11.43	50.33	12.29	53.27
EVOH/MWCNT	12.38	53.46	8.72	57.63

We can conclude that multi-walled carbon nanotubes improved the tensile properties of EVOH. The dispersion of the fibres inside the matrix during the preparation of the composites might lead to poor dispersion of the nanotubes inside the polymer matrix. If agglomerates of nanotubes occur inside the fibre, the chances are they will be distributed as agglomerates inside the polymer matrix, leading to a decrease in their reinforcement properties [50]. We could conclude some dispersion of the nanotubes did take place to cause the reinforcing effect, but better dispersion is necessary to obtain a higher increase in the mechanical properties. This method proved to be a way to disperse nanotubes through a polymer matrix; however, optimisation is necessary to improve the alignment and dispersion of nanotubes inside the nanofibres and nanocomposites. Once again, remelting and remolding of the composites might have resulted in better properties, but this was not possible within the scope of this study.

5.3.3 Attaching fluorophores to carbon nanotubes

We observed that it was quite difficult to see the carbon nanotubes inside a fibre mat. The size of the nanotubes as well as the fibres overlapping makes it very hard to be able to see them inside. Therefore, another method was required to determine the distribution of the nanotubes within the fibres.

Some work has been published that describe the attachment of fluorescent dye molecules to the nanotubes which render the nanotubes visible with a fluorescent microscope. In many cases Fluorescein and Rhodamine B has been used, though it is found that when these dye molecules are attached to carbon nanotubes, the carbon nanotubes will quench the fluorescence of the dye

molecules [51-57]. Though this is true, there is still enough fluorescence of the dye molecules to distinguish the nanotubes inside a material.

In our case, Rhodamine B was added beforehand to functionalized MWCNT in an acetone solution with 1 drop op H_2SO_4. After the functionalization, the nanotubes were washed repeatedly with water, to make sure that all the unreacted Rhodamine B is removed. These dyed nanotubes were then added to the electrospinning solution. After electrospinning, the the nanofibre mat was examined with a fluorescence microscope.

It was difficult to determine the amount of dye needed for the solution, since too much dye might make it impossible to observe the individual nanotubes. In Figure 5.42 the three different images obtained by microscopy can be seen. **A** is the transmission image and **B** the fluorescent image, while **C** is the overlay of the two. The bright red fluorescence seen in **B** could, however, be due to the auto-fluorescence of the carbon nanotubes. It can also be seen in the overlay of two images. It is therefore not clear what the dispersion of the nanotubes was like.

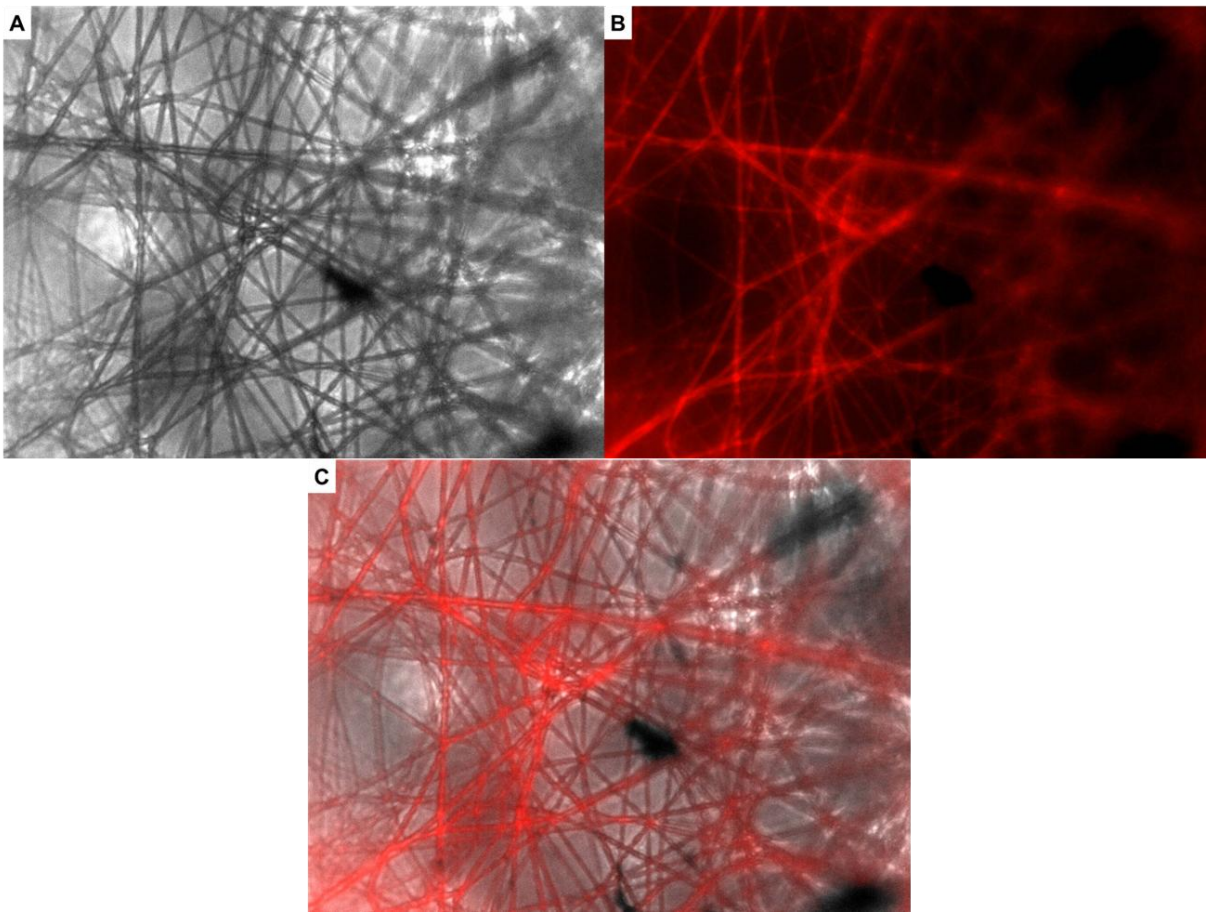

Figure 5.42. Fluorescence and transmission images of EVOH fibres containing dyed MWCNT

It is possible to use fluorescein with an isocyanate group (FITC) as a marker dye. These molecules are reported to react with the side walls of the (non-functionalized) nanotubes, forming non-covalent bonds [52]. The nanotubes used in this study were –COOH functionalized, so it was

expected to find covalent interaction between the isocyanate and carboxylic acid groups, as well as some side-wall binding as well. The multi-wall carbon nanotubes were treated with FITC as described in Chapter 3. Once again, care was taken to remove any loose or unbound dye molecules before drying the dyed MWCNT.

The dried, dyed MWCNT were added to EVOH and electrospun. These electrospun fibres were placed under the microscope. The FITC will be seen as a green fluorescence signal when placed under the fluorescence microscope.

In Figure 5.43 the images of the electrospun fibres filled with the dyed MWCNT can be seen. We can still see that the nanotubes tend to agglomerate inside the fibres, but there is some dispersion visible in the fibres although agglomerated.

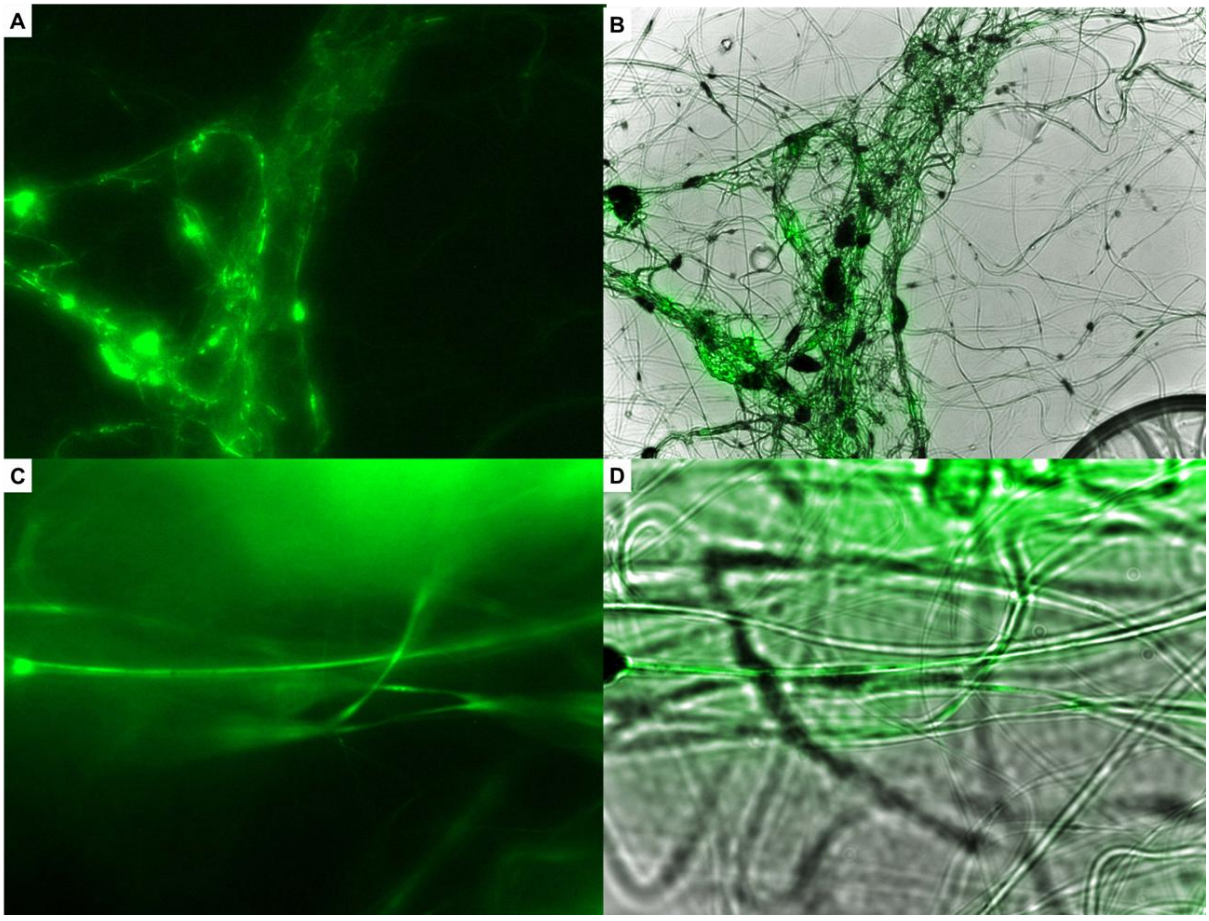

Figure 5.43. Fluoroscence images of EVOH fibres with FITC attached to MWCNT, B and D are the transmission and fluorescence overlay of A and C respectively

It is clear that the carbon nanotubes are well dispersed in the electrospun fibres, but is it necessary to use the fibres to disperse the MWCNT in the polymer matrix during the preparation of nanocomposites? In the next experiment, the fibres with the dyed MWCNT were used in the preparation of these nanocomposites. In **A** (Figure 5.44) the nanotubes, not encapsulated within electrospun fibres, were placed between two LDPE films and heated to form a composite. The next

two samples were prepared by placing the electrospun fibre mat containing the dyed MWCNT between (**B**) LDPE and (**C**) EVOH films. In both cases the composites were formed at a temperature high enough to melt the EVOH fibres. From Figure 5.44, it is clear that the distribution of MWCNT in **A** is not as good as in **B** and **C**, with **C** clearly giving the best dispersion. The latter is a clear indication that the interaction between the matrix and the EVOH fibres play a role in the dispersion of the fibres upon melting. Whilst EVOH and LDPE might be compatible, the dispersion is much better when the EVOH fibres are placed between two EVOH films prior to melting. In **A** the nanotubes are static before melting occurs, and they tend not to flow in the melt. A better dispersion could be seen in **B**, indicating that the fibres with the nanotubes inside provide better dispersion of the nanotubes, but agglomeration still occurs, as is evidenced by the bright spots. Dispersion in **C** looks the best, with the nanotubes not as agglomerated as in B, but well dispersed throughout the matrix. It must be noted that the fibre mats used in the preparation of composites B and C were prepared separately, and the dispersion of the MWCNT might also be influenced by the dispersion within the fibres. Having said that, however, it seems clear that agglomeration occurs after melting in the case of the LDPE nanocomposite. It seems that the functionalized nanotubes do not want to associate with the LDPE, but would rather agglomerate. In the case of the EVOH nanocomposite, the interaction between the functionalized MWCNT and the matrix appears to be as good as that between the MWCNT and the EVOH fibres, which should be expected.

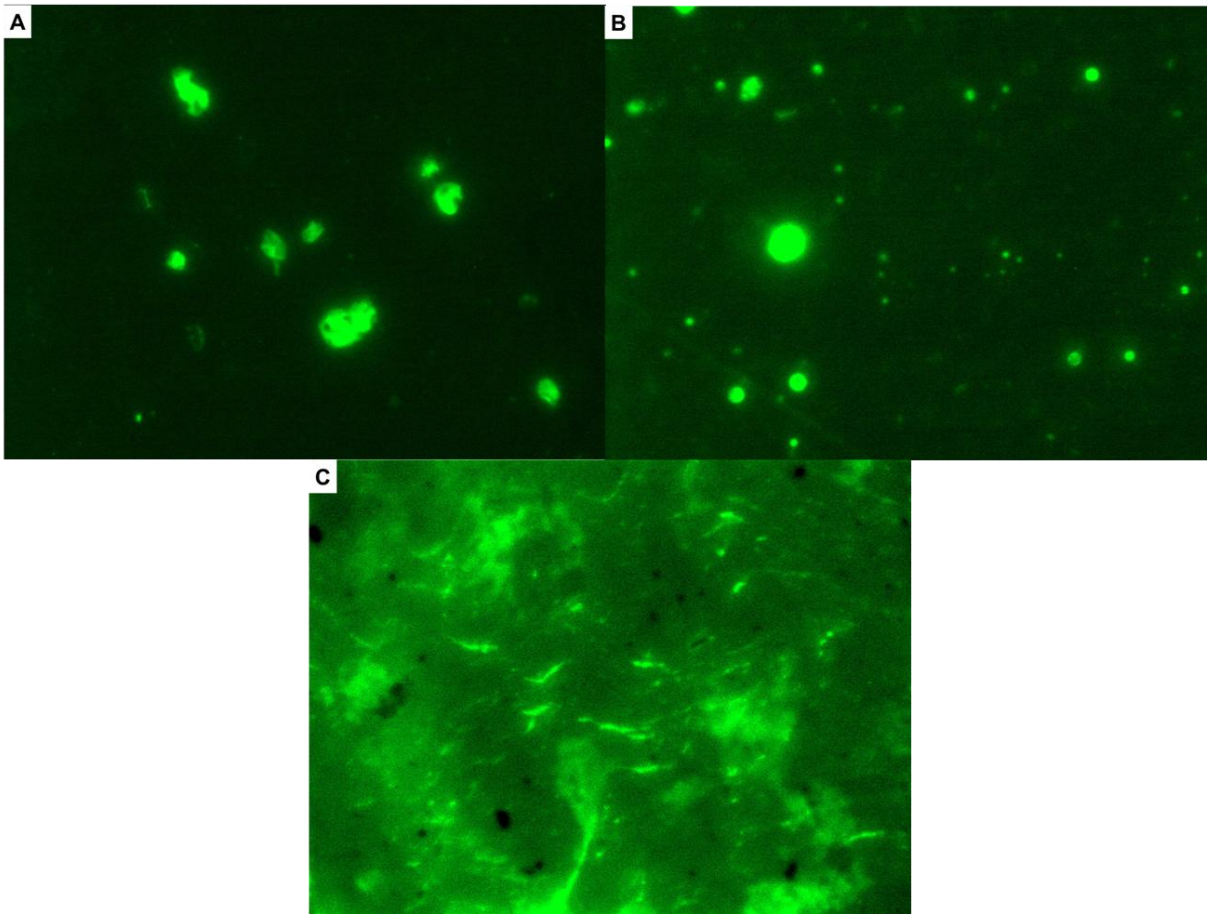

Figure 5.44. Fluoroscence images of A) LDPE with MWCNT, B) LDPE with MWCNT inside fibres and C) EVOH with MWCNT inside fibres. In B and C samples were heated to melt fibres.

One of the main concerns may be that the dye may react with the hydroxyl group of the EVOH and what is seen is the fluorescent of the fibres and the nanotubes which will not be a true reflection of the dispersion of the nanotubes. Further optimisation of the system is still required. It is also not clear at this point how the dye bonds to the nanotubes and this will be a discussion point in further research.

In conclusion, some aspects may be pointed out:

- The use of electrospun nanofibers seems to be a facile way of introducing MWCNT into a polymer matrix.
- The interaction of the MWCNT with the electrospun fiber and the interaction of the MWCNT with the matrix within which it is placed might differ, and this could affect the distribution of the nanotubes within the polymer with which the nanocomposite is formed.
- The use of the “single polymer composite” approach, i.e using the same polymer as the matrix to electrospin the “carrier” fibres seems to be the most effective way of dispersing the MWCNT in the polymer matrix.

- Suitable fluorescent dyes appear to be a good way of following the dispersion of nanofillers in polymer matrices, particularly in those cases where the nanofillers are difficult to see by conventional techniques.

5.4 References

1. Park, S. H.; Lee, G. J.; Im, S. S.; Suh, K. D. *Polymer Engineering and Science* **1998**, *9,* 1420-1425.

2. Ruiz, C.; Sanchez-Chaves, M.; Cerrada, M. L.; Fernandez-Garcia, M. *Journal of Polymer Science, Part A: Polymer Chemistry* **2008**, *21,* 7238-7248.

3. Ogata, N.; Lu, G.; Iwata, T.; Yamaguchi, S.; Nakane, K.; Ogihara, T. *Journal of Applied Polymer Science* **2007**, *2,* 1368-1375.

4. Fernandez, M. J.; Fernandez, M. D. *Polymer* **2005**, *5,* 1473-1483.

5. Sánchez-Chaves, M.; Ruiz, C.; Cerrada, M. L.; Fernández-García, M. *Polymer* **2008**, *12,* 2801-2807.

6. Kenawy, E.; Layman, J. M.; Watkins, J. R.; Bowlin, G. L.; Matthews, J. A.; Simpson, D. G.; Wnek, G. E. *Biomaterials* **2003**, *6,* 907-913.

7. Martinez-Sanz, M.; Olsson, R. T.; Lopez-Rubio, A.; Lagaron, J. M. *Cellulose* **2011**, *2,* 335-347.

8. Layman, J. M.; Wnek, G. E.; Kenawy, E. United States Patent US 2003/0215624 A1, 2003.

9. Ramakriskna, S.; Fujihara, K.; Teo, W. E.; Lim, T. C.; Ma, Z. *An Introduction to Electrospinning and Nanofibers;* World Scientific Publishing Co. Pte. Ltd: Singapore, 2005; .

10. Burger, C.; Hsiao, B. S.; Chu, B. *Annual Review of Materials Research* **2006**, 333-368.

11. Frenot, A.; Chronakis, I. S. *Current Opinion in Colloid and Interface Science* **2003**, 64-75.

12. Baumgarten, P. K. *Journal of Colloid and Interface Science* **1971**, *1,* 71-79.

13. Hsu, C.; Shivkumar, S. *Macromolecular Materials and Engineering* **2004**, *4,* 334-340.

14. Son, W. K.; Youk, J. H.; Lee, T. S.; Park, W. H. *Polymer* **2004**, *9,* 2959-2966.

15. Wannatong, L.; Sirivat, A.; Supaphol, P. *Polymer International* **2004**, *11,* 1851-1859.

16. Bhardwaj, N.; Kundu, S. C. *Biotechnology Advances* **2010**, *3,* 325-347.

17. Deitzel, J. M.; Kleinmeyer, J.; Harris, D.; Beck Tan, N. C. *Polymer* **2001**, *1,* 261-272.

18. Demir, M. M.; Yilgor, I.; Yilgor, E.; Erman, B. *Polymer* **2002**, *11,* 3303-3309.

19. Eda, G.; Shivkumar, S. *Journal of Material Science* **2006**, *17,* 5704-5708.

20. Ding, W.; Wei, S.; Zhu, J.; Chen, X.; Rutman, D.; Guo, Z. *Macromolecular Materials and Engineering* **2010**, *10,* 958-965.

21. Liu, Y.; Li, C.; Chen, S.; Wachtel, E.; Koga, T.; Sokolov, J. C.; Rafailovich, M. H. *Journal of Polymer Science, Part B: Polymer Physics* **2009**, *24,* 2501-2508.

22. Liu, Y.; Chen, S.; Zussman, E.; Korach, C. S.; Zhao, W.; Rafailovich, M. *Macromolecules* **2011**, *11,* 4439-4444.

23. Baji, A.; Mai, Y.; Wong, S.; Abtahi, M.; Chen, P. *Composites Science and Technology* **2010**, *5,* 703-718.

24. Kongkhlang, T.; Tashiro, K.; Kotaki, M.; Chirachanchai, S. *Journal of the American Chemical Society* **2008**, *46,* 15460-15466.

25. Dhanalakshmi, M.; Jog, J. P. *eXPRESS Polymer Letters* **2008**, *8,* 540-545.

26. Shebani, A. N. The effect of wood composition and compatibilisers on polyethylene/wood fibre composites, Stellenbosch University, Stellenbosch, 2010.

27. Chen, D.; Wang, R.; Tjiu, W. W.; Liu, T. *Composites Science and Technology* **2011***, 13,* 1556-1562.

28. Wang, X.; Huang, Z.; Chen, L. *Fibers and Polymers* **2011***, 3,* 359-365.

29. Huang, Z. -.; Zhang, Y. -.; Kotaki, M.; Ramakrishma, S. *Composites Science and Technology* **2003**, 2223-2253.

30. Bergshoef, M. M.; Vancso, G. J. *Advances in Materials* **1999***, 16,* 1362-1365.

31. Kim, J.; Reneker, D. H. *Polymer Composites* **1999***, 1,* 124-131.

32. Zucchelli, A.; Focarete, M. L.; Gualandi, C.; Ramakrishna, S. *Polymers in Advanced Technology* **2011***, 3,* 339-349.

33. Pedicini, A.; Farris, R. J. *Polymer* **2003***, 22,* 6857-6862.

34. Tang, C.; Liu, H. *Composites, Part A* **2008***, 10,* 1638-1643.

35. Jose, M. V.; Dean, D.; Tyner, J.; Price, G.; Nyairo, E. *Journal of Applied Polymer Science* **2007**, 3844-3850.

36. Liu, L. -.; Tasis, D.; Prato, M.; Wagner, H. *Advanced Materials* **2007***, 9,* 1228-1233.

37. Cooper, C. A.; Ravich, D.; Lips, D.; Mayer, J.; Wagner, H. D. *Composites Science and Technology* **2002***, 7-8,* 1105-1112.

38. Eitan, A.; Fisher, F. T.; Andrews, R.; Brinson, L. C.; Schadler, L. S. *Composites Science and Technology* **2006***, 9,* 1162-1173.

39. Breuer, O.; Sundararaj, U. *Polymer Composites* **2004**, *6,* 630-645.

40. Yeo, L. Y.; Friend, J. R. *Journal of Experimental Nanoscience* **2006**, *1-4,* 177-209.

41. Choi, J.; Park, E. J.; Park, D. W.; Shim, S. E. *Synthetic Methods* **2010**, *23-24,* 2664-2669.

42. Alvarez, V. A.; Ruseckaite, R. A.; Vazquez, A. *Journal of Applied Polymer Science* **2003**, *11,* 3157-3163.

43. Thostenson, E. T.; Chou, T. *Journal of Physics D: Applied Physics* **2002**, *16,* L77-L80.

44. Dror, Y.; Salalha, W.; Khalfin, R. L.; Cohen, Y.; Yarin, A. L.; Zussman, E. *Langmuir* **2003**, *17,* 7012-7020.

45. Sahoo, N. G.; Rana, S.; Cho, J. W.; Li, L.; Chan, S. H. *Progress in Polymer Science* **2010**, *7,* 837-867.

46. Qian, D.; Dickey, E. C.; Andrews, R.; Rantell, T. *Applied Physics Letters* **2000**, *20,*.

47. Zhao, C.; Hu, G.; Justice, R.; Schaefer, D. W.; Zhang, S.; Yang, M.; Han, C. C. *Polymer* **2005**, *14,* 5125-5132.

48. Kim, G. -.; Michler, G. H.; Pötschke, P. *Polymer* **2005**, *18,* 7346-7351.

49. Safadi, B.; Andrews, R.; Grulke, E. A. *Journal of Applied Polymer Science* **2002**, *14,* 2660-2669.

50. Ko, F.; Gogotsi, Y.; Ali, A.; Naguib, N.; Ye, H.; Yang, G.; Li, C.; Willis, P. *Advanced Materials* **2003**, *14,* 1161-1165.

51. Singh, D. K.; Giri, P. K.; Iyer, P. K. *Journal of Physical Chemistry C* , Ahead of Print.

52. Nakayama-Ratchford, N.; Bangsaruntip, S.; Sun, X.; Welsher, K.; Dai, H. *Journal of the American Chemical Society* **2007**, *9,* 2448-2449.

53. Ahmad, A.; Kurkina, T.; Kern, K.; Balasubramanian, K. *Journal of Physical Chemistry* **2009**, *13,* 2251-2255.

54. Zanarini, S.; Vinante, M.; Pasquardini, L.; Sanginario, A.; Giorcelli, M.; Bianco, S.; Gerbaldi, C.; Nair, J. R.; Lunelli, L.; Vanzetti, L.; Paolucci, F.; Marcaccio, M.; Prodi, L.; Tagliaferro, A.; Pederzolli, C.; Demarchi, D.; Civera, P. *Electrochimica Acta* **2011**, *25,* 9269-9276.

55. Liu, Q.; Chen, B.; Wang, Q.; Shi, X.; Xiao, Z.; Lin, J.; Fang, X. *Nano Lett.* **2009**, *3,* 1007-1010.

56. Serag, M. F.; Kaji, N.; Gaillard, C.; Okamoto, Y.; Terasaka, K.; Jabasini, M.; Tokeshi, M.; Mizukami, H.; Bianco, A.; Baba, Y. *ACS Nano* **2011**, *1,* 493-499.

57. Serag, M. F.; Kaji, N.; Venturelli, E.; Okamoto, Y.; Terasaka, K.; Tokeshi, M.; Mizukami, H.; Braeckmans, K.; Bianco, A.; Baba, Y. *ACS Nano* **2011**, *11,* 9264-9270.

Chapter 6

Conclusions and recommendations

6.1 Electrospinning of polyolefins

6.1.1 Conclusions

The original aim of this study was to successfully electrospin polyolefins from solution. The following objectives were successfully achieved.

- A suitable solvent system was found by which polypropylene copolymers could be electrospun at room temperature. The polymer was dissolved in a solvent system comprising out of cyclohexane/acetone/DMF at 100 °C in an oilbath. The solution was taken out of the oilbath for solution electrospinning at room temperature. This solvents system allowed the solution electrospinning at room temperature without the polymer crystallizing out of solution.
- The optimum spinning conditions were established for the different copolymers to achieve the thinnest fibres. The optimum spinning conditions differed for the different copolymers. For the 1-decene copolymers, the thinnest fibres (in the nanometre range) were obtained for the 10A copolymer however all these samples were particularly beaded. The other copolymers in this range did not produce nanofibres and the fibre diameters were in the micrometre range. For the 1-octene copolymers the fibre diameters were mostly in the micrometre range, however one sample of polymer 8A could be electrospun to obtain nanofibres. The 1-tetracene produced nanofibres for most of the samples, although these samples as well were particularly beaded.
- The influence of the different parameters on the fibre diameter was investigated. This was done by keeping to parameters constant and varying the third parameter. The influence of the different parameters varied for the different copolymers. It was quite clear that the solubility and the related properties were different for the 1-octene, 1-decene and 1-tetradecene copolymers.
- Under the initial conditions, the fibres of all the different propylene copolymers were very beaded. Different salts were added to the electrospinning solutions, trying to increase the conductivity of the solutions. With increased conductivity the charges carried by the jet will be more and with an increase in charges the jet will be stretched more in the electrical field. All these factors contributed to the formation of beadless fibres. In the end it was found that by the addition of only 0.2 wt% LiCl beadless fibres could be electrospun.

- The crystallinity of for fibres produced from the 1-octene and 1-decene copolymers was more than that of the pure polymer powders. During electrospinning the chains inside the polymer will have time to align before reaching the collector plate, leading to an increase in crystallinity. However for polymer 1-tetradecene copolymers the crystallinity of the fibres was more or less half than that of the polymer powder. It is possible that the length of the side-chains on the copolymer prevents rapid crystallization during the electrospinning process, in addition the presence of the 1-tetradecene might influence the solubility to such an extent that precipitation from solution during the spinning process is more rapid than for the other 2 copolymers.
- Different collectors were also investigated, but in the end it was found that between spinning unto ice, foil on ice of just foil, foil still seemed to be the best collector.
- The electrospinning of isotactic polypropylene was also attempted, but dissolving of the polymer proved to be difficult. These polymers had lower molecular weight than those of the copolymers which could be dissolved quite easily. This solution melting temperatures of the copolymers was investigated and even though these polymers had the same amount of comonomer, crystallinity and more or less the same molecular weight, their solution melting temperatures differed greatly. It was found that though believed otherwise previously, the type and amount of comonomer have an influence on the solubility of the copolymer.

6.2 Electrospinning of polyethylene vinyl alcohol

6.2.1 Conclusions

The aims of this section were to electrospin EVOH and use the EVOH nanofibres as reinforcement in a polymer matrix as well as way to disperse MWCNT in a polymer matrix.

The following objectives was successfully achieved

- A suitable solvent was found for the solution electrospinning of EVOH. Isopropanol/water gave very thick fibres. DMF and DMSO gave the thinnest fibres with the best morphology, but the polymer stayed in solution the longest in DMSO. DMOS also has a higher dielectric constant and is less toxic than DMF. LiCl was added to the solution to ensure the electrospinning of beadless fibres.
- Spinning conditions was optimised for both DMF and DMSO. It was found with DMSO an even slower flow rate could be used to obtain nanofibres.
- The influence of the various spinning parameters on the fibre diameter was investigated. Two parameters were again kept constant while varying the third.

  For DMF the fibre diameter increased with an increase in voltage and a 20 kV beaded fibres were formed. At high voltage the jet might become instable, leading to inconsistent whipping and causing the formation of beads along the fibres.

The flow rate did not seem to influence the fibre diameter that much,

The greater the distance the smaller the fibre diameter. At shorter distances the fibres will arrive faster at the collector not having enough time to be stretched and elongated before arriving at the collector. At shorter distances the solvent also might not have enough time to evaporate, leading to wet fibres being collected which also leads to thicker fibre diameters.

For the DMSO system exactly the same trends were found when varying the different electrospinning parameters.

- The crystallinity of the fibres was lower than that of the pure polymer. The chains inside the polymer did not get enough time to realign and crystallize during electrospinning and therefore the fibres will have a lower crystallinity than that of the pure polymer.
- Both aligned and unaligned fibres were successfully incorporated in a LDPE matrix by film pressing. The morphology of the fibres was still intact after the melt formation of the composites.
- The stress at 5% strain as well as the ultimate tensile strength increased for both samples with aligned and unaligned fibres compared to the pure LDPE. The fibres are great for reinforcement since the stress that is applied to the composite will be transferred to the fibres leading to better mechanical properties. Those containing unaligned fibres had a bigger impact on the stress at 5% strain. The unaligned fibres had greater crystallinity than that of the aligned fibres, greater crystallinity will lead to a stronger material, and this explains why the reinforcement of the unaligned fibres is better than that of the aligned fibres.

  What should be taken in to account is that it was not possible to determine the amount of fibres incorporated in the matrix and therefore the results may differ between samples.
- MWCNT were successfully incorporated through electrospinning inside EVOH nanofibres. TEM confirmed the presence inside the fibres, although some agglomeration of the nanotubes still occurred. The nanotubes did not influence the morphology of the fibres, although the fibre diameter was thicker for fibres with MWCNT. FE-SEM on the fracture surface of the fibres containing MWCNT could not confirm the presence of the nanotubes. TGA however confirmed that more nanotubes were incorporated when using DMSO as solvent then when using DMF.
- Composites were successfully created containing MWCNT. The fibres were placed inside the polymer matrix and then melted so that just the MWCNT remained inside the polymer matrix. The EVOH fibres were both imbedded in LDPE and EVOH matrices.
- The mechanical properties of the LDPE containing MWCNT did not show a great increase and it was suspected that the EVOH polymer plays a bigger role in influencing the polymer properties than the MWCNT.

The EVOH polymer containing the MWCNT however did show an increase in the modulus at 4% strain and the ultimate tensile strength. Greater increase in mechanical properties can be achieved if less agglomeration of the nanotubes inside the fibres takes place.

- Fluorescent dye molecules were attached to the nanotubes and from fluorescent images the dispersion of the nanotubes inside the fibres as well as the polymer matrix could be seen. From these images it could be seen that some agglomeration of the nanotubes did still take place. When comparing samples in which nanotubes were just added to the matrix and samples in which nanotubes were added by the means of nanofibres it was quite clear that better dispersion of nanotubes took place by adding the nanotubes through nanofibres. The way in which these dye molecules attach to the nanotubes is not clear yet.

6.2.2 Recommendations for future work

- The use of EVOH nanofibres opens up a whole new area of research. Not only could these fibres be used as reinforcement, but as a way to disperse MWCNT inside a polymer matrix.
- The precise incorporation of the fibres inside a polymer matrix is still a problem. Further investigation is needed to attempt to find a sufficient way to incorporate these fibres inside the polymer.
- The use of fluorescent molecules attached to carbon nanotubes could also be used to determine the dispersion of nanotubes inside a polymer matrix or inside nanofibres. Further investigation is needed into how these dye molecules attach to the surface of the nanotubes.
- The ability to functionalize and attach dye molecules to the surface of MWCNT indicates that this approach could be extended to, for example, the surface of nanofibres, or the different components of complex polymers.
- The fact that the dispersion of functionalized MWCNT in LDPE and in EVOH differs significantly, even when delivered to the matrix by means of a “carrier” fibre like EVOH, indicates that the same approach should be tried with non-functionalized MWCNT. These nanotubes might be more compatible with an all-hydrocarbon polymer like LDPE.